CZECH TECHNICAL UNIVERSITY IN PRAGUE

Faculty of Civil Engineering

Department of Concrete and Masonry Structures

Design of a prestressed concrete road viaduct close to Lisbon

Diploma Thesis

Study programme: Civil Engineering

Branch of study: Structural and Transportation Engineering

Diploma Thesis supervisor: doc. Ing. Roman Šafář, Ph.D.

Bc. Magdaléna Kábelová

2022

CZECH TECHNICAL UNIVERSITY IN PRAGUE
Faculty of Civil Engineering
Thákurova 7, 166 29 Prague 6, Czech Republic

DIPLOMA THESIS ASSIGNMENT FORM

I. PERSONAL AND STUDY DATA

Surname: Kábelová Name: Magdaléna Personal number: 468645

Assigning Department: Concrete and Masonry Structures

Study programme: Stavební inženýrství

Branch of study: Konstrukce a dopravní stavby

II. DIPLOMA THESIS DATA

Diploma Thesis (DT) title: Návrh silničního mostu z předpjatého betonu u Lisabonu

Diploma Thesis title in English: Design of a presstressed concrete road viaduct close to Lisbon

Instructions for writing the thesis:
Elaborate drawings, structural analysis and technical report.

List of recommended literature:
Šafář, R.: Concrere Bridges - Lectures, CTU in Prague 2015
Šafář, R., Petřík, M., Tej, P.: Concrete Bridges - Worked Examples, CTU in Prague 2016

Name of Diploma Thesis Supervisor: doc. Ing. Roman Šafář, Ph.D.

DT assignment date: 16th September 2021 DT submission date: 2nd January 2022

DT Supervisor's signature Head of Department's signature

III. ASSIGNMENT RECEIPT

I declare that I am obliged to write the Diploma Thesis on my own, without anyone's assistance, except for provided consultations. The list of references, other sources and consultants' names must be stated in the Diploma Thesis and in referencing I must abide by the CTU methodological manual "How to Write University Final Theses" and the CTU methodological instruction "On the Observation of Ethical Principles in the Preparation of University Final Theses".

Assignment receipt date Student's name

Sworn declaration

I hereby declare that I have completed my diploma thesis independently, by using the literature mentioned and with the help of professional consultations of doc. Ing. Roman Šafář, Ph.D. and Ing. António Batista, Ph.D.

9th January 2022, Prague ……

Bc. Magdaléna Kábelová

Acknowledgments

I would like to express my gratitude to the supervisors of the thesis doc. Ing. Roman Šafář, Ph.D. and Ing. António Lopes Batista, Ph.D for their valuable advice and professional guidance, which contributed to the completion of this diploma thesis.

Furthermore, I would like to thank my friends and family for the support they provided me throughout the study and development of this thesis.

Abstract

The aim of the diploma thesis is a design of a bridge structure (road viaduct V1) located close to Lisbon.

The thesis contains a technical report that includes details of the structure and the considered design options.

The structural analysis deals with the solution of a structure with six spans of the lengths 40.0 + 4 x 50.0 + 40.0 m. Its main part is the design of the superstructure, which consists of a post-tensioned double beam cast-in-situ.

The design includes load analysis, determination of internal forces, design of prestressing and main safety checks.

Drawings of the final structure were prepared as well.

Keywords

road viaduct, bridge, double-beam, prestressed concrete

Table of contents

Introduction 9

Technical report 11

1. Identification data of the bridge 11
2. Basic data of the bridge 11
3. Justification of the bridge and its location 12
   - 3.1. Purpose of the bridge 12
   - 3.2. Road data, obstacle data 12
   - 3.3. Territorial conditions 12
   - 3.4. Geotechnical conditions 12
4. Technical solution of the viaduct 13
   - 4.1. Variants of the superstructure 13
     - 4.1.1. Box girder built on a movable scaffolding system 13
     - 4.1.2. Arch bridge 14
     - 4.1.3. System of UHPFRC precast segments for bridge structures 15
     - 4.1.4. Composite steel-concrete structure 16
   - 4.2. Description of the chosen solution 17
     - 4.2.1. Superstructure 17
     - 4.2.2. Substructure 17
     - 4.2.3. Bridge equipment 18
5. Construction of the bridge 19

Structural analysis 21

1. Structure 21
   - 1.1. Empirical formulas for structural design 21
     - 1.1.1. Superstructure 21
     - 1.1.2. Substructure 22
   - 1.2. Scheme of the structure for structural analysis 23
   - 1.3. Calculation model 23
   - 1.4. Characteristics of a cross section 27
   - 1.5. Effective width of flanges 27
2. Materials 29
   - 2.1. Concrete 29
   - 2.2. Prestressing reinforcement 30
   - 2.3. Reinforcing steel 31

3. Actions 31
3.1. Permanent loads 31
3.1.1. Self-weight of the superstructure g_0 31
3.1.2. Self-weight of bridge equipment $(g - g_0)$ 31
3.1.3. Uneven settlements of supports 35
3.2. Variable loads 35
3.2.1. Traffic loads 35
3.2.2. Horizontal forces 39
3.2.3. Thermal actions 40
3.2.4. Wind load 42
3.2.5. Construction load 44
3.3. Accidental actions 44
3.3.1. Seismic action 44
3.4. List of loads 48
4. Internal forces 49
4.1. Analysis of internal forces 49
4.1.1. Permanent and variable actions 49
4.1.2. Accidental actions 62
4.2. Combinations of actions 64
5. Prestressing 70
5.1. Design principles 70
5.1.1. Cover layer 70
5.1.2. Clear spacing between ducts 70
5.2. Design of prestressing reinforcement 70
5.3. Prestressing layout 71
6. Serviceability limit states 72
6.1. Introduction 72
6.2. Stress limit of concrete 72
6.2.1. Finished structure 72
6.2.2. Construction stages 72
6.3. Determination of normal stresses 73
6.4. Resulting normal stresses 74
6.4.1. Construction stages - check of the case without the action of the fresh concrete 76
6.4.2. Construction stages - check of the case with the action of the fresh concrete on the scaffolding system 80
6.4.3. Finished structure – check of limit stresses 84

7. Ultimate limit states 86
7.1. Introduction 86
7.2. Resulting internal forces 86
7.3. Check of the cross section at span 87
7.3.1. Check of the cross section at span – beginning of service life 88
7.4. Check of the cross section at pier 90
7.4.1. Check of the cross section at pier– end of service life 91
8. Conclusion 93

Introduction

The thesis was written during a study stay in Lisbon, Portugal within the Erasmus+ programme. The project was developed under the dual supervision of Ing. António Batista, Ph.D. from the NOVA School of Science and Technology in Lisbon and doc. Ing. Roman Šafář, Ph.D. from the Czech Technical University in Prague.

The details of the thesis assignment have been provided by the NOVA School and Technology in Lisbon as well as some of the standards and literature used.

The aim of the diploma thesis is to elaborate a case study and to design a bridge structure (road viaduct V1) located close to Lisbon which has to meet provided requirements.

The thesis is composed of a written part (technical report and structural analysis) and a set of drawings.

The first task was a proposal of several variants of the structure. Subsequently, the best solution has been chosen for a more detailed elaboration. For the final choice, multiple aspects have been considered, such as functionality, materials, construction method and the aesthetics of the structure.

Another part of the thesis is focused on modelling, calculations, structural analysis and main safety checks of the bridge.

The drawing part of the thesis includes a cross section, longitudinal section, plan, arrangement of supports and prestressing reinforcement.

CZECH TECHNICAL UNIVERSITY IN PRAGUE

Faculty of Civil Engineering

Department of Concrete and Masonry Structures

Design of a prestressed concrete road viaduct close to Lisbon

Part A
Technical report

Technical report

1. Identification data of the bridge

Name of the structure	New construction Caparica
County	Setúbal
Cadastral territory	Lisbon
Country	Portugal
Structure number	V1
Structure name	Road viaduct V1
Obstacle bellow the bridge	valley

2. Basic data of the bridge

Number of spans	6
Bridge deck position	upper bridge deck
Intended service life	100 years (permanent bridge)
Route course on the bridge	horizontally direct, vertically constant longitudinal slope of 1 %
Principal material	concrete (prestressed, reinforced)
Structural arrangement	continuous girder
Length of the bridge	299.560 m
Length of superstructure	281.500 m
Length of spans	40.000 + 4 x 50.000 +040.000 span 2, 3, 4, 5: 50.000 m
Support angle	100 g – perpendicular
Clear width of the carriageway	12.000 m
Clear width between outer handrails	14.000 m
Width of the superstructure	14.500 m
Width of the bridge	15.100 m
Considered traffic actions	EN 1991-1-2: Eurocode 1– Actions on structures – Part 1-2: Traffic loads on bridges NP EN 1991-1-2: Eurocódigo 1 – Acções em estruturas – Parte 1-2: Ações gerais – Ações em estruturas expostas ao fogo

NP EN 1991-2: Eurocódigo 1 – Ações em estruturas - Parte 2: Ações de tráfego em pontes

According to NP EN 1991-2, the bridge is classified as Class II: bridges on routes with more common traffic characteristics, including roads and motorways. Heavy traffic is not expected on these routes.

3. Justification of the bridge and its location

3.1. Purpose of the bridge

The purpose of the bridge is to carry a road across a 27.3 metres deep valley in the maximum.

3.2. Road data, obstacle data

Road data

Width layout	3,5 metres wide lanes with 2,5 metres wide shoulders, centrally located road axis
Directional conditions	straight line
Road level height at the bridge site	from 48.0 to 51.0 metres above sea level
Height conditions at the bridge site	constant longitudinal slope of 1 %

Obstacle data

The bridge carries a road over a valley for almost 300 m. The maximum depth of the ground below the road level is 27.3 metres.

3.3. Territorial conditions

The viaduct is located in the extravilan in the cadastral territory of Lisbon, Portugal, near the Caparica area.

3.4. Geotechnical conditions

No specific geotechnical survey was performed at the bridge site. For the purposes of the thesis, it is assumed that the foundation ground is composed by soft limestone (allowable stresses 500 kPa at 3 m depth).

4. Technical solution of the viaduct

4.1. Variants of the superstructure

4.1.1. Box girder built on a movable scaffolding system

The first option considered is a bridge structure with 5 spans of variable length. The maximum span length 60 m is placed in the deepest part of the valley, while towards the ends of the bridge, the span lengths are decreasing. In the cross section, the structure is in the form of a box girder. The cross-section depth of the beam is 1/20 of the maximum span length, which is 3.0 m. This depth was chosen with regard to the considered technology of construction – casting in place on a movable scaffolding system.

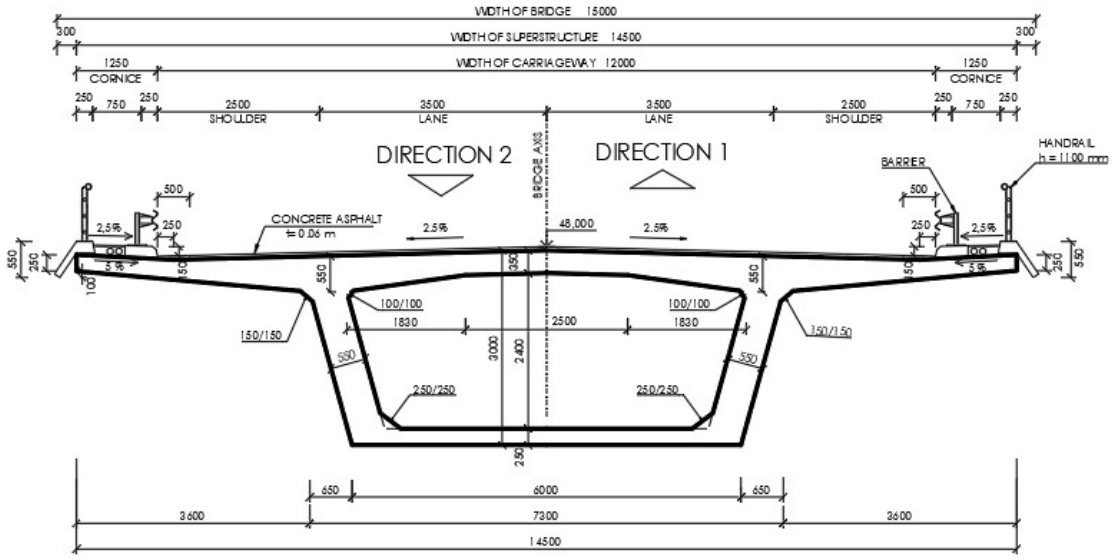

Figure 1: Box girder built on a movable scaffolding system – cross section

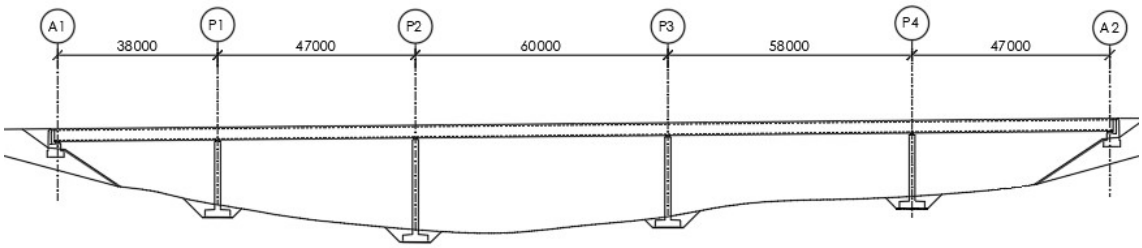

Figure 2: Box girder built on a movable scaffolding system – longitudinal section

4.1.2. Arch bridge

Another variant of the bridge structure is an arch bridge. The arch is placed in the deepest part of the valley, then the structure continues using standard spans. The span between the springers of the arch is 91.0 m, its rise is 22.3 m. The load from the bridge deck is transferred to the arch by vertical struts evenly distributed along the length of the arch.

In the cross section, the structure is a box girder with a depth of 3.5 m. The outermost spans of the bridge would be built on a scaffolding system, the arch part would be built by a cantilever method with temporary stay cables.

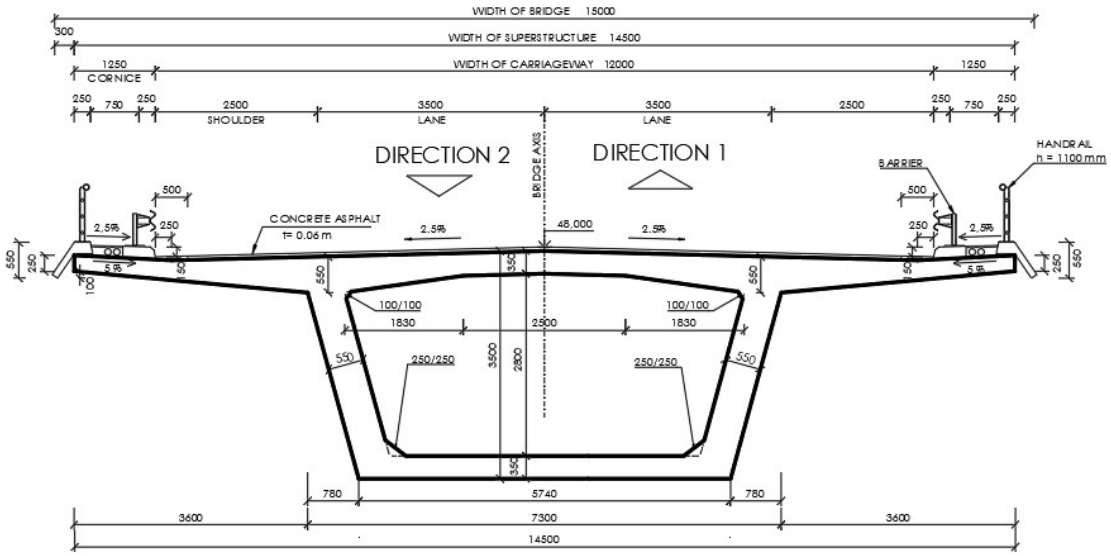

Figure 3: Arch bridge – cross section

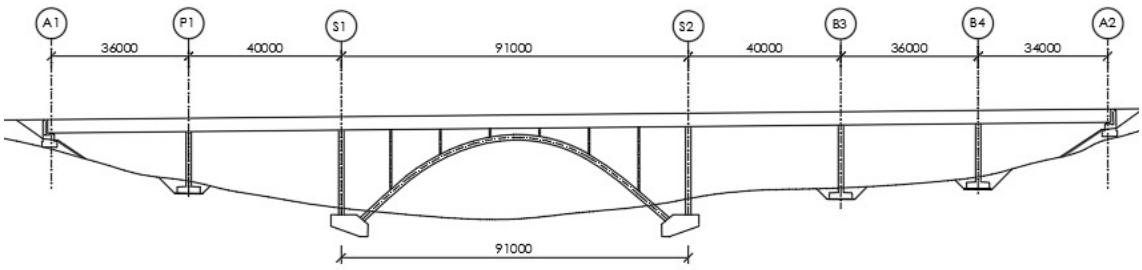

Figure 4: Arch bridge – longitudinal section

4.1.3. System of UHPFRC precast segments for bridge structures

The third bridge alternative is a bridge structure composed of a system of UHPFRC precast segments for bridge structures. The bridge has six spans of the length of 32.0 + 42.0 + 50.0 + 46.0 + 42.0 + 32.0 m. The system is made of ultra-high-performance fibre-reinforced concrete elements connected by post-tensioning. The structure consists of two 2.5 m deep main box segmental girders, cross beams and a deck slab with longitudinal stiffeners.

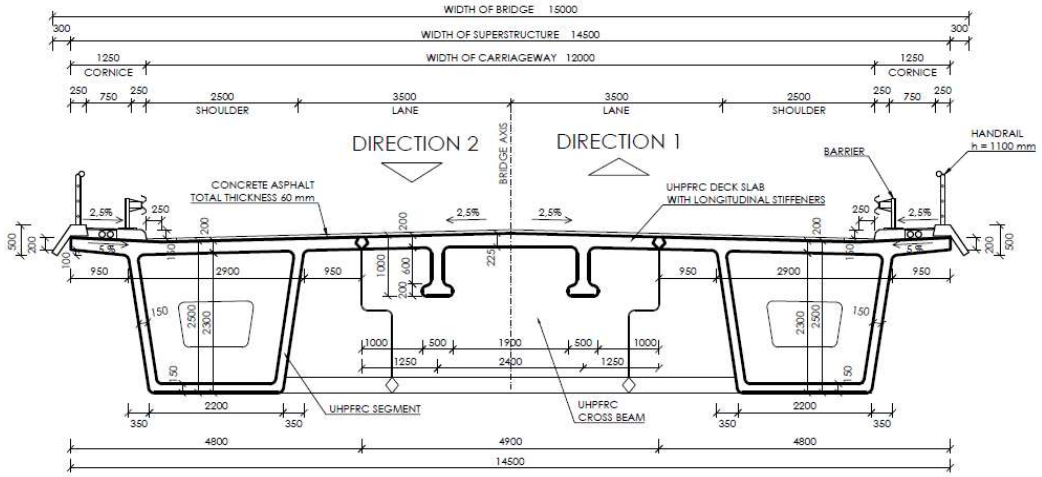

Figure 5: System of UHPFRC precast segments – cross section

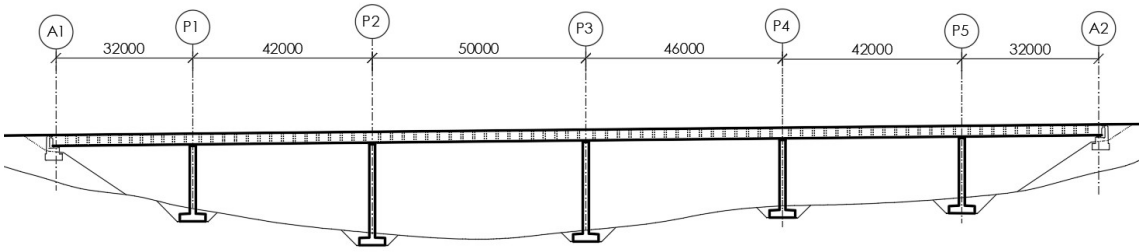

Figure 6: System of UHPFRC precast segments – longitudinal section

4.1.4. Composite steel-concrete structure

The selection of the superstructure also included the option of a composite steel-concrete structure. This option was intended for an eight-spanned bridge with a typical span length of 40 m. The superstructure consists of two main steel welded girders with a depth of 1.7 m which are connected with a cast-in-situ reinforced concrete deck slab of a maximum thickness of 550 mm above the girders. Towards the centre and edges of the slab, the thickness is decreased by haunches. Along the length of the structure, the steel girders are stiffened by vertical stiffeners (on the inner sides at spans and from both sides above supports) and connected together by cross beams at regular intervals.

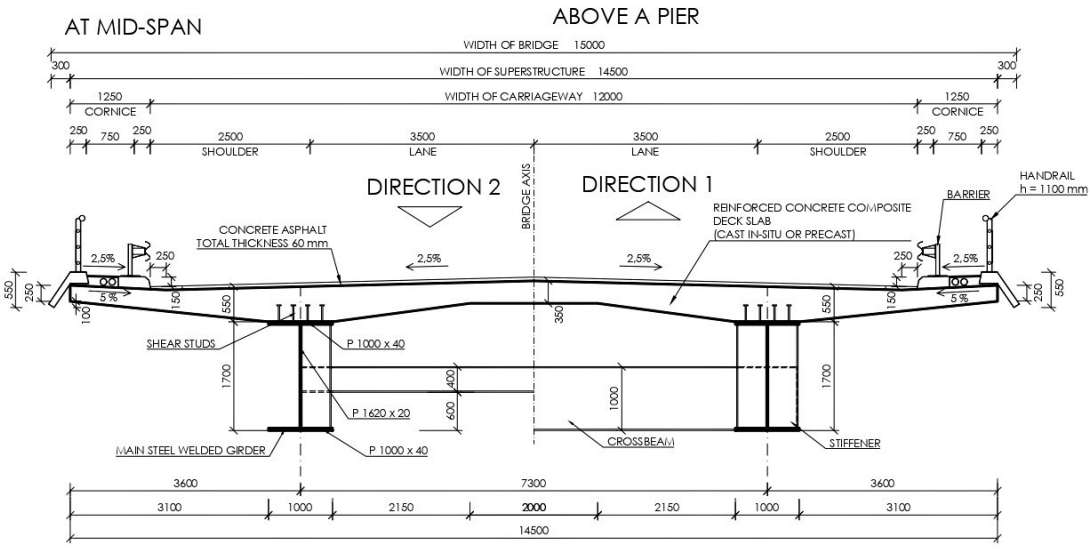

Figure 7: Composite steel-concrete structure – cross section

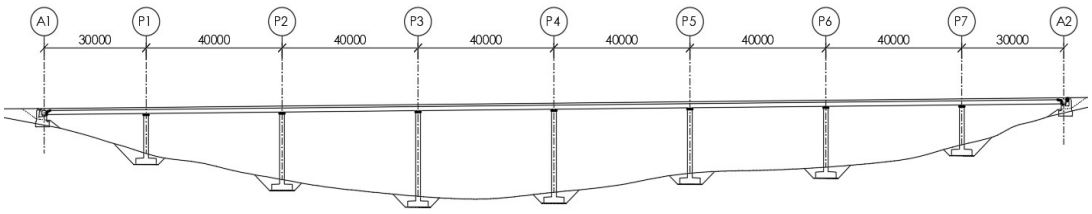

Figure 8: Composite steel-concrete – longitudinal section

4.2. Description of the chosen solution

4.2.1. Superstructure

The bridge structure considered in this thesis has six spans of the length of 40 + 4 x 50 + 40 m.

Superstructure of the bridge is continuous, double-beam, cast-in-situ, made of post-tensioned prestressed concrete. Depth of the cross section is 3.000 m.

The axial distance of the main beams is 7.700 m, their width is 1.200 m at the lower surface and 1.400 m at the upper surface. Thickness of the deck slab is 0.550 m above the main beams, 0.350 m in the central part of the slab and 0.250 m at the ends of the lateral cantilevers.

The superstructure is supported by pot bearings.

Total width of the superstructure is 14.5 m. The upper surface of the bridge deck is made in a roof-like slope of 2.5 % towards the edges of the structure, under the cornices there is a counter slope of 5 %, the change of slope is located 1.5 m from the outer edge of the structure.

The main beams are connected by end cross beams above the end abutments; lateral cantilevers are stiffened by ribs in this area.

The superstructure is made of concrete C40/50– XS1, XD1, XC4.

Prestressing reinforcement is made of internal bonded tendons composed of 26 strands of the diameter of 15.7 mm with f_{pk} = 1860 MPa and of the relaxation class 2 (strands and wires with low relaxation). The tendons are placed in plastic ducts, grouted finally by cement mortar. Passive reinforcement is made of steel B500B.

4.2.2. Substructure

The superstructure is supported by five intermediate piers of variable height and by two end abutments.

The heights of piers vary from 14.550 m to 22.880 m, and they consist of two independent shafts with a square cross section with sides of 1.700 m and 2.200 m. The axial distance of the shafts is the same as the axial distance of main beams, which is 7.700 m. In about two thirds of their height, the shafts of the piers are stiffened with a cross beam. Both shafts of each pier are placed on one common foundation block of a rectangular shape.

The end supports are made as low bridge abutments made from concrete C30/37 – XS1, XD1, XC4. Their width in the transverse direction is the same as the width of the superstructure, i.e., 14.5 m, longitudinally, the load-bearing part of the abutment is 3.0 m wide.

A gap of 0.5 m is left between the lower surface of the superstructure and the upper surface of abutments. Here, the structure is placed on pot bearings and this gap also allows the access for inspections and eventual repairs or replacements of the bridge bearings.

The top surface of abutments below bearings is made in the slope of 4 % towards its back side, where a small drainage channel for water is placed.

A free vertical space between the end face of the superstructure and the closing wall is 750 mm wide.

At the top of closing walls, transition slabs are fixed by hinges and there is also a place for anchoring of expansion joints.

The embankment behind the abutment is closed by parallel wing walls, which are monolithically connected to the abutments and placed on the same foundation block. The wing walls are made also of concrete C30/37 – XS1, XD1, XC4.

Foundation blocks of abutments are 4.0 m wide, and they are supported by bored piles with of the diameter of 1.2 m. Subbase concrete below foundations is of the class of C12/15 – X0.

4.2.3. Bridge equipment

4.2.3.1. Pavement

The bridge has an asphalt concrete pavement with a total thickness of 60 mm including a waterproofing layer, made of bituminous sheets.

4.2.3.2. Bridge cornices

The bridge cornices are partly precast, partly cast-in-situ, made of concrete C30/37 – XS1, XD3, XC4. The upper surface of cornices is made in the traverse slope of 2.5 % towards the axis of the bridge and it is made rough. The height of kerbs is 150 mm.

The cornices have a total width of 1550 mm, of which 1250 mm lie directly on the bridge superstructure.

The cornices also serve as a place for 750 mm wide service footways, which are bordered by steel barriers and a steel railing.

4.2.3.3. Barriers

Steel barriers are installed on both sides of the carriageway on the inner 500 mm of the bridge cornices. The level of retention of the barriers should be NH2.

4.2.3.4. Handrail

The outer edges of the cornices are equipped by steel bridge handrail 1100 mm high with a vertical filling.

4.2.3.5. Water drainage system

Drainage of water from the bridge surface is ensured by a roof-like slope towards the cornices into a gutter which is 250 mm from the edge of the kerb. In this axis, water drainage gullies are placed, connected to a longitudinal pipe, which is finished at the lower end of the bridge.

4.2.3.6. Transition areas of the bridge

The transition zones consist of a soil fill behind the foundations, watertight layer, permeable coarse-grained soil located directly behind the abutment and partly under the transition slab, placed on the top of transition zones. The remaining area is backfilled with well compacted soil. Used materials and processes of manufacture must correspond to the relevant codes.

On the top of transition zones, 9.0 m long transition slabs are made of concrete C25/30 – XC3, connected to the top of closing walls of abutments by hinges.

The back side of abutments should be covered by a waterproofing and a water drainage layer. A drainage pipe of a diameter of 150 mm is located at the bottom of the transition zone to drain water away.

5. Construction of the bridge

Construction of the bridge should be made by the following steps.

- Removal of topsoil, relocation of technical networks
- Manufacture of bored piles
- Excavations
- Construction of bridge supports (substructure)
- Installation of the movable scaffolding system
- Manufacture of the superstructure – in the following steps
- Transport of MSS (movable scaffolding system) to the next span, preparation of formwork, reinforcement, casting and prestressing of the superstructure and grouting of the ducts – when the sufficient concrete strength is reached (assumed after 7 days) – in following stages
    - span 1 with a cantilevered overlap to span 2
    - rest of the span 2, cantilevered overlap to span 3
    - rest of the span 3, cantilevered overlap to span 4
    - rest of the span 4, cantilevered overlap to span 5
    - rest of the span 5, cantilevered overlap to span 6
    - rest of the span 6

  Note: During construction of the superstructure, longitudinal horizontal forces will be temporarily taken by the abutment A1. After finish of the whole superstructure, fixed points will be transferred to piers P2, P3 and P4.

- Insulation of the substructure
- Backfilling of transition areas
- Waterproofing layer on the deck
- Reinforcement and casting of cornices
- Manufacture of pavement layers
- Installation of railings and barriers
- Finishing works

A more detailed description of individual construction stages related to the casting and prestressing of the structure is presented in the structural analysis.

CZECH TECHNICAL UNIVERSITY IN PRAGUE

Faculty of Civil Engineering

Department of Concrete and Masonry Structures

Design of a prestressed concrete road viaduct close to Lisbon

Part B
Structural analysis

Structural analysis

1. Structure

1.1. Empirical formulas for structural design

1.1.1. Superstructure

The shape of the superstructure is designed as a double-beam. The individual dimensions are based on the following relationships. The total width of the structure is divided into distances *a* and *b*, which define the axes of the main beams.

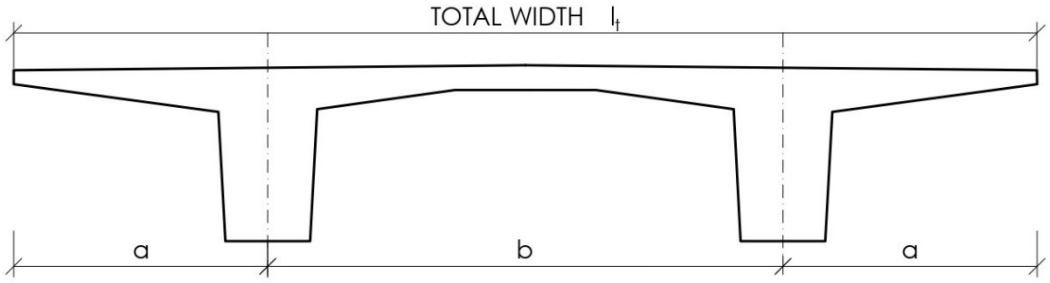

Figure 9: Scheme for empirical design

The distances *a* and *b* must be such that no torsional force is exerted in the marked sections due to load *p*. This means that the bending moments at the points adjacent to the beams must be identical.

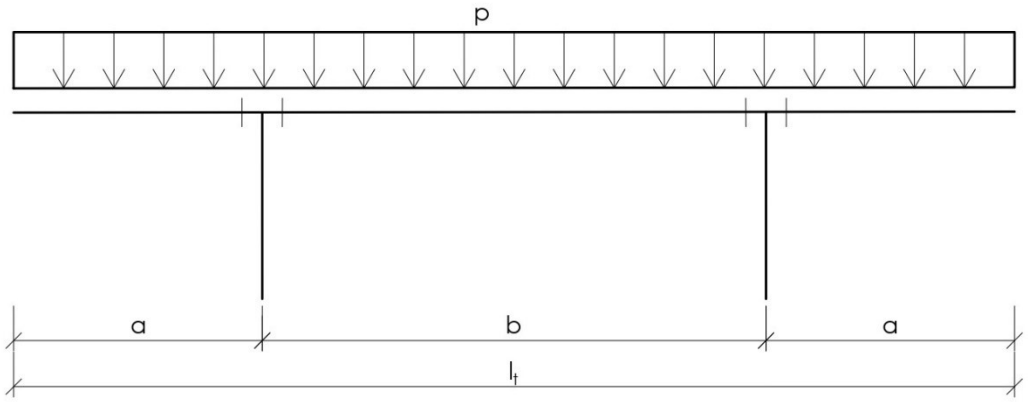

Figure 10: Scheme for dimensioning of the double-beam

From the balance of bending moments, the following relations then result:

$$a = 0.41\, b$$

$$b = 0.55\, l_t$$

Lateral cantilevers have a variable thickness with a minimum 200 mm at the edges of the structure.

The slab between the main beams should be at least 250 mm thick. For the distance *b*> 5 m, haunches with length of 0.3 *b* at each side should be used in the uppermost area. The thickness of the slab next to the beams should be approximately *a*/8, in the middle of the cross section it should be approximately *b*/25.

The depth of the cross section should be between 1/16 and 1/18 of the span length.

Using the previous recommendations, the shape of the cross-section was designed.

1.1.2. Substructure

The initial design of the cross section of the piers was developed based on the following parameters:

- The first parameter considers the stress from a constant load of approximately 4 MPa,
- According to the second recommendation, the slenderness of the piers should be less than or equal to 70,
- Dimensions of the top of supports as well as dimensions of the lower surface of the superstructure (the main beams in this case) must enable a placement of bridge bearings. In some cases, also a space for hydraulic jacks needed for lifting the superstructure for repairs or replacement of bearings is required,
- Using such criteria, the required cross-sectional area *A* and a moment of inertia *I* could be determined. These two characteristics were the basis for designing the exact shape of the cross section of piers.

$$\sigma = \frac{N}{A} \cong 4\ MPa$$

$$A = \frac{N}{4000}$$

$$\lambda = \frac{l_0}{i} \leq 70$$

$$l_0 = \eta \cdot l$$

$$\frac{\eta \cdot l}{\sqrt{\frac{I}{A}}} = 70$$

$$I = \frac{\eta^2 \cdot l^2 \cdot A}{70^2}$$

1.2. Scheme of the structure for structural analysis

Details of the structure are shown in the attached drawings. For the structural analysis, the shape of the structure (cross section as well as longitudinal section) was slightly simplified according to Figure 11.

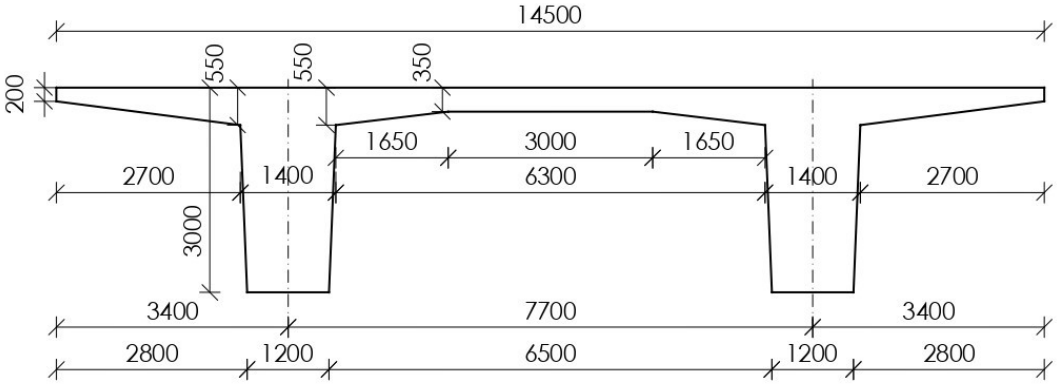

Figure 11: Cross section simplified for the structural analysis

1.3. Calculation model

For calculation of internal forces, a 3D calculation combined model (using shell as well as bar elements) in the SCIA Engineer software was used. The superstructure was modelled as a variable thickness slab with ribs for the beams, the supports are modelled as bars.

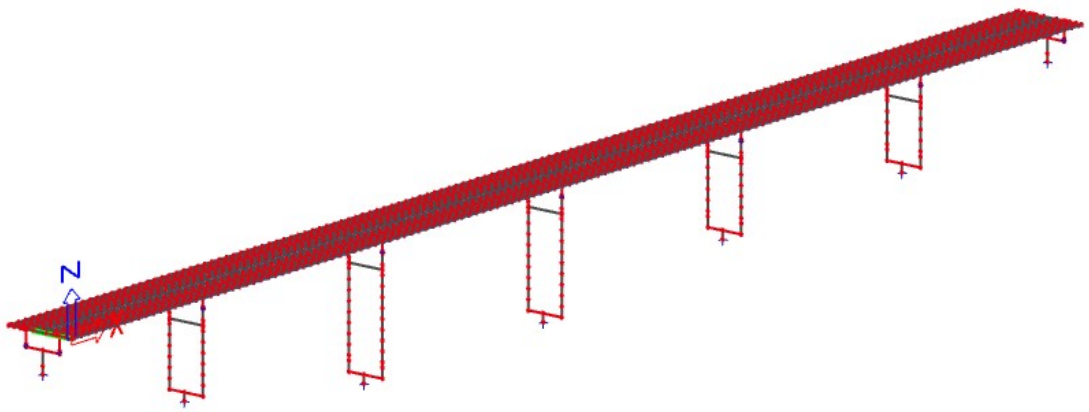

Figure 12: 3D model

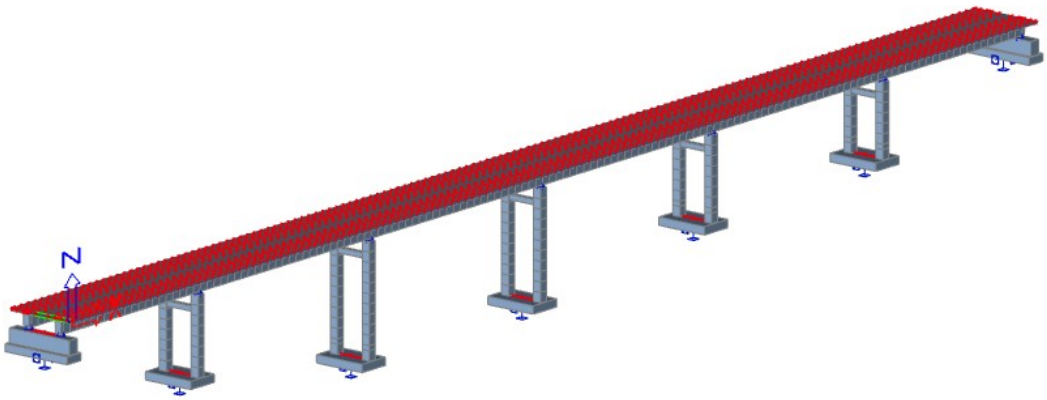

Figure 13: Rendered 3D model

Moreover, a 2D planar model was created for time-dependent analysis (TDA) in the SCIA Engineer software as well. These calculations reflect construction stages, prestressing and time-dependent effects such as creep and shrinkage of concrete and relaxation of prestressing steel.

For the planar model it was necessary to define individual construction stages and their schedule, which can be found in Table 1. A graphical representation of construction steps is shown in the following figures.

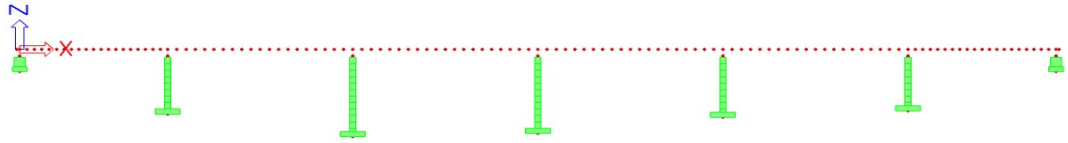

Figure 14: Casting the substructure

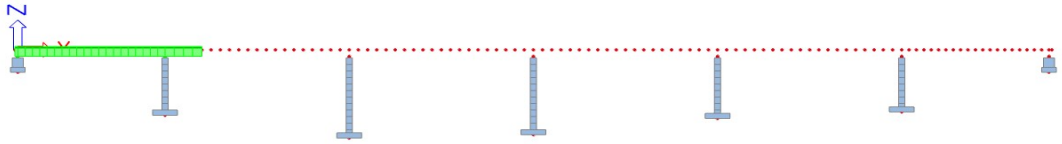

Figure 15: Casting the span 1

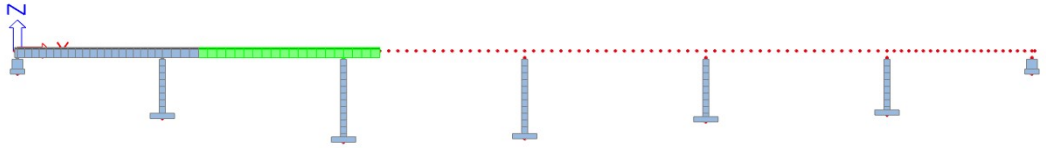

Figure 16: Casting the span 2

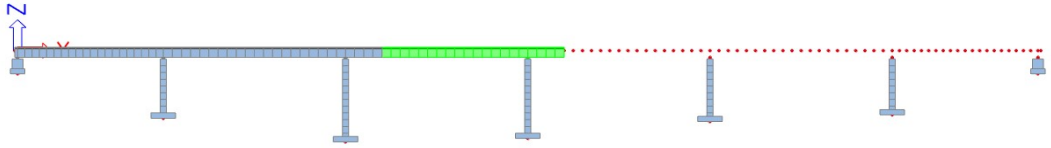

Figure 17: Casting the span 3

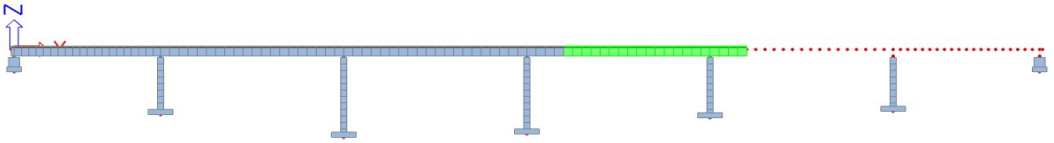

Figure 18: Casting the span 4

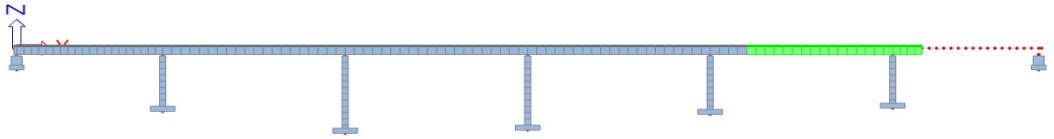

Figure 19: Casting the span 5

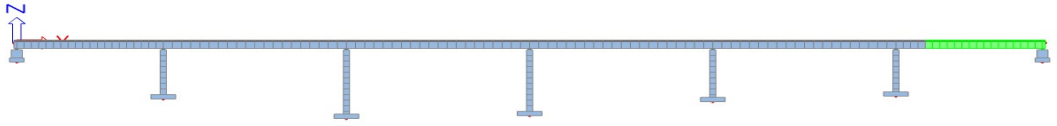

Figure 20: Casting the span 6

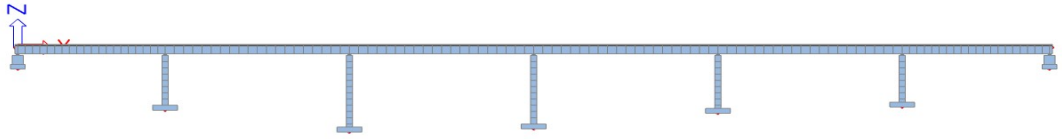

Figure 21: Completed structure

Table 1: Construction stages

Construction stages	
Stage	Age (days)
Casting the span 1	0
Prestressing the structure - span 1	30
Casting the span 2	31
Prestressing the structure - span 2	51
Casting the span 3	52
Prestressing the structure - span 3	72
Casting the span 4	73
Prestressing the structure - span 4	93
Casting the span 5	94
Prestressing the structure - span 5	114
Casting the span 6	115
Prestressing the structure - span 6	135
Application of self-weight of equipment	136
Beginning of service	225
3 years	315
5 years	1095
10 years	1825
20 years	3650
50 years	7300
70 years	18250
End of service life - age of 100 years	25550
Casting the span 1	36500

Note: The end time of the casting is set as negative -6 days, which means that the casting is completed 6 days before the end of the "Casting the span" stage.

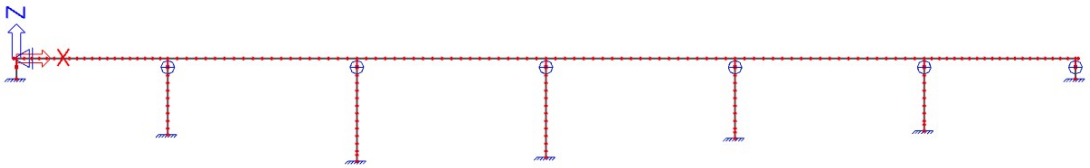

Figure 22: Bar 2D model

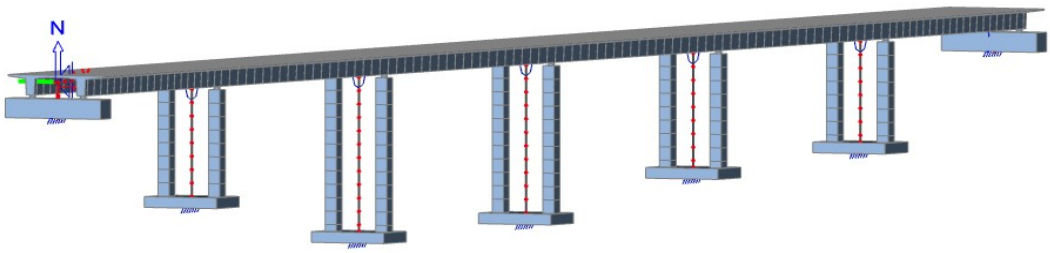

Figure 23: Rendered 2D model

To calculate the effects of short-term loads during construction, individual models were created for each stage separately. Figure 1Figure 24 shows the model for the first stage of construction. The models for the other stages are developed in a similar way.

Figure 24: Model for short-term loads during construction – stage 1

1.4. Characteristics of a cross section

The cross-sectional characteristics were determined using AutoCAD.

Area	A = 12.470 m^2
Overall depth of the cross section	h = 3.000 m
Height of neutral axis	z_c = 2.001 m
Moment of inertia	I_y = 10.513 m^4
Section modulus – upper fibers	W_t = 10.513 / (3.000 – 2.001) = = 10.524 m^3
Section modulus – lower fibers	W_b = 10.513/ 2.001 = 5.254 m^3

1.5. Effective width of flanges

Shear lag should also be included in the structural model, due to which normal stresses are not uniformly distributed over the width of the cross section, but the maximum stress is at the beam location, and it is decreased towards the edges of the structure. To express this effect, the effective width of flanges needs to be defined.

$$b_{eff} = \sum b_{eff,i} + b_w \leq b$$

$$b_{eff,i} = 0.2\, b_i + 0.1 l_0 \leq 0.2 l_0$$

$$b_{eff,i} \leq b_i$$

In this case:

The middle of 40 m span:

$$l_0 = 0.7 \cdot l = 0.7 \cdot 40.0 = 28.0\, m$$

$$b_{eff,1} = 0.2 \cdot 2.700 + 0.1 \cdot 28.0 = 3.340\, m \leq 0.2 \cdot 28.0 = 5.6\, m$$

$$b_{eff,2} = 0.2 \cdot 3.150 + 0.1 \cdot 28.0 = 3.430\, m \leq 0.2 \cdot 28 = 5.6\, m$$

$$b_{eff} = 3.340 + 3.430 + 1.400 = 8.170\, m$$

The entire cross section is contributing to the stress distribution.

The middle of 50 m span:

$$l_0 = 0.7 \cdot l = 0.7 \cdot 50.0 = 35.0\ m$$

$$b_{eff,1} = 0.2 \cdot 2.700 + 0.1 \cdot 35.0 = 4.040\ m \leq 0.2 \cdot 35.0 = 7.0\ m$$

$$b_{eff,2} = 0.2 \cdot 3.150 + 0.1 \cdot 35.0 = 4.130\ m \leq 0.2 \cdot 35 = 7.0\ m$$

$$b_{eff} = 4.040 + 4.130 + 1.400 = 9.570\ m$$

The entire cross section is contributing to the stress distribution.

Above the supports P1 and P5:

$$l_0 = 0.15 \cdot (l_1 + l_2) = 0.15 \cdot (40 + 50) = 13.5\ m$$

$$b_{eff,1} = 0.2 \cdot 2.700 + 0.1 \cdot 13.5 = 1.890\ m \leq 0.2 \cdot 13.5 = 2.7\ m$$

$$b_{eff,2} = 0.2 \cdot 3.150 + 0.1 \cdot 13.5 = 1.980\ m \leq 0.2 \cdot 13.5 = 2.7\ m$$

$$b_{eff} = 1.890 + 1.980 + 1.400 = 5.270\ m < 7.250\ m$$

Flange width should be reduced.

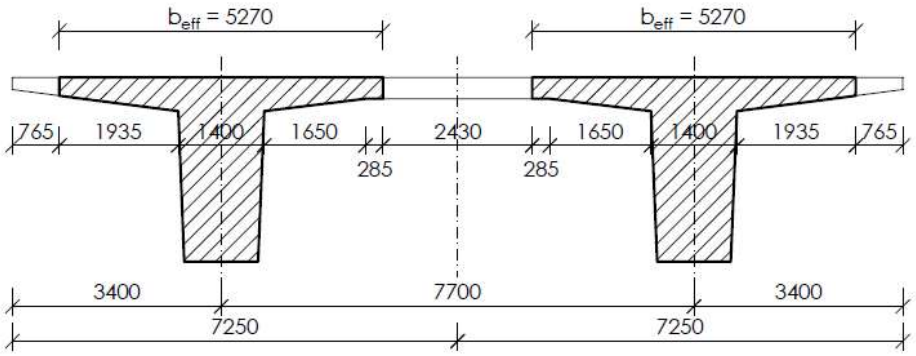

Figure 25: Effective cross section above the piers P1 and P5

For calculation purposes, the cross section was reduced in this way to decrease the moment of inertia. However, to maintain the cross-sectional area, narrow strips were added to the centre of gravity to replace the missing area, but not to change the moment of inertia.

Other spans:

$$l_0 = 0.15 \cdot l_2 + l_3 = 0.15 \cdot 50 + 50 = 57.5\ m$$

$$b_{eff,1} = 0.2 \cdot 2.700 + 0.1 \cdot 57.5 = 6.290\ m \leq 0.2 \cdot 57.5 = 11.5\ m$$

$$b_{eff,2} = 0.2 \cdot 3.150 + 0.1 \cdot 57.5 = 6.380\ m \leq 0.2 \cdot 57.5 = 11.5\ m$$

$$b_{eff} = 6.290 + 6.380 + 1.400 = 14.070\ m$$

The entire cross section is contributing to the stress distribution.

2. Materials

2.1. Concrete

The superstructure is made of concrete C40/50 – XS1, XD1, XC4. The mechanical characteristics for this strength class are as below:

- Characteristic compressive cylinder strength of concrete at 28 days
  f_{ck} = 40.0 MPa
- Mean value of concrete cylinder compressive strength
  f_{cm} = 48.0 MPa
- Design value of concrete compressive strength
  $f_{cd} = \alpha_{cc} \times f_{ck} / \gamma_c = 1.0 \times 40 / 1{,}5 = 26.67$ MPa

  Partial safety factor for concrete $\gamma_c = 1.5$ (persistent and transient design situations)

  Coefficient taking account long-term effects on the compressive strength and unfavourable effects resulting from the way the load is applied $\alpha_{cc} = 1.0$
- Mean characteristic value of axial tensile strength of concrete
  f_{ctm} = 3.5 MPa
- Upper characteristic value of axial tensile strength of concrete
  $f_{ctk,\,0,95}$ = 4.6 MPa
- Lower value of axial tensile strength of concrete
  $f_{ctk,\,0,05}$ = 2.5 MPa
- Secant modulus of elasticity of concrete
  E_{cm} = 35.0 MPa
- Tangent modulus of elasticity - normal weight concrete at 28 days
  $E_c = 1.05 \times E_{cm} = 1.05 \times 35.0 = 36.750$ MPa
- Ultimate compressive strain in concrete
  ε_{cu2} = 3.5 ‰
- Compressive strain in concrete at the peak stress f_c
  ε_{c2} = 2.0 ‰
- Poisson's ratio
  $v = 0.2$
- Linear coefficient of thermal expansion
  $\alpha = 10 \times 10^{-6}\ K^{-1}$
- Characteristic compressive cylinder strength of concrete at the age of the application of the prestressing (t = 7 days)
  $f_{ck}(t) = f_{cm}(t) - 8$ MPa
  $f_{cm}(t) = \beta_{cc}(t) \times f_{cm}$

  where: f_{cm} is the mean compressive strength at 28 days

f_{cm} (t) is the mean compressive strength at the age of t days

$$\beta_{cc}(t) = \exp\left\{s\left[1 - \sqrt{\frac{28}{t}}\right]\right\}$$

where: β_{cc} (t) is a coefficient which depends on the age of the concrete t

$$\beta_{cc}(t = 7) = \exp\left\{0{,}20\left[1 - \sqrt{\frac{28}{7}}\right]\right\} = 0.819$$

f_{cm} (t=7) = β_{cc} (t=7) x f_{cm} = 0.819 x 48 = 39.312 MPa
f_{ck} (t=7) = f_{cm} (t=7) − 8 MPa = 39.312 − 8 = 31.312 MPa

- Value of axial tensile strength of concrete at the age of the application of the prestressing (t = 7 days)
  f_{ctm} (t) = (β_{cc} (t))$^{\alpha}$ x f_{ctm} = 0.819^{1} x 3.5 = 2.867 MPa

2.2. Prestressing reinforcement

The prestressing reinforcement consists of tendons composed of strands of a diameter of 15.7 mm. The strands are made of Y1860S7 prestressing steel, and their mechanical characteristics are described below.

- Characteristic tensile strength of prestressing steel
  f_{pk} = 1860.0 MPa
- Characteristic 0,1 % proof-stress of prestressing steel
  $f_{p0,1k}$ = 0.88 x f_{pk} = 0.88 x 1860.0 = 1638.8 MPa
- Design tensile stress of prestressing steel
  f_{pd} = $f_{p0,1k}$ / γ_s = 1638.8 / 1.15 = 1423.304 MPa
- Partial factor for prestressing steel (persistent and transient design situations)
  γ_s = 1.15
- Design value of modulus of elasticity of prestressing steel
  E_p = 195.0 GPa
- Cross sectional area of a prestressing strand
  A_{p1} = 150 mm^2

In terms of classifying prestressing reinforcement into a class indicating relaxation behaviour, the prestressing reinforcement is categorised as class 2: wires or strands of low relaxation. Plastic ducts of a diameter of 120 mm are used for prestressing tendons.

2.3. Reinforcing steel

Steel B500B is used for passive reinforcement. It has the following properties:

- Characteristic yield strength of reinforcement
  f_{yk} = 500.0 MPa
- Design yield strength of reinforcement
  $f_{yd} = f_{yk} / \gamma_s = 500 / 1.15 = 434.783$ MPa

  Partial factor for reinforcing (persistent and transient design situations) $\gamma_s = 1.15$
- Design value of modulus elasticity of reinforcing steel
  E_s = 200.0 GPa

3. Actions

3.1. Permanent loads

3.1.1. Self-weight of the superstructure g_0

The self-weight of the superstructure was automatically calculated by SCIA Engineer. The volume weight of the prestressed concrete was considered to be 26 kN/m^3, of which 24 kN/m^3 is a normal weight concrete, 1 kN/m^3 passive reinforcement and 1 kN/m^3 prestressing reinforcement.

3.1.2. Self-weight of bridge equipment ($g - g_0$)

Reinforced concrete cornices

Average thickness above the superstructure		0.139 m
Area of the cornice next to the superstructure		0.046 m^2
Surface load over the superstructure	25 x 0.139 =	3.475 kN/m^2
Linear load along the edge of the superstructure	25 x 0.046 =	1.150 kN/m

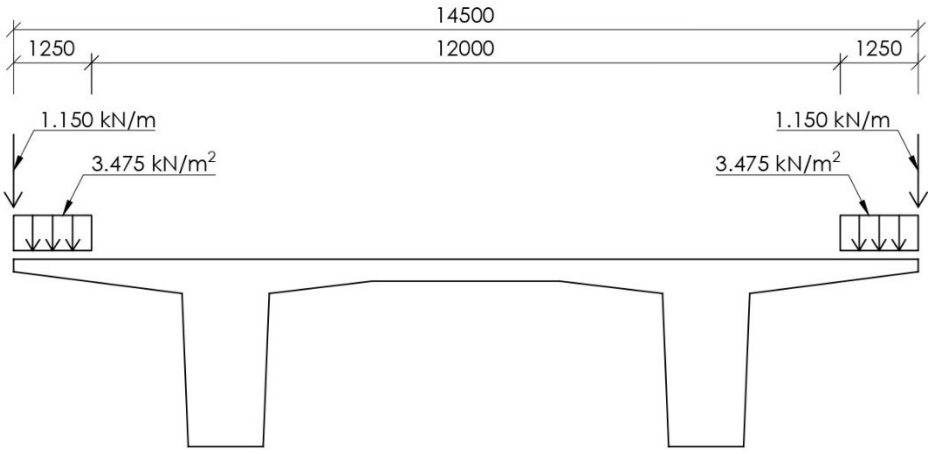

Figure 26: Self-weight of cornices

Handrails

The load of the handrails is assumed as a linear load along the edge of the structure equal to 0.500 kN/m.

Barriers

The weight of the steel barriers is distributed over the width of the cornice. The value of the linear load of the barriers applied to the superstructure is 1.000 kN/m.

Surface load per cornice width 1.000/1.250 = 0.800 kN/m^2

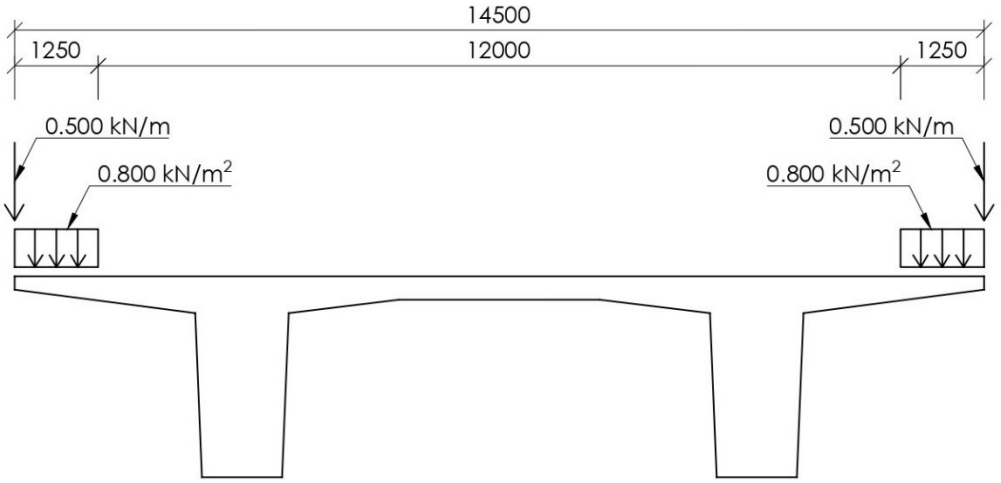

Figure 27: Self-weight of handrails and barriers

Pavement layers

The thickness of the pavement layers is 60 mm. A density of concrete asphalt equal to 25 kN/m^3 was taken into account.

Concrete asphalt 25 x 0.060 = 1.500 kN/m^2

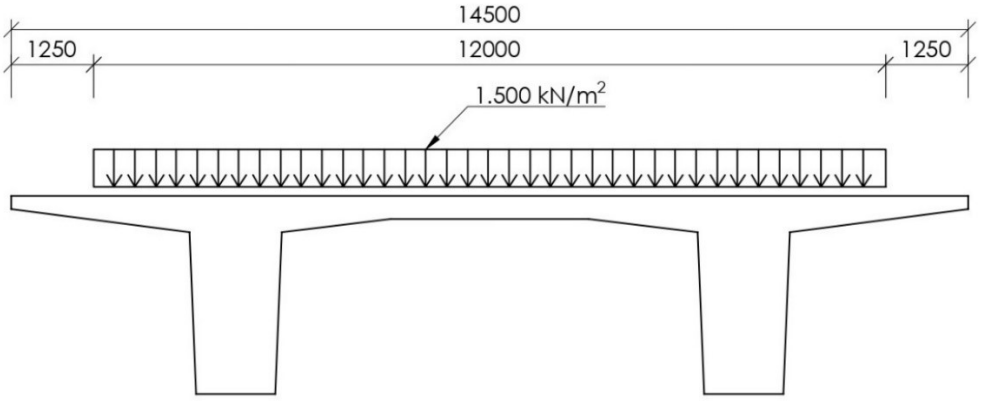

Figure 28: Self-weight of pavement layers

3.1.2.1. Mean value

Linear load along the edge of the superstructure

Handrail	1 x 0.500 =	0.500 kN/m
Weight of the cornice	1 x 25 x 0.046 =	1.150 kN/m
	Total	1.650 kN/m

Surface load at the cornice area

Weight of the cornice	1 x 25 x 0.139 =	3.475 kN/m^2
Barriers	1 x 0.800 =	0.800 kN/m^2
	Total	4.275 kN/m2

Pavement

Concrete asphalt	1 x 25 x 0.060 =	1.500 kN/m^2

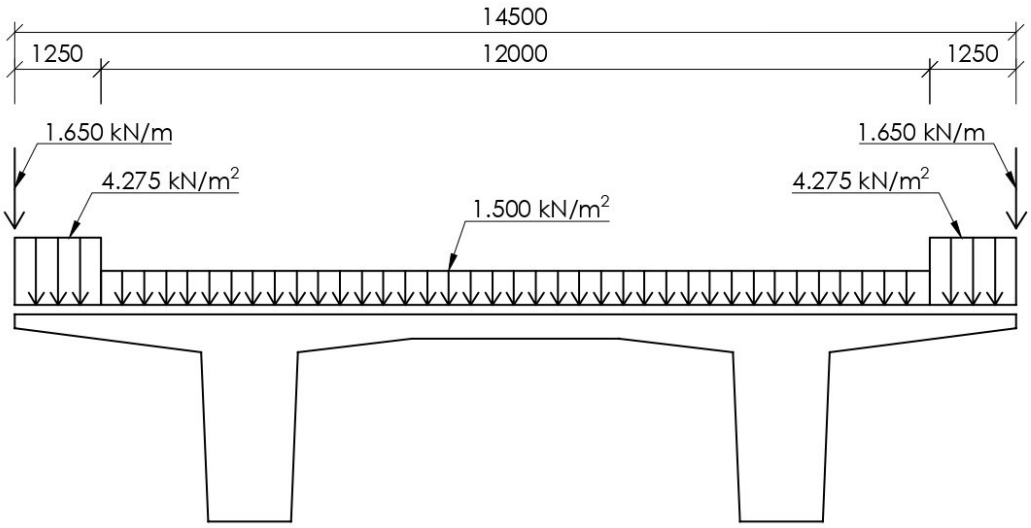

Figure 29: Self-weight of bridge equipment: mean value

Conversion to linear load (2D model)

Linear load along the superstructure

Handrail	2 x 0.500 =	1.000 kN/m
Weight of the cornice	2 x 25 x 0.046 =	2.300 kN/m
	Total	3.300 kN/m

Surface load at the cornice area

Weight of the cornice	2 x 25 x 0.139 x 1.250 =	8.688 kN/m
Barriers	2 x 0.800 x 1.250 =	2.000 kN/m
	Total	10.688 kN/m

Pavement

Concrete asphalt	1 x 25 x 0.060 x 12.0 =	18.000 kN/m
Total mean value $(g-g_0)_m$ =	3.300+10.688+18.000 =	31.988 kN/m

3.1.2.2. Upper characteristic value

This value differs from the mean value by using a k_{sup} factor equal to 1.4, which is used to multiply the load of the pavement (and waterproofing) layers.

Linear load along the edge of the superstructure

Handrail	1 x 0.500 =	0.500 kN/m
Weight of the cornice	1 x 25 x 0.046 =	1.150 kN/m
	Total	1.650 kN/m

Surface load at the cornice area

Weight of the cornice	1 x 25 x 0.139 =	3.475 kN/m^2
Barriers	1 x 0.800 =	0.800 kN/m^2
	Total	4.275 kN/m^2

Pavement

Concrete asphalt	1,4 x 25 x 0,060 =	2.100 kN/m^2

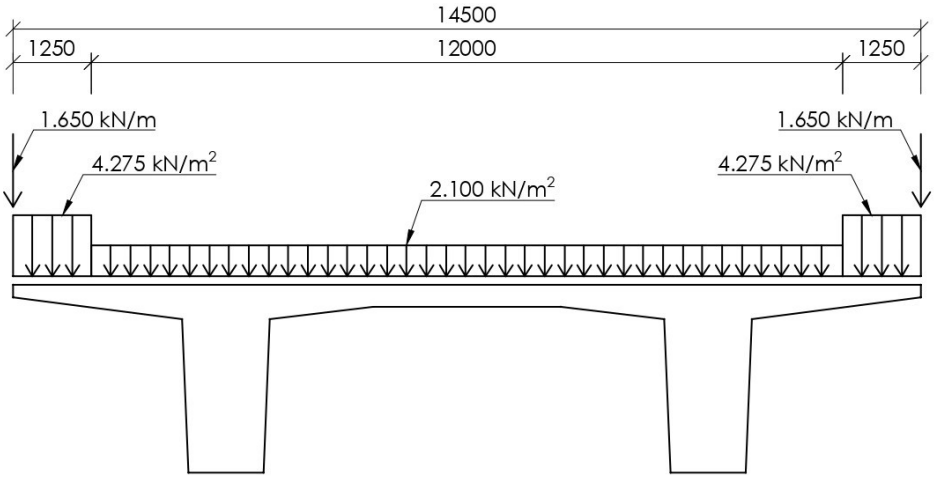

Figure 30: Self-weight of bridge equipment: Upper characteristic value

3.1.2.3. Lower characteristic value

This value differs from the mean value by using a k_{inf} factor equal to 0.8, which is used to multiply the load of the pavement (and waterproofing) layers.

Linear load along the edge of the superstructure

Handrail	1 x 0.500 =	0.500 kN/m
Weight of the cornice	1 x 25 x 0.046 =	1.150 kN/m
	Total	1.650 kN/m

Surface load at the cornice area

Weight of the cornice	1 x 25 x 0.139 =	3.475 kN/m^2
Barriers	1 x 0.800 =	0.800 kN/m^2
	Total	4.275 kN/m^2

Pavement

Concrete asphalt	0.8 x 25 x 0.060 =	1.200 kN/m^2

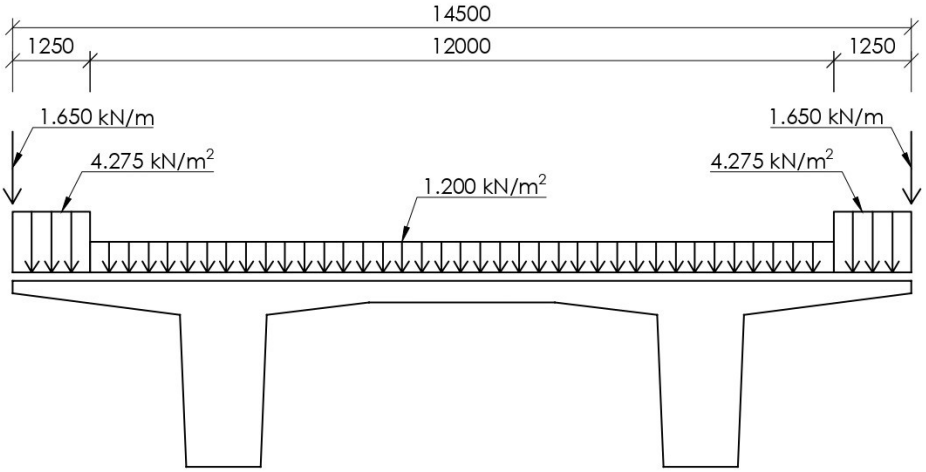

Figure 31: Self-weight of bridge equipment: lower characteristic value

3.1.3. Uneven settlements of supports

Another loading cases are used for uneven settlements of supports. Settlements of each support are considered separately in the calculations; these settlements are equal to 5 mm.

3.2. Variable loads

3.2.1. Traffic loads

The total carriageway width of 12.0 m is divided into three 3.0 m wide notional lanes and the remaining area which is also 3.0 m wide.

3.2.1.1. Load Model 1 – LM1

3.2.1.1.1. Axle forces – tandem system (TS)

The first part of the Load Model 1 is a pair of two local forces, such that each pair is equal to Q_k x α_Q. In this case, the distribution of these forces over a contact area of 0.4 x 0.4 m was assumed. Furthermore, the dispersion of axle forces into the bridge deck centreline at an angle of 45° was considered. The centreline of the smallest slab thickness 350 mm was used as the centreline of the slab. Therefore, the forces are spread out over the area $(400 + 2 \times (60 + 350/2))^2 = 870^2 =$ $= 756900\ mm^2 = 0.757\ m^2$.

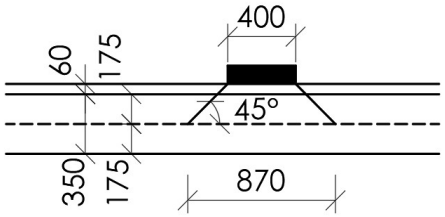

Figure 32: Dispersion of axle forces of LM1 TS

In Portugal, two classes of bridges are distinguished to select the parameters α_Q and α_q. Class I includes road bridges where a major part of the traffic is expected to be an international heavy traffic and vehicles. Road bridges with more normal traffic characteristics belong to the Class II. The viaduct V1 is intended to be a Class II.

The values of the forces Q_k, the adjustment factor α_Q and the load distributed to the level of the centreline can be seen in Table 2.

Table 2: Load Model 1 – tandem system – characteristic values of action

	Axle forces		Total value of axle forces	Load distributed over the area of each wheel
	Q_k	α_Q	$Q_k \times \alpha_Q$	$Q_k \times \alpha_Q / 2 \times 0.87^2$
Lane 1	300 kN	0.9	270 kN	178.4 kN/m^2
Lane 2	200 kN	0.8	160 kN	105.7 kN/m^2
Lane 3	100 kN	0.8	80 kN	52.8 kN/m^2
Remaining area	0 kN	-	0 kN	0 kN/m^2

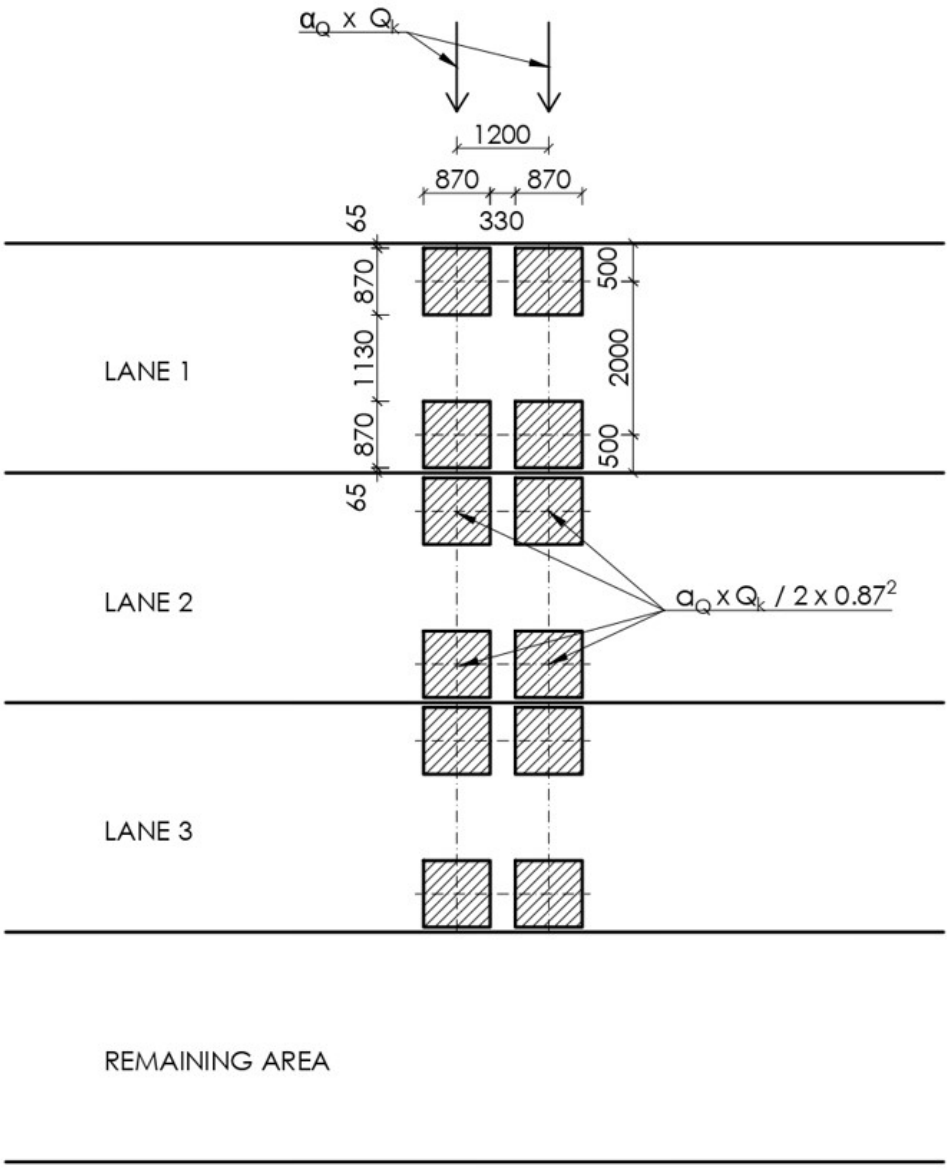

Figure 33: Scheme of the Load Model 1 – tandem system

3.2.1.1.2. Uniformly distributed load (UDL)

The second part of Load Model 1 is uniformly distributed load, in this case the individual notional lanes are loaded by values shown in Table 3.

For this type of load, the even and odd spans were loaded, then always two spans loaded or unloaded side by side and the remaining spans were loaded in checkerboard order. All maximum effects were obtained by these load cases.

Table 3: Load Model 1 – uniformly distributed load – characteristic values of action:

	q_k	α_q	$q_k \times \alpha_q$
Lane 1	9.0 kN/m^2	0.7	6.3 kN
Lane 2	2.5 kN/m^2	1.0	2.5 kN
Lane 3	2.5 kN/m^2	1.0	2.5 kN
Remaining area	2.5 kN/m^2	1.0	2.5 kN

3.2.1.2. Load Model 3 – LM3

Special vehicle 1200/150 was applied for the Load Model 3.

The special vehicle under consideration is a 1200/150 vehicle, i.e., an eight-axle vehicle with an axle load of 150 kN. This vehicle is positioned in the notional lane 1; for this loading case, the carriageway is defined without emergency lanes, shoulders, and guide strips for the load distribution.

Uniformly distributed load according to Load Model 1 (LM1 UDL) is placed in the other lanes (lane 2 and the others) at the same time as the special vehicle. All other traffic is excluded.

Also, the dispersion of axle forces into the bridge deck centreline at an angle of 45° was considered by the same way as in the Load Model 1 (LM1 TS).

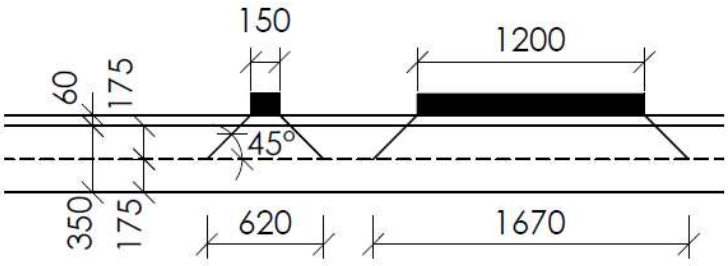

Figure 34: Dispersion of axle forces of LM3

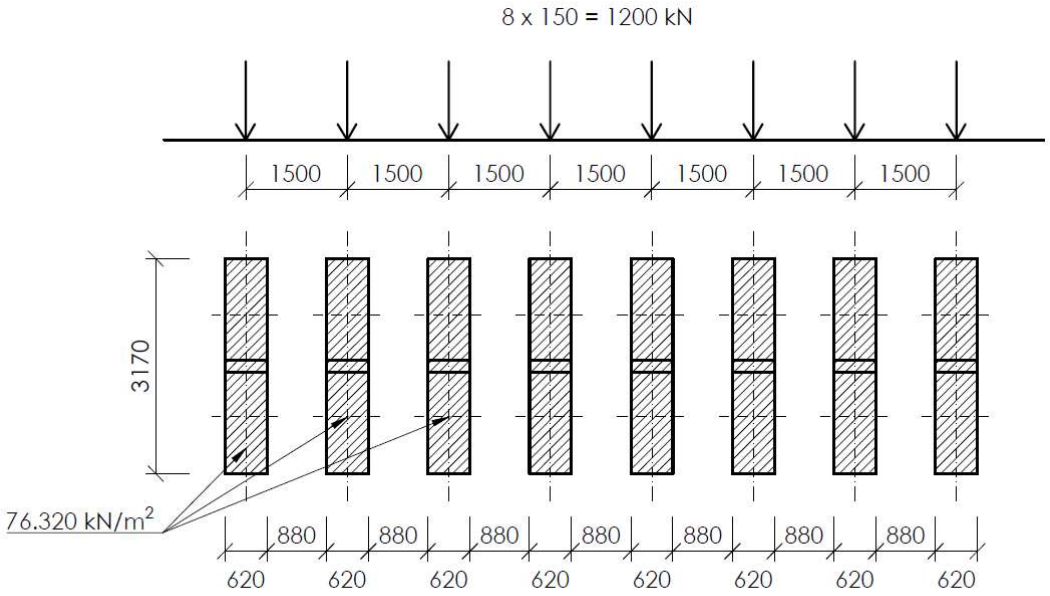

Figure 35: Scheme of the Load Model 3 – special vehicle 1200/150

Load distributed over the area of one axle is 150 / (3.170 x 0.620) = 76.320 kN/m^2.

3.2.1.3. Load Model 4 – LM4

Load Model 4 caused by a crowd of people is considered as uniformly distributed load of 5 kN/m^2. This load is applied over the whole width of the deck between outer handrails. The maximum effects were obtained by loading conditions identical to the uniformly distributed load of the Load Model 1.

3.2.1.4. Action of footways

Uniformly distributed load of 5 kN/m^2 is assumed on footways.

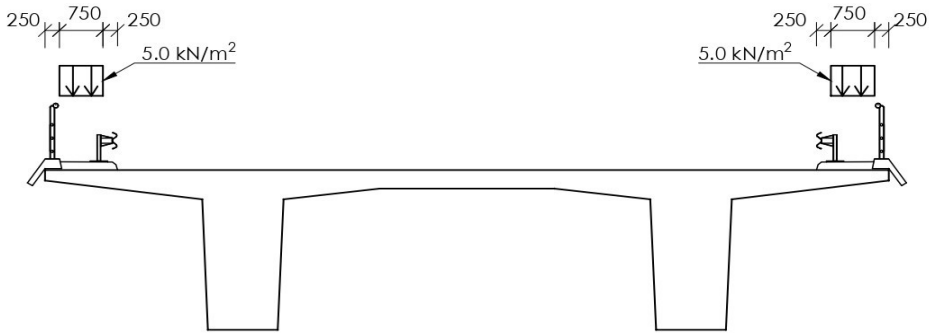

Figure 36: Action of footways

3.2.2. Horizontal forces

Braking and acceleration forces were also included in the calculation.

Braking force Q_{lk} is a longitudinal force, and it is acting at the level of the running surface of the carriageway. The value of Q_{lk} is calculated of the maximum vertical load of the Load Model 1 and it is limited by 900 kN

$$Q_{lk} = 0.6\ \alpha_{Q1}\ (2Q_{1k}) + 0.10\ \alpha_{q1}\ q_{1k}\ w_1\ L$$

$$150\ \alpha_{Q1}\ (kN) \leq Q_{1k} \leq 900\ (kN)$$

In this case:

$$Q_{lk} = 0.6 \times 0.9 \times 2 \times 300 + 0.1 \times 0.7 \times 9.0 \times 3 \times 280 = 853.2\ kN \leq 900\ kN$$

Acceleration forces are taken into account with the exact value as the braking forces, but in the reverse direction.

Moreover, the transverse braking forces are included in the model as 25 % of the longitudinal braking forces.

$$Q_{xk} = 0.25 \times Q_{lk} = 0.25 \times 853.2 = 213.3\ kN$$

These point forces were distributed over the wheel area in much by the same way as for the vertical load in Load Model 1.

Table 4: Horizontal forces overview

	Longitudinal direction				Transverse direction	
	Braking force	Number of wheels	Force per one wheel	Load distributed over the area of each wheel	Braking force	Load distributed over the area of each wheel
	Q_{lk}	n	Q_{lk} / n	Q_{lk} / n / 0.87^2	Q_{xk} = 0.25 x Q_{lk}	Q_{xk} / 0.87^2
Lane 1	853.2 kN	12	71.1 kN	93.9 kN/m^2	5.9 kN	7.8 kN/m^2
Lane 2	853.2 kN		71.1 kN	93.9 kN/m^2	5.9 kN	7.8 kN/m^2
Lane 3	853.2 kN		71.1 kN	93.9 kN/m^2	5.9 kN	7.8 kN/m^2
Remaining area	0 kN	-	0 kN	93.9 kN/m^2	5.9 kN	7.8 kN/m^2

3.2.3. Thermal actions

3.2.3.1. Uniform temperature component

The uniform temperature change component depends on the maximum shade air temperature T_{max} and the minimum shade air temperature T_{min}, which are defined on the basis of location. The Caparica area is classified in the standard as Zone B, where these temperatures are as follows:

Shade air temperature T_{max} = 40 °C
T_{min} = 0 °C

In the case of concrete bridge structures and for the climatic conditions of Portugal, the values of the maximum uniform temperature component of the structure $T_{e,max}$ and of the minimum uniform temperature component of the structure $T_{e,min}$ can be considered equal to T_{max} and T_{min}.

Uniform bridge temperature component of the structure:

$T_{e,max} = T_{max}$ = 40 °C
$T_{e,min} = T_{min}$ = 0 °C

The value of the initial temperature of the structure at the time of its completion was set as 15 °C, which is used in Portugal when no more detailed temperature data is available for the area.

Initial temperature T_0 = 15 °C

The range of uniform bridge temperature component was obtained from previous data. The structure is uniformly loaded by the maximum contraction range component and by the maximum expansion range of the uniform bridge temperature component. The values of these temperatures are:

Maximum expansion range of the uniform bridge temperature component

$$\Delta T_{N,exp} = T_{e,max} - T_0 = 40 - 15 = 25\ °C$$

Maximum contraction range of the uniform bridge temperature component

$$\Delta T_{N,con} = T_0 - T_{e,min} = 0 - 15 = -15\ °C$$

3.2.3.2. Temperature difference component

The temperature difference component reflects the temperature differences between the upper and lower surface of the deck. For differential temperature loading, a linear temperature change along the height of the cross-section was considered

The effects of temperature differences are taken into account using an equivalent linear temperature difference components $\Delta T_{M,heat}$ and $\Delta T_{M,cool}$.

The component $\Delta T_{M,heat}$ is applied for heating by sunlight, that means that the top surface is warmer than the bottom one. On the contrary, $\Delta T_{M,cool}$ is assumed for cooling, which indicates that the bottom surface is warmer than the top.

Equivalent linear temperature difference components:

Top warmer than bottom $\Delta T_{M,heat} = 15\ °C$

Bottom warmer than top $\Delta T_{M,cool} = 5\ °C$

These values of an equivalent linear temperature difference components are based on the thickness of pavement layers of 50 mm. For other surface thicknesses, the temperature effects must be multiplied by the k_{sur} factor, the values (important for this case) of which are given in Table 5.

Table 5: Values of the factor k_{sur}

Surface thickness [mm]	k_{sur} top warmer than bottom	k_{sur} bottom warmer than top
unsurfaced	0.8	1.1
waterproofing bituminous sheets	1.5	1.0
50	1.0	1.0
100	0.7	1.0

Construction stages – completed structure with waterproofing bituminous sheets only

Top surface warmer $k_{sur} = 1.5$

Bottom surface warmer $k_{sur} = 1.1$

Completed bridge

Top surface warmer	$k_{sur} = 1.0 - (1.0 - 0.7) / 50 \times 60 = 0.84$
Bottom surface warmer	$k_{sur} = 1.0$

The individual effects of the uniform and differential temperature change do not have to be calculated as the full values in both cases, but a reduction using coefficients ω_N (for uniform temperature component) and ω_M (for temperature difference component) can be applied to obtain a the combination of actions.

Conditions depending on weather, the following combinations of actions should be considered.

$\Delta T_{M,heat} + \omega_N \Delta T_{N,exp}$
$\Delta T_{N,exp} + \omega_M \Delta T_{M,heat}$

$\Delta T_{M,cool} + \omega_N \Delta T_{N,con}$
$\Delta T_{N,con} + \omega_M \Delta T_{M,cool}$

The values of these reduction factors in Portugal are $\omega_N = 0.8$ and $\omega_M = 0.8$.

3.2.4. Wind load

The bridge site is classified as a terrain of the category II. Continental Portugal belongs to the zone B. The values for these categories are as follows.

Fundamental value of the basic wind velocity		$v_{b,0}$ 30 m/s
Roughness length	z_0	0.05 m
Minimum height	z_{min}	2.0 m
Air density	ρ	1.25 kg/m^3

Force coefficient for wind action on bridge deck in the x-direction

$$C_{f,x} = c_{fx,0}$$

Wind load factor

$$C = c_e \times c_{f,x}$$

$$C = c_e \times c_f$$

Basic wind velocity

$$v_b = c_{dir} \times c_{season} \times v_{b,0}$$

Wind force in the x-direction

$$F_w = 0.5 \times \rho \times v_b^2 \times C \times b_{ref}$$

Transverse direction (y direction)

Superstructure

Without traffic

Width in x direction		b 14.5 m
Depth in z direction	d_{tot}	3.0 m
	b/d_{tot}	4.83
Force coefficient	$c_{fx,0}$	1.3
Exposure factor	c_e	3.0
Wind load factor	C	3.9
Directional factor	c_{dir}	1.0
Season factor	c_{season}	1.0
Basic wind velocity	v_b	30 m/s

Wind force $F_w = 0.5 \times 1.25 \times 30^2 \times 3.9 \times 3.0 = 6.58$ kN/m

With traffic

Width in x direction	b	14.5 m
Depth in z direction	d_{tot}	5.0 m
	b/d_{tot}	2.90
Force coefficient	$c_{fx,0}$	1.63
Exposure factor	c_e	3.0
Wind load factor	C	4.89
Directional factor	c_{dir}	1.0
Season factor	c_{season}	1.0
Basic wind velocity	v_b	30 m/s

Wind force $F_w = 0.5 \times 1.25 \times 30^2 \times 4.89 \times 5.0 = 13.75$ kN/m

Pier

Height	l	23.0 m
Width	d	1.7 m
	b	1.7 m
	d/b	1.0
Force coefficient	$c_{fx,0}$	2.1
Effective slenderness	λ	12.60
Solidity ratio	φ	1.0
End-effect factor	ψ_λ	0.74
Reduction factor	ψ_r	1.0
Force coefficient	c_f	1.55
Exposure factor	c_e	3.0

Wind load factor	C	4.65
Directional factor	c_{dir}	1.0
Season factor	c_{season}	1.0
Basic wind velocity	v_b	30 m/s
Wind force	Fw = 0.5 x 1.25 x 302 x 4.65 x 1.7 = 4.44 kN/m	

Longitudinal direction (x direction)

In the longitudinal direction, a wind load of 25 % of the traverse wind force component was taken into account for the deck. Piers are exposed to the total value of the load in both directions.

Superstructure

Without traffic

Wind force	$F_{w,x}$ = 0.25 x 6.58 = 1.65 kN/m
Wind force for area of the deck	$f_{w,x}$ = 1.65/14.5 = 0.11 kN/m^2

With traffic

Wind force	$F_{w,x}$ = 0.25 x 13.75 = 3.44 kN/m
Wind force for area of the deck	$f_{w,x}$ = 3.44/14.5 = 0.24 kN/m^2

Piers

Wind force	$F_{w,x} = F_{w,y}$ = 0.5 x 1.25 x 302 x 4.65 x 1.7 = 4.44 kN/m

3.2.5. Construction load

During construction, a uniform load of q_{constr} = 1.0 kN/m^2 on the structure is considered. This load includes the weight of persons moving on the structure during construction, the weight of tools, etc.

3.3. Accidental actions

3.3.1. Seismic action

3.3.1.1. Types of seismic action

In Portugal, there are two scenarios of earthquake generation that may happen:

- a scenario called "away", generally referring to earthquakes with an epicenter in the Atlantic area, and which corresponds to the seismic action Type 1

- a scenario named "near", usually referring to earthquakes with an epicenter in the Continental territory

3.3.1.2. Parameters of seismic action

The first parameter needed for the analysis of earthquake load is the reference peak ground acceleration, which varies depending on the location. The reference peak ground acceleration values according to the two types of seismic action in Portugal are different.

For the type 1 of seismic action, the Caparica area belongs to zone 1.1, for which the reference acceleration is α_{gR} = 1.3 m/s^2.

In view of the second type of seismic action, the bridge site is located in the zone 2.3, for which the reference acceleration is equal to α_{gR} = 1.7 m/s^2.

The calculation also depends on the type of terrain (subsoil). In the case of the viaduct V1, the terrain type is classified as type A – solid rock.

3.3.1.3. Seismic load representation

The design value of the seismic load is expressed as a load with a return period probability of 475 years. The earthquake motion is given by the elastic response spectrum of the subsurface. The shape of the acceleration spectrum is the same for both horizontal directions, which are orthogonal and independent each of the other.

The parameters for the calculation of the elastic response spectrum are given in Table 6 depending on the terrain type and the reference peak acceleration.

Table 6: Elastic response spectrum parameters

Elastic response spectrum		
	Type 1	Type 2
Return period	475 years	475 years
Coefficient	1	1
a_{gr} =	1,5	1,7
a_g =	1,5	1,7
η =	1	1
S_{max} =	1	1
S =	1	1
TB =	0,1	0,1
TC =	0,6	0,25
TD =	2	2

To avoid non-linear calculations, the elastic response spectrum is reduced and is referred to as the design acceleration spectrum. This spectrum shall be input to the calculation. The parameters for the calculation of the design response spectrum are given in Table 7.

Table 7: Design response spectrum parameters

Design response spectrum		
	Type 1	Type 2
Return period	475 years	475 years
Coefficient	1	1
a_{gr} =	1,5	1,7
a_g =	1,5	1,7
η =	1	1
S_{max} =	1	1
S =	1	1
TB =	0,1	0,1
TC =	0,6	0,25
TD =	2	2
q =	2	2
β =	0,2	0,2

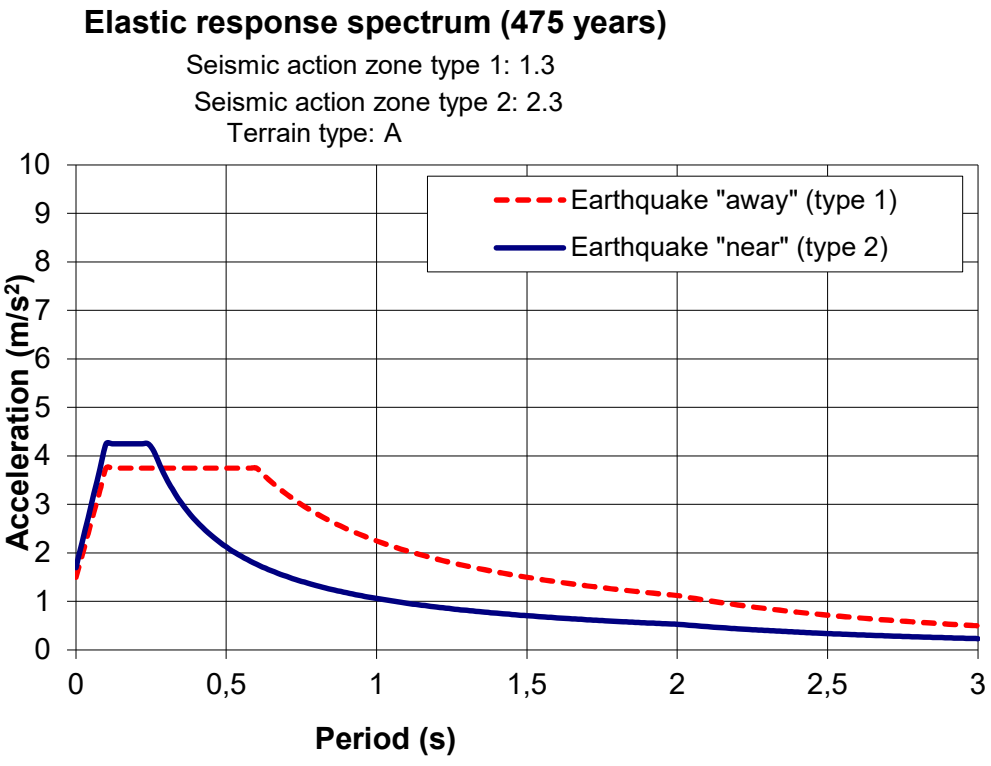

Figure 37: Elastic response spectrum

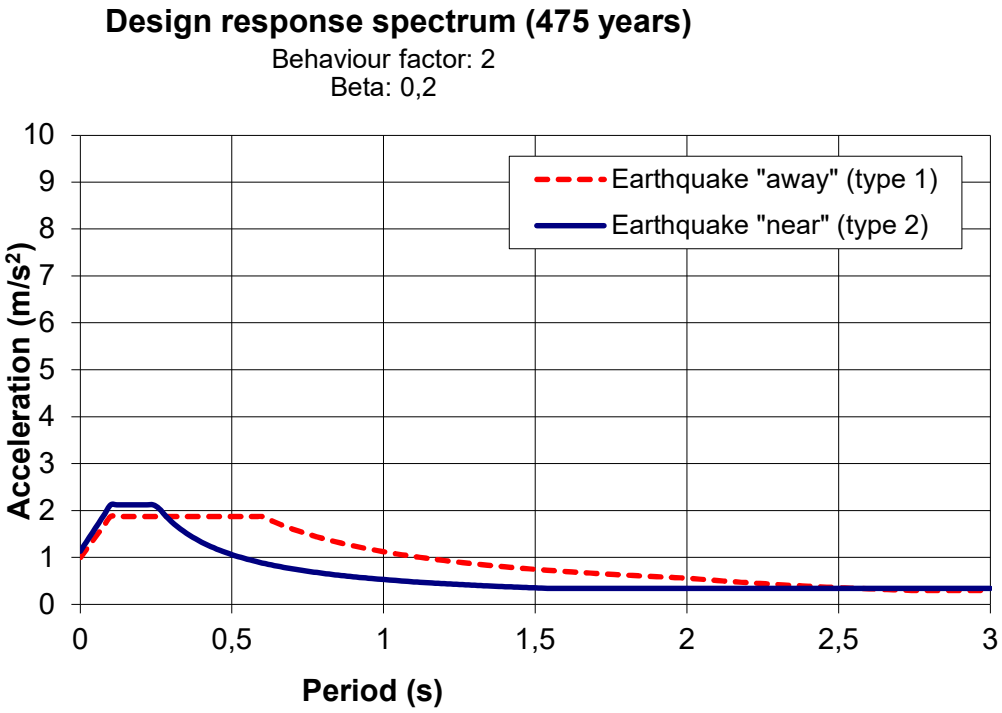

Figure 38: Design response spectrum

3.4. List of loads

All of the mentioned loads were input into the SCIA Engineer structural model and classified into load cases and group of loads.

Table 8: Overview of load cases

Load case/group of loads	Description
Self-weight of structure	Automatically calculated by software. The density of prestressed concrete was considered to be 26 kN/m^3.
Self-weight of equipment	The load is assumed in three values (lower, upper, mean) along the entire length of the structure.
Uneven settlements	Individual settlement of each support by 5 mm.
LM1 TS	Movable load system along the length of the structure.
LM1 UDL	Uniformly distributed load placed to generate extreme effects.
LM3 TS	Movable load system along the length of the structure.
LM3 UDL	Uniformly distributed load placed to generate extreme effects.
LM4	Uniformly distributed load of 5 kN/m^2 over the width of the structure placed to generate extreme effects.
Sidewalks	Uniformly distributed load of 5 kN/m^2 over the width of the sidewalks placed to generate extreme effects.
Uniform temperature change without reduction	Uniform temperature change without reducing effects.
Uniform temperature change with reduction	Uniform temperature change with reduction effects.
Differential temperature change without reduction	Differential temperature change without reducing effects.
Differential temperature change with reduction	Differential temperature change with reduction effects between fixed bearings on the middle piers.
Transverse wind	Continuous loads applied to the structure in the transverse direction.
Longitudinal wind	Continuous loads applied to the structure in the longitudinal direction.
Construction load	Uniform load of 1 kN/m^2 on the structure during construction to generate the extreme effects
Seismic action	Structure loaded by a spectrum of accelerations in the horizontal direction.

4. Internal forces

4.1. Analysis of internal forces

4.1.1. Permanent and variable actions

The envelopes of internal force courses caused by each load group on one main beam are shown in the following figures. The analysis was carried out in SCIA Engineer. It was more appropriate to represent the normal forces and some other internal forces on a 2D model in order to eliminate the effect of redistribution of forces in the transverse direction and the effect of the fineness of the element division.

4.1.1.1. Self-weight of superstructure (here, as for a complete construction in one step)

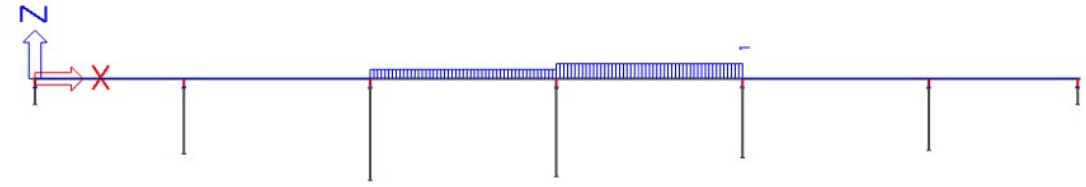

Figure 39: Normal force N: Self-weight of superstructure

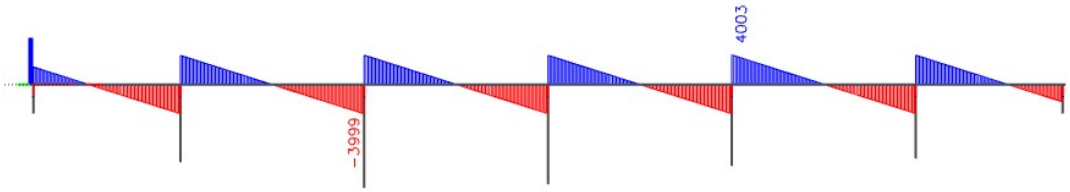

Figure 40: Shear force V_z: Self-weight of superstructure

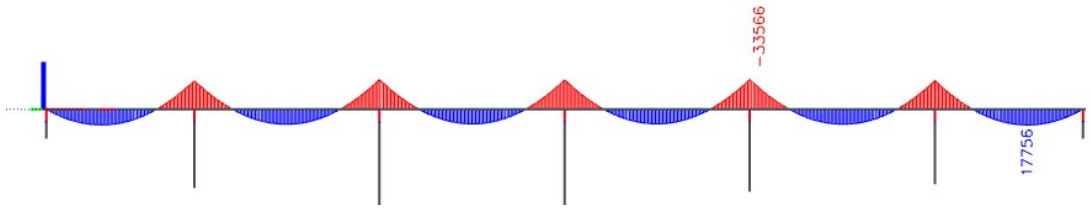

Figure 41: Bending moment M_y: Self-weight of superstructure

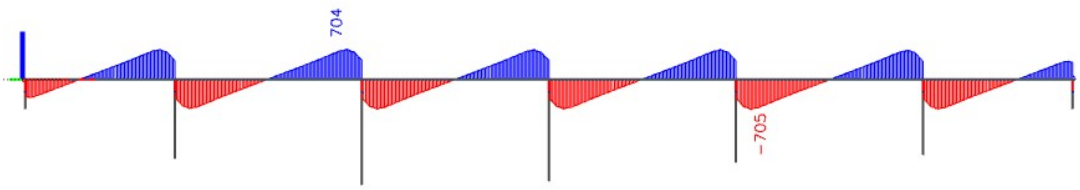

Figure 42: Torsion moment M_x: Self-weight of superstructure

4.1.1.2. Self-weight of equipment

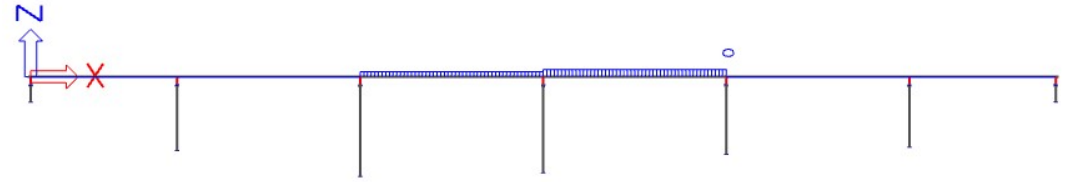

Figure 43: Normal force N: Self-weight of equipment

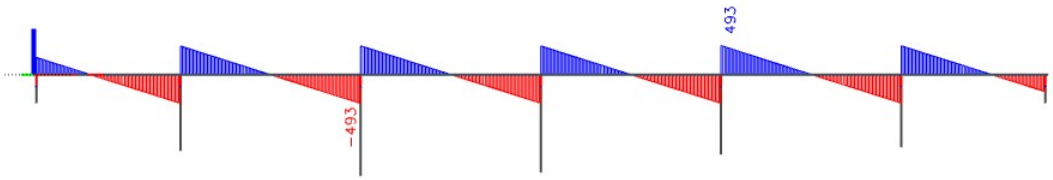

Figure 44: Shear force V_z: Self-weight of equipment

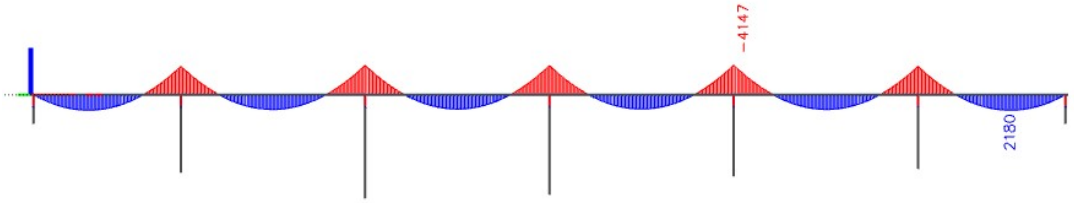

Figure 45: Bending moment M_y: Self-weight of equipment

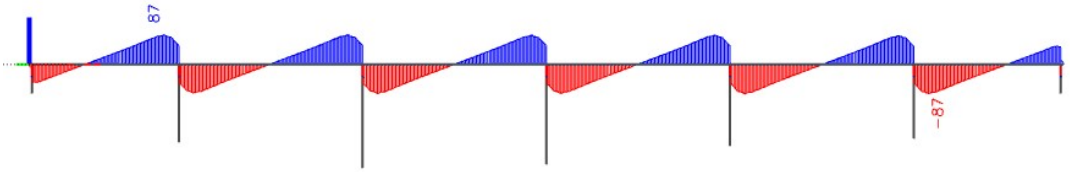

Figure 46: Torsion moment M_x: Self-weight of equipment

4.1.1.3. Uneven settlements

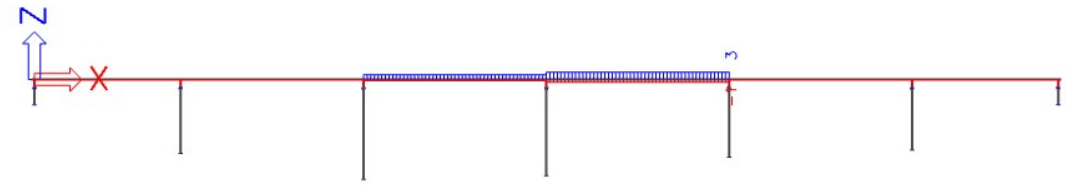

Figure 47: Normal force N: Uneven settlements

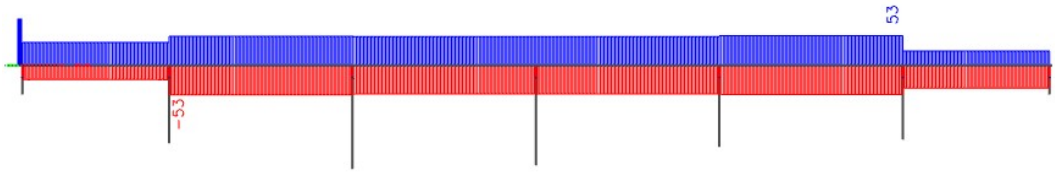

Figure 48: Shear force V_z: Uneven settlements

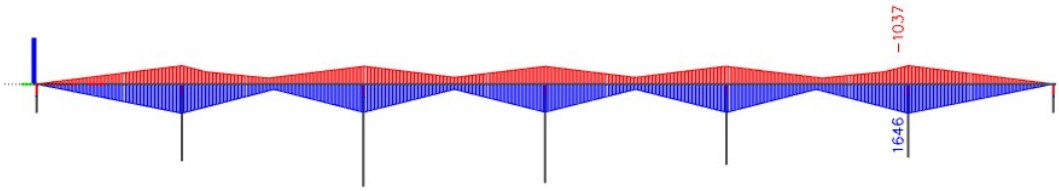

Figure 49: Bending moment M_y: Uneven settlements

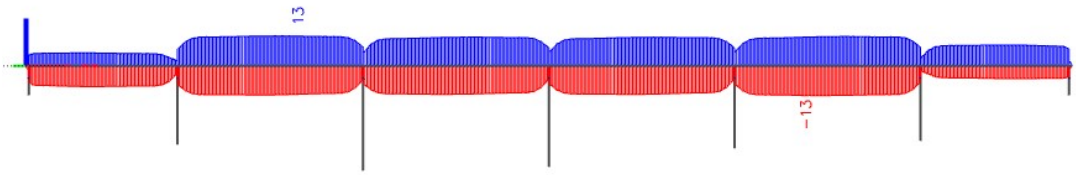

Figure 50: Torsional moment M_x: Uneven settlements

4.1.1.4. Load Model 1 – tandem system

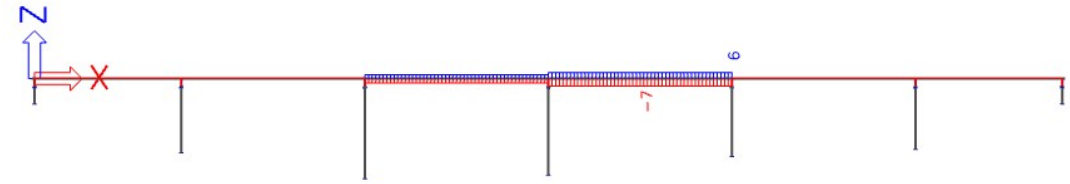

Figure 51: Normal force N: LM1 TS

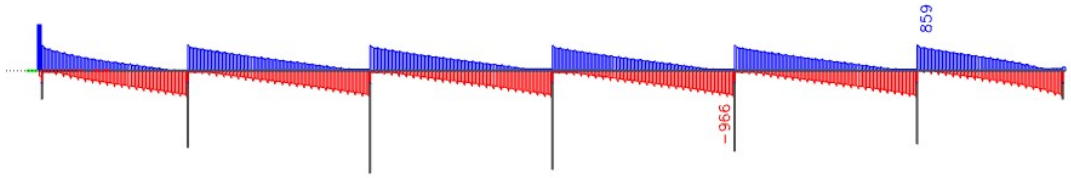

Figure 52: Shear force V_z: LM1 TS

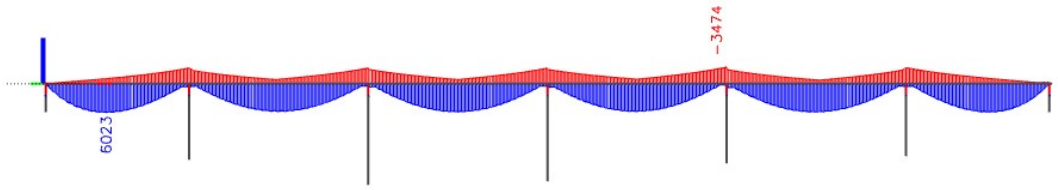

Figure 53: Bending moment M_y: LM1 TS

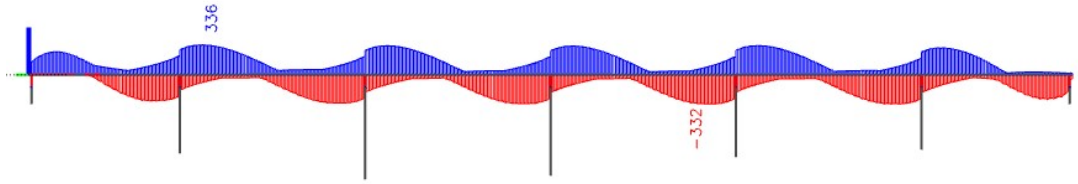

Figure 54: Torsion moment M_x: LM1 TS

4.1.1.5. Load Model 1 – uniformly distributed load

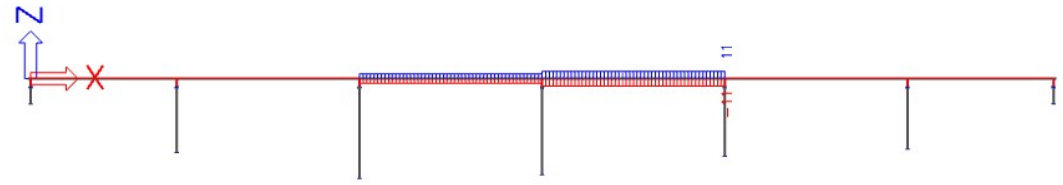

Figure 55: Normal force N: LM1 UDL

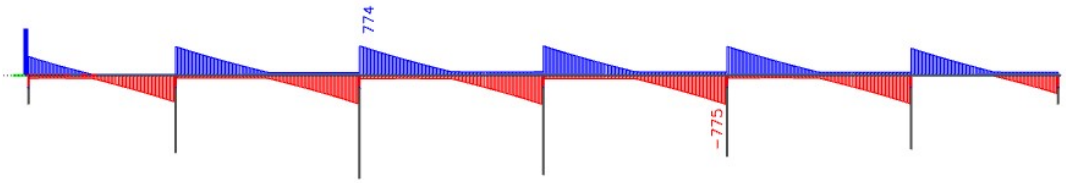

Figure 56: Shear force V_z: LM1 UDL

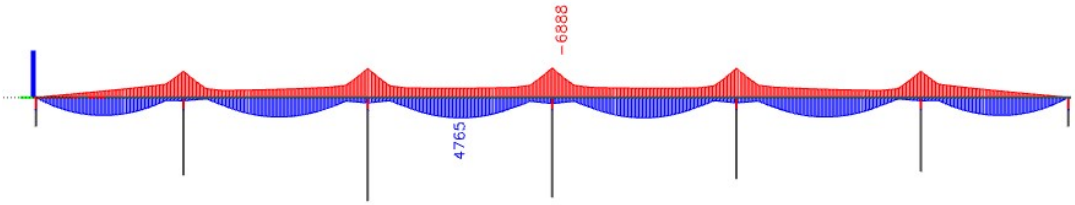

Figure 57: Bending moment M_y: LM1 UDL

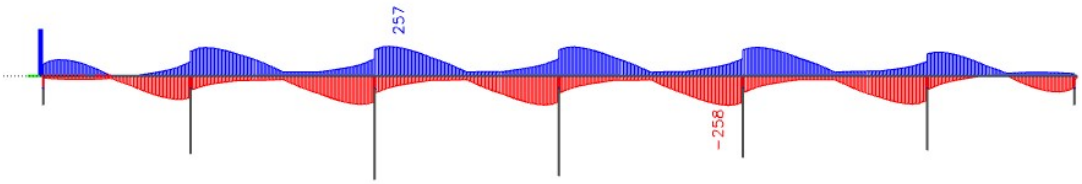

Figure 58: Torsion moment M_x: LM1 UDL

4.1.1.6. Load on sidewalks – internal forces in a beam due to the live load on the walkway above this beam

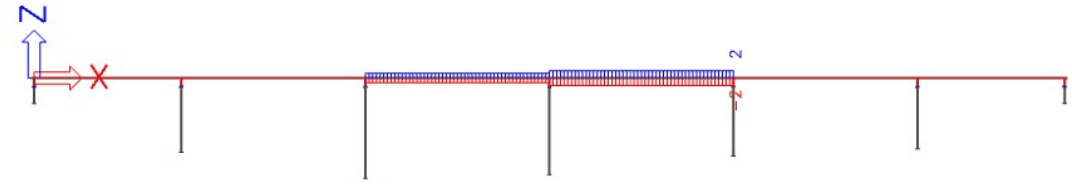

Figure 59: Normal force N: Load on sidewalks

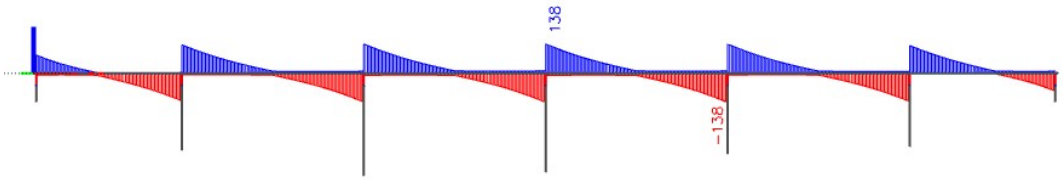

Figure 60: Shear force V_z: Load on sidewalks

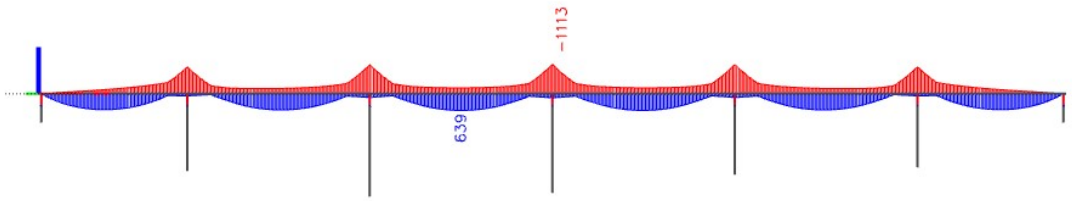

Figure 61: Bending moment M_y: Load on sidewalks

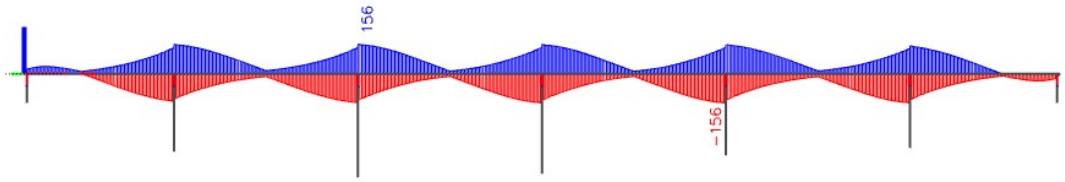

Figure 62: Torsion moment M_x: Load on sidewalks

4.1.1.7. Load Model 3 – the vehicle 1200/150

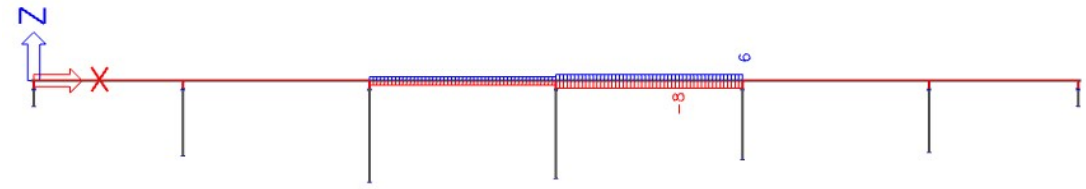

Figure 63: Normal force N: LM3 TS

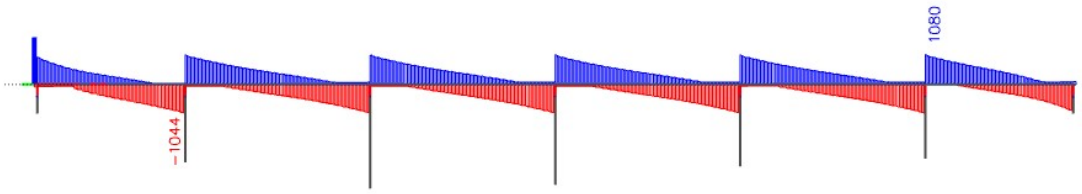

Figure 64: Shear force V_z: LM3 TS

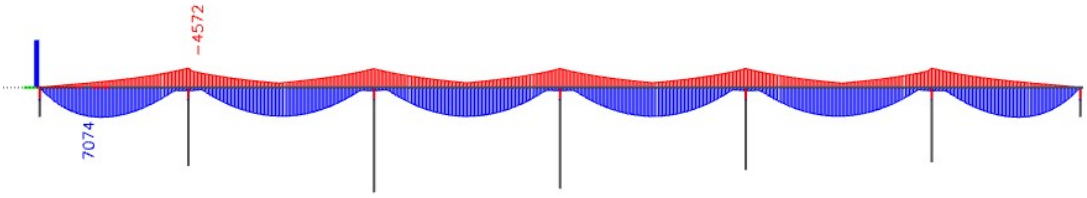

Figure 65: Bending moment M_y: LM3 TS

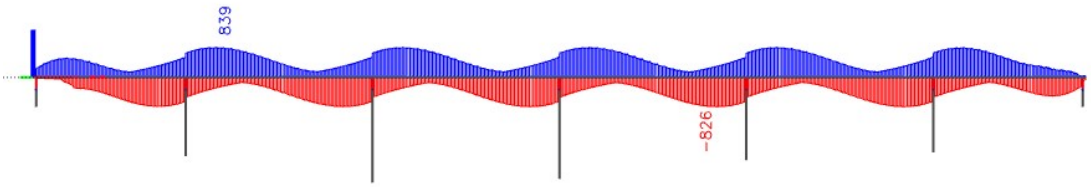

Figure 66: Torsion moment M_x: LM3 TS

4.1.1.8. Load Model 3 – corresponding uniformly distributed load

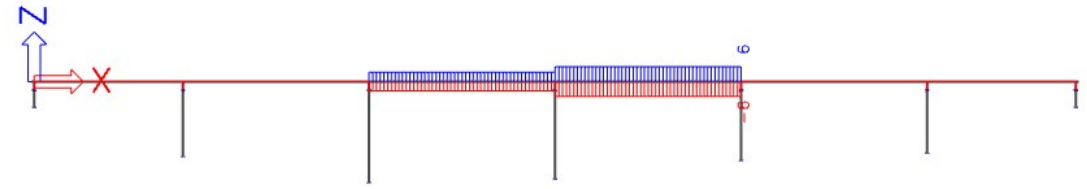

Figure 67: Normal force N: LM3 UDL

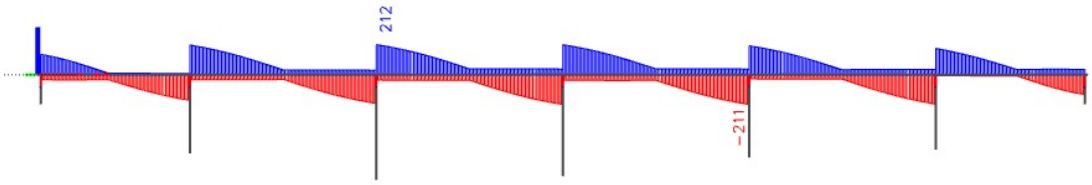

Figure 68: Shear force V_z: LM3 UDL

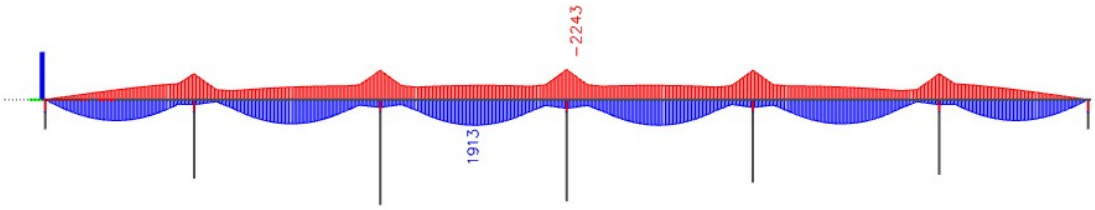

Figure 69: Bending moment M_y: LM3 UDL

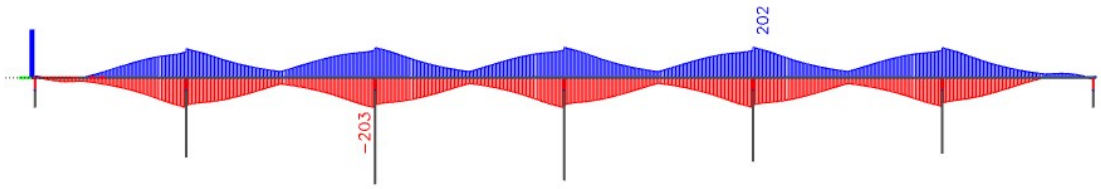

Figure 70: Torsion moment M_x: LM3 UDL

4.1.1.9. Load Model 4 – crowd of people

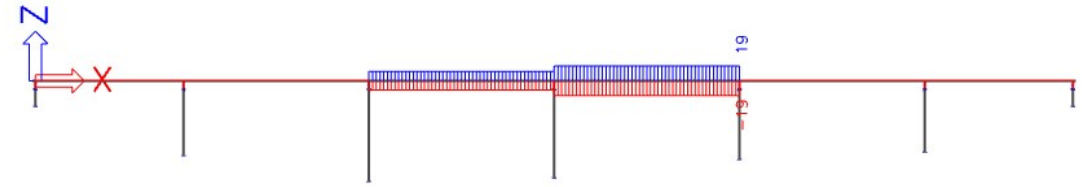

Figure 71: Normal force N: LM4

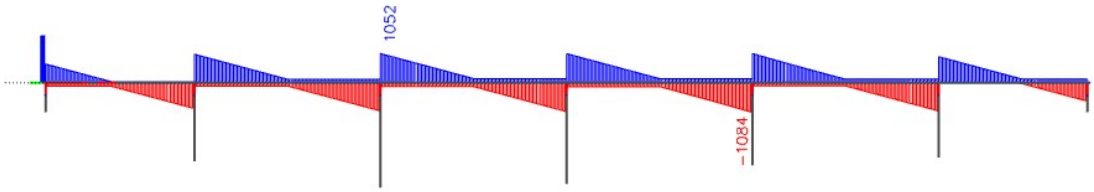

Figure 72: Shear force V_z: LM4

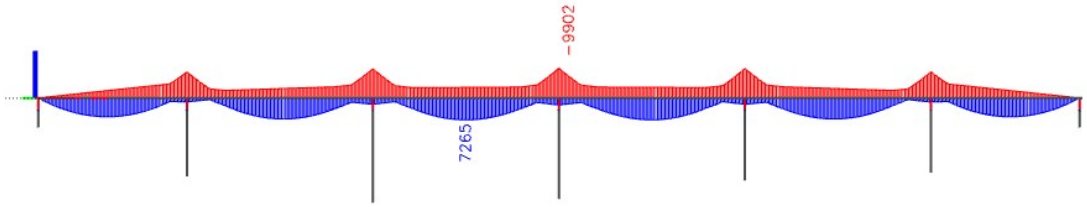

Figure 73: Bending moment M_y: LM4

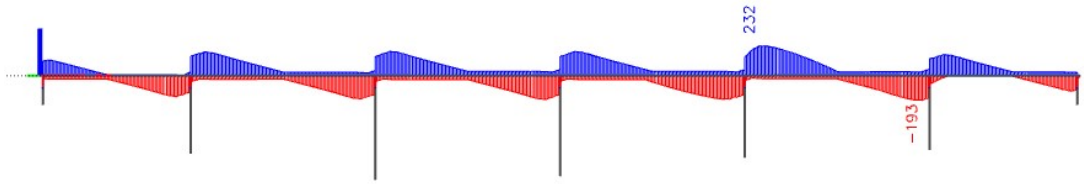

Figure 74: Torsion moment M_x: LM4

4.1.1.10. Temperature changes – uniform component

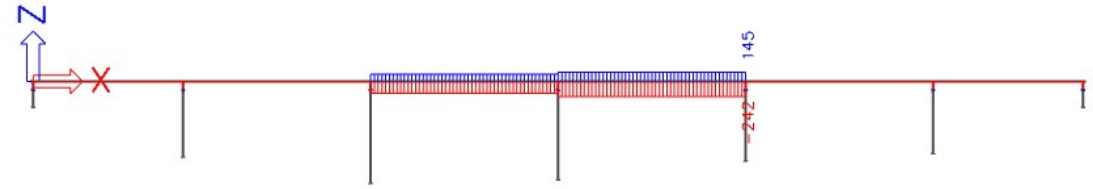

Figure 75: Normal force N: Uniform temperature load

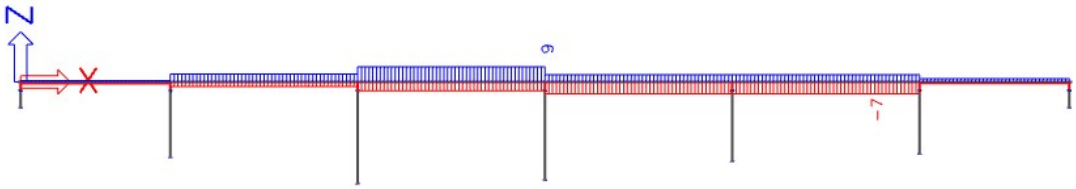

Figure 76: Shear force V_z: Uniform temperature load

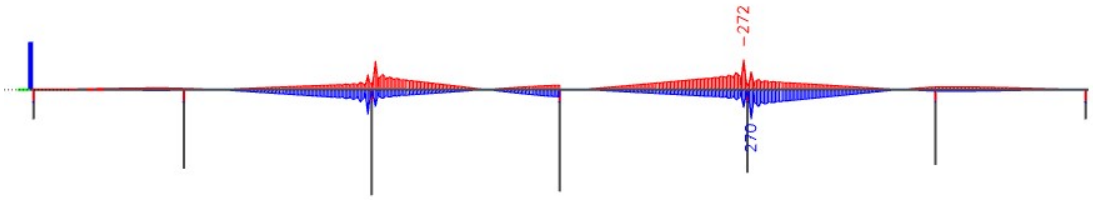

Figure 77: Bending moment M_y: Uniform temperature load

Figure 78: Torsion moment M_x: Uniform temperature load

4.1.1.11. Temperature changes – vertical linearly varying component

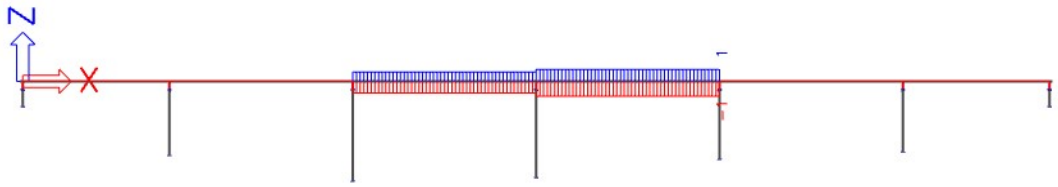

Figure 79: Normal force N: Differential temperature load

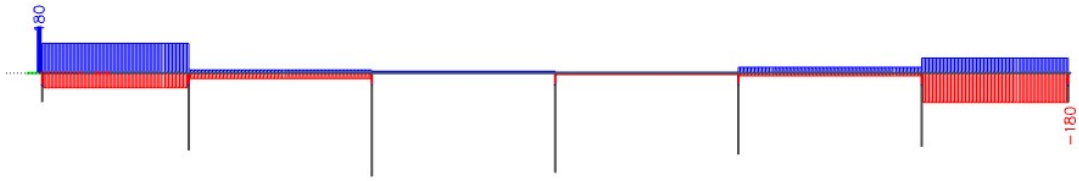

Figure 80: Shear force V_z: Differential temperature load

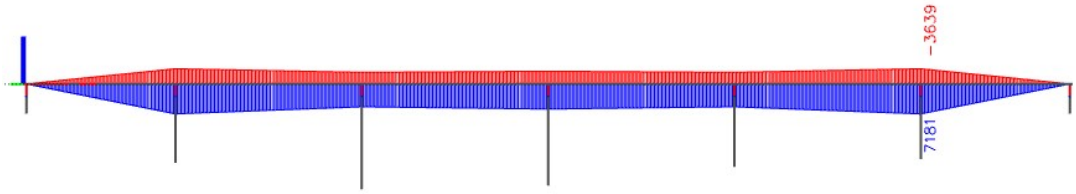

Figure 81: Bending moment M_y: Differential temperature load

Figure 82: Torsion moment M_x: Differential temperature load

4.1.1.12. Wind load – longitudinal direction

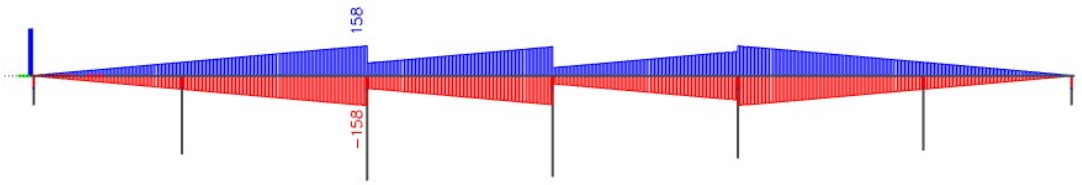

Figure 83: Normal force N: Wind load – longitudinal direction

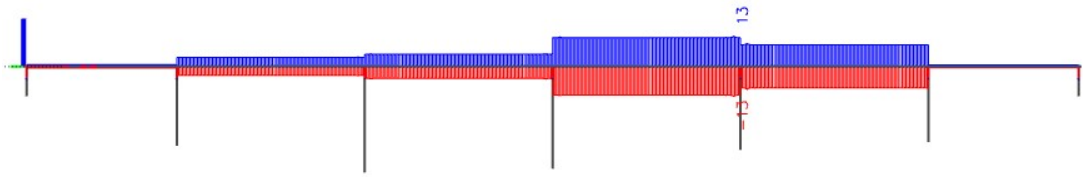

Figure 84: Shear force V_z: Wind load – longitudinal direction

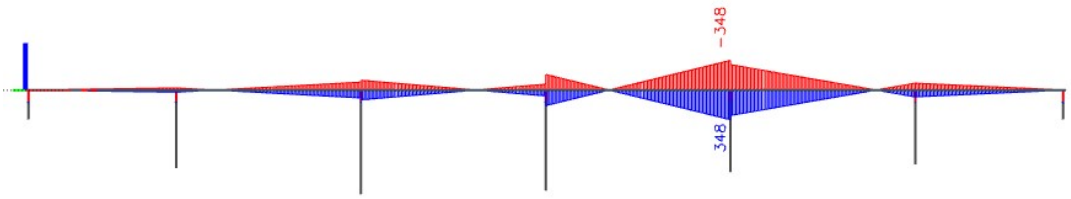

Figure 85: Bending moment M_y: Wind load – longitudinal direction

Figure 86: Torsion moment M_x: Wind load – longitudinal direction

4.1.1.13. Wind load – transverse direction

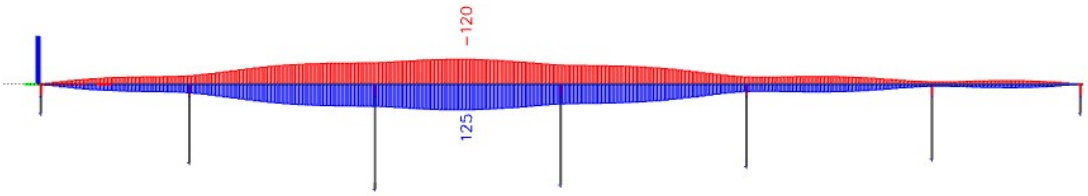

Figure 87: Normal force N: Wind load – transverse direction

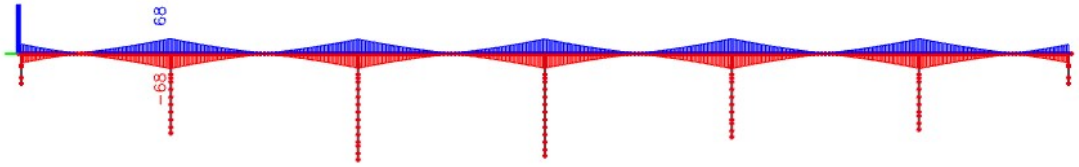

Figure 88: Shear force V_z: Wind load – transverse direction

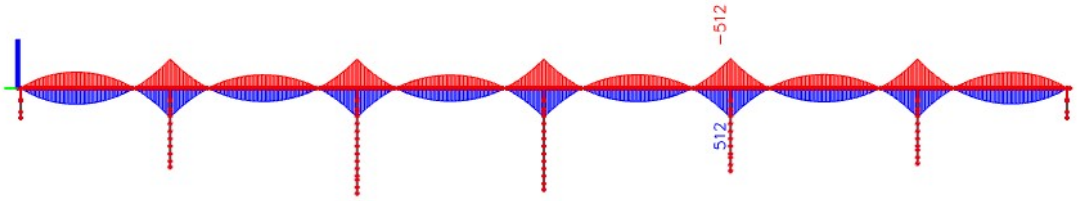

Figure 89: Bending moment M_y: Wind load – transverse direction

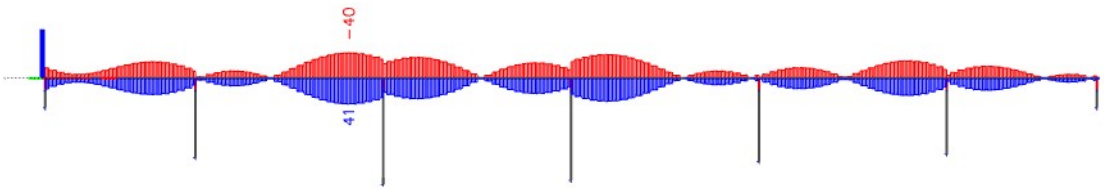

Figure 90: Torsion moment M_x: Wind load – transverse direction

4.1.2. Accidental actions

The design acceleration spectra for both types of the earthquake generation were entered as loading cases into the SCIA software. Masses corresponding to the self-weight of the structure and to the self-weight of the equipment were also generated in the model. The mode shapes of the oscillations were found by modal analysis.

Figure 91: First mode shape of the structure

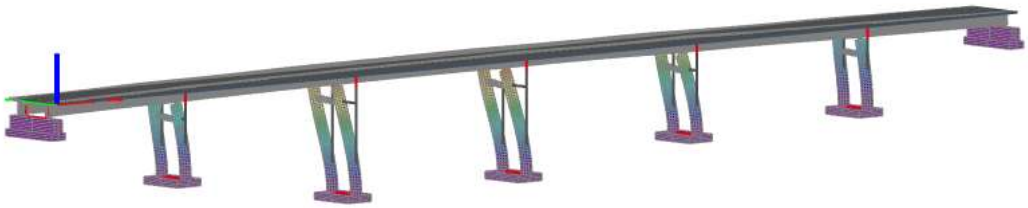

Figure 92: Second mode shape of the structure

Combinations of actions for seismic design situations were set up according to the following expression.

$$\sum_{j\geq 1} G_{k,j}\text{"} + \text{"}P + \text{"} \mathrm{A_{Ed}} + \text{"} \sum_{i>1} \psi_{2,i} Q_{k,i}$$

The seismic analysis was performed with superposition of results by SRSS method separately for each direction and type of earthquake generation, therefore 4 combinations of results were obtained.

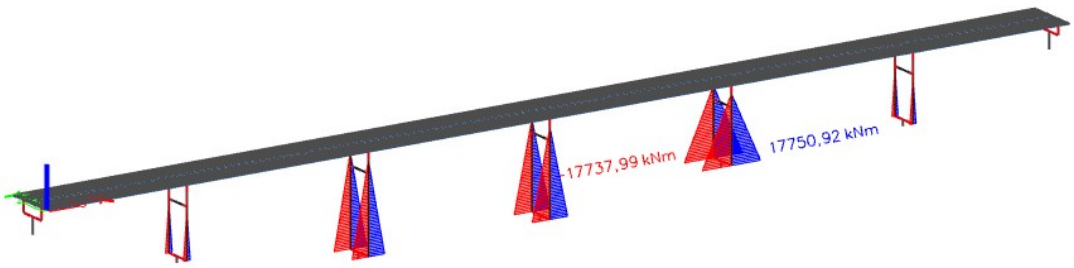

Figure 93: Bending moments in piers: Combination of seismic action – direction x

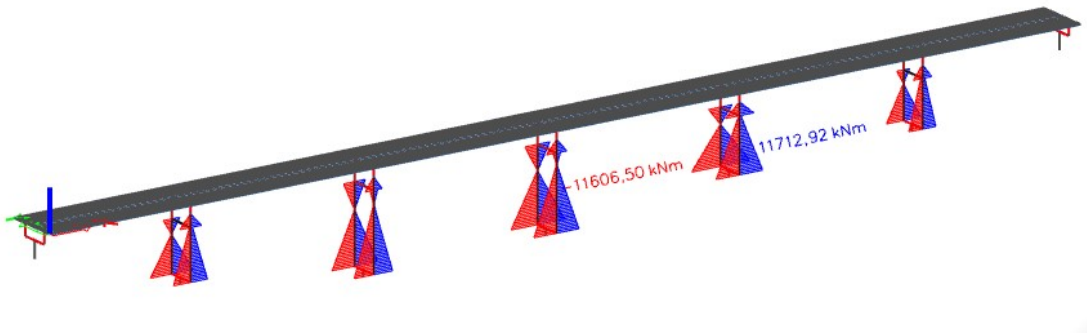

Figure 94: Bending moments in piers: Combination of seismic action – direction y

The figures indicate that significant bending moments would be generated at the base of the piers with fixed bearings in accidental situations such as an earthquake. For this purpose, a detailed dynamic calculation would be required, and the substructure would also need to be dimensioned for seismic actions.

Nevertheless, this is not a part of the thesis.

4.2. Combinations of actions

Load combinations according to EN 1990 were set up for the design of the structure. For these purposes, load cases without prestressing effects were assumed.

Ultimate limit states

Combinations of actions for persistent or transient design situations are expressed as:

6.10

$$\sum_{j\geq 1} \gamma_{G,j} G_{k,j}" + "\gamma_p P" + "\gamma_{Q,1} Q_{k,1}" + " \sum_{i>1} \gamma_{Q,i} \psi_{0.i} Q_{k,i}$$

Or alternatively for STR and GEO limit states, the less favourable of the following expressions:

6.10a

$$\sum_{j\geq 1} \gamma_{G,j} G_{k,j}" + "\gamma_p P" + "\gamma_{Q,1} \psi_{0.i} Q_{k,1}" + " \sum_{i>1} \gamma_{Q,i} \psi_{0.i} Q_{k,i}$$

6.10b

$$\sum_{j\geq 1} \xi_j \gamma_{G,j} G_{k,j}" + "\gamma_p P" + "\gamma_{Q,1} Q_{k,1}" + " \sum_{i>1} \gamma_{Q,i} \psi_{0.i} Q_{k,i}$$

Combination of action for a seismic design situation is defined as:

$$\sum_{j\geq 1} G_{k,j}" + "P +" \mathrm{A_{Ed}} + " \sum_{i>1} \psi_{2,i} Q_{k,i}$$

Serviceability limit states

For serviceability limit states, the combinations of actions are represented by the following expressions:

Characteristic combination

$$\sum_{j\geq 1} G_{k,j}" + "P" + "Q_{k,1}" + " \sum_{i>1} \psi_{0,i} Q_{k,i}$$

Frequent combination

$$\sum_{j\geq 1} G_{k,j}" + "P" + "\psi_{1,i} Q_{k,1}" + " \sum_{i>1} \psi_{2,i} Q_{k,i}$$

Quasi-permanent combination

$$\sum_{j\geq 1} G_{k,j}" + "P" + " \sum_{i>1} \psi_{2,i} Q_{k,i}$$

The partial factors γ, the reduction factor ξ and the combination coefficients ψ, valid for road bridges, are considered in the above equations. Their values for each type and set of loads are given in Table 9 and Table 10.

Table 9: Partial factors γ and reduction factor ξ

Loads	Unfavourable effects	Favourable effects
Permanent actions	$\gamma_{G,sup} = 1,35$	$\gamma_{G,inf} = 1,35$
Prestressing – ultimate limit states (favourable effects)	$\gamma_{G,f} = 1,0$	$\gamma_{G,fav} = 1,0$
Uneven settlements – linear elastic analysis	$\gamma_{G,set} = 1,20$	$\gamma_{G,set} = 0,0$
Uneven settlements – non-linear analysis	$\gamma_{G,set} = 1,35$	$\gamma_{G,set} = 0,0$
Traffic actions – road bridges, pedestrians and cyclists	$\gamma_{Q} = 1,35$	$\gamma_{Q} = 0,0$
Other traffic and variable actions	$\gamma_{Q} = 1,5$	$\gamma_{Q} = 0,0$
Reduction factor	$\xi = 0,85$	

Table 10: Values of combination coefficients ψ (road bridges)

Action	Symbol		Ψ_0	Ψ_1	Ψ_2
Traffic loads	gr1a – LM1 + pedestrians or cycle-track loads	TS – tandem system	0,75	0,75	0,0
		UDL – uniformly distributed load	0,40	0,40	0,0
		Pedestrian + cycle-track loads	0,40	0,40	0,0
	gr2 – horizontal forces		0	0	0
	gr4 – LM4 – crowd of people		0,0	-	0,0
	gr5 – LM3 – special vehicles		0,0	-	0,0
Thermal actions	T_k		0,60	0,60	0,50
Construction loads	Q_c		1,00		

The group of loads according to Table 10 with the corresponding coefficients were used to form the combinations of actions.

These coefficients of the individual load cases entering into the combinations are given in the following tables for the finished structure.

Table 11: SLS – combination factors – leading traffic action

Overview of combinations and values of factor for load cases																							
Serviceability limit states																							
Leading variable action		gr1a						gr4						gr5									
Accompanying variable action		Temperature						Temperature						Temperature									
		Wind						Wind						Wind									
Combination		Characteristic		Frequent		Quasi-permanent		Characteristic		Frequent		Quasi-permanent		Characteristic		Frequent		Quasi-permanent					
Temperature reduction		ω_N	ω_M	ω_N	ω_M	ω_N	ω_M	ω_N	ω_M	ω_N	ω_M	ω_N	ω_M	ω_N	ω_M	ω_N	ω_M	ω_N	ω_M				
Load case/group	coef																						
Self-weight of structure	γ_G	1	1	1	1	1	1	1	1	1	1	1	1	1	1	1	1	1	1				
	ξ_G																						
Self-weight of equipment	γ_G	1	1	1	1	1	1	1	1	1	1	1	1	1	1	1	1	1	1				
	ξ_G																						
Uneven settlements	γ_{Gset}	1	1	1	1	1	1	1	1	1	1	1	1	1	1	1	1	1	1				
	ξ_G																						
LM1 TS	γ_Q	1	1	1	1	1	1																
	ψ_0																						
	ψ_1			0,75	0,75																		
	ψ_2					0	0																
LM1 UDL	γ_Q	1	1	1	1	1	1																
	ψ_0																						
	ψ_1			0,4	0,4																		
	ψ_2					0	0																
LM3 TS	γ_Q													1	1			1	1				
	ψ_0																						
	ψ_1																						
	ψ_2																	0	0				
LM3 UDL	γ_Q													1	1	1	1	1	1				
	ψ_0																						
	ψ_1															0,4	0,4						
	ψ_2																	0	0				
LM4	γ_Q							1	1			1	1										
	ψ_0																						
	ψ_1																						
	ψ_2											0	0										
Sidewalks	γ_Q	1	1	1	1	1	1																
	ψ_0																						
	ψ_1			0,4	0,4																		
	ψ_2					0	0																
	coef	0,6	0,6	0,6	0,6	0,6	0,6																
Uniform temperature without reduction	γ_Q		1		1		1		1		1		1		1		1						
	ψ_0		0,6						0,6						0,6								
	ψ_1																						
	ψ_2				0,5		0,5				0,5		0,5				0,5		0,5				
Uniform temperature with reduction	γ_Q	1		1		1		1		1		1		1		1		1					
	ψ_0	0,6						0,6						0,6									
	ψ_1																						
	ψ_2			0,5		0,5				0,5		0,5				0,5		0,5					
Diff. temperature without reduction	γ_Q	1		1		1		1		1		1		1		1		1					
	ψ_0	0,6						0,6						0,6									
	ψ_1																						
	ψ_2			0,5		0,5				0,5		0,5				0,5		0,5					
Diff. temperature with reduction	γ_Q		1		1		1		1		1		1		1		1		1				
	ψ_0		0,6						0,6						0,6								
	ψ_1																						
	ψ_2				0,5		0,5				0,5		0,5				0,5		0,5				
Wind	γ_Q	1	1	1	1	1	1	1	1	1	1	1	1	1	1	1	1	1	1				
	ψ_0	0,6	0,6					0,6	0,6					0,6	0,6								
	ψ_1																						
	ψ_2			0	0	0	0			0	0	0	0			0	0	0	0				

Table 12: SLS – combination factors – leading action temperature

Overview of combinations and values of factor for load cases																			
Serviceability limit states																			
Leading variable action		Temperature						Temperature						Temperature					
Accompanying variable action		gr1a						gr4						gr5					
		Wind						Wind						Wind					
Combination		Characteristic		Frequent		Quasi-permanent		Characteristic		Frequent		Quasi-permanent		Characteristic		Frequent		Quasi-permanent	
Temperature reduction		ω_N	ω_M	ω_N	ω_M	ω_N	ω_M	ω_N	ω_M	ω_N	ω_M	ω_N	ω_M	ω_N	ω_M	ω_N	ω_M	ω_N	ω_M
Load case/group	coef																		
Self-weight of structure	γ_G	1	1	1	1	1	1	1	1	1	1	1	1	1	1	1	1	1	1
	ξ_G																		
Self-weight of equipment	γ_G	1	1	1	1	1	1	1	1	1	1	1	1	1	1	1	1	1	1
	ξ_G																		
Uneven settlements	γ_{Gset}	1	1	1	1	1	1	1	1	1	1	1	1	1	1	1	1	1	1
	ξ_G																		
LM1 TS	γ_Q	1	1	1	1	1	1												
	ψ_0	0,75	0,75																
	ψ_1																		
	ψ_2			0	0	0	0												
LM1 UDL	γ_Q	1	1	1	1	1	1												
	ψ_0	0,4	0,4																
	ψ_1																		
	ψ_2			0	0	0	0												
LM3 TS	γ_Q													1	1	1	1	1	1
	ψ_0													0	0				
	ψ_1																		
	ψ_2															0	0	0	0
LM3 UDL	γ_Q													1	1	1	1	1	1
	ψ_0													0,4	0,4				
	ψ_1																		
	ψ_2															0	0	0	0
LM4	γ_Q							1	1	1	1	1	1						
	ψ_0							0	0										
	ψ_1																		
	ψ_2									0	0	0	0						
Sidewalks	γ_Q	1	1	1	1	1	1												
	ψ_0	0,4	0,4																
	ψ_1																		
	ψ_2			0	0	0	0												
	coef	0,6	0,6	0,6	0,6	0,6	0,6												
Uniform temperature without reduction	γ_Q		1		1		1		1		1		1		1		1		1
	ψ_0																		
	ψ_1				0,6						0,6						0,6		
	ψ_2						0,5						0,5						0,5
Uniform temperature with reduction	γ_Q	1		1		1		1		1		1		1		1		1	
	ψ_0																		
	ψ_1			0,6						0,6						0,6			
	ψ_2					0,5						0,5						0,5	
Diff. temperature without reduction	γ_Q	1		1		1		1		1		1		1		1		1	
	ψ_0																		
	ψ_1			0,6						0,6						0,6			
	ψ_2					0,5						0,5						0,5	
Diff. temperature with reduction	γ_Q		1		1		1		1		1		1		1		1		1
	ψ_0																		
	ψ_1				0,6						0,6						0,6		
	ψ_2						0,5						0,5						0,5
Wind	γ_Q	1	1	1	1	1	1	1	1	1	1	1	1	1	1	1	1	1	1
	ψ_0	0,6	0,6					0,6	0,6					0,6	0,6				
	ψ_1																		
	ψ_2			0	0	0	0			0	0	0	0			0	0	0	0

Table 13: ULS – combination factors – leading action traffic

Overview of combinations and values of factor for load cases													
Ultimate limit states, Mext													
Leading variable action		gr1a				gr4				gr5			
Accompanying variable action		Temperature				Temperature				Temperature			
		Wind				Wind				Wind			
Expression		6.10a		6.10b		6.10a		6.10b		6.10a		6.10b	
Temperature reduction		ω_N	ω_M	ω_N	ω_M	ω_N	ω_M	ω_N	ω_M	ω_N	ω_M	ω_N	ω_M
Load case	Coef.												
Self-weight of structure	γ_G	1,35	1,35	1,35	1,35	1,35	1,35	1,35	1,35	1,35	1,35	1,35	1,35
	ξ_G	1	1	0,85	0,85	1	1	0,85	0,85	1	1	0,85	0,85
Self-weight of equipment	γ_G	1,35	1,35	1,35	1,35	1,35	1,35	1,35	1,35	1,35	1,35	1,35	1,35
	ξ_G	1	1	0,85	0,85	1	1	0,85	0,85	1	1	0,85	0,85
Uneven settlements	γ_{Gset}	1,2	1,2	1,2	1,2	1,2	1,2	1,2	1,2	1,2	1,2	1,2	1,2
	ξ_G	1	1	0,85	0,85	1	1	0,85	0,85	1	1	0,85	0,85
LM1 TS	γ_Q	1,35	1,35	1,35	1,35								
	ψ_0	0,75	0,75										
	ψ_1												
	ψ_2												
LM1 UDL	γ_Q	1,35	1,35	1,35	1,35								
	ψ_0	0,4	0,4										
	ψ_1												
	ψ_2												
LM3 TS	γ_Q									1,35	1,35	1,35	1,35
	ψ_0									0	0		
	ψ_1												
	ψ_2												
LM3 UDL	γ_Q									1,35	1,35	1,35	1,35
	ψ_0									0,4	0,4		
	ψ_1												
	ψ_2												
LM4	γ_Q					1,35	1,35	1,35	1,35				
	ψ_0					0	0						
	ψ_1												
	ψ_2												
Sidewalks	γ_Q	1,35	1,35	1,35	1,35								
	ψ_0	0,4	0,4										
	ψ_1												
	ψ_2												
	coef	0,6	0,6	0,6	0,6								
Uniform temperature without reduction	γ_Q		1,5		1,5		1,5		1,5		1,5		1,5
	ψ_0		0,6		0,6		0,6		0,6		0,6		0,6
	ψ_1												
	ψ_2												
Uniform temperature with reduction	γ_Q	1,5		1,5		1,5		1,5		1,5		1,5	
	ψ_0	0,6		0,6		0,6		0,6		0,6		0,6	
	ψ_1												
	ψ_2												
Diff. temperature without reduction	γ_Q	1,5		1,5		1,5		1,5		1,5		1,5	
	ψ_0	0,6		0,6		0,6		0,6		0,6		0,6	
	ψ_1												
	ψ_2												
Diff. temperature with reduction	γ_Q		1,5		1,5		1,5		1,5		1,5		1,5
	ψ_0		0,6		0,6		0,6		0,6		0,6		0,6
	ψ_1												
	ψ_2												
Wind	γ_Q	1,5	1,5	1,5	1,5	1,5	1,5	1,5	1,5	1,5	1,5	1,5	1,5
	ψ_0	0,6	0,6	0,6	0,6	0,6	0,6	0,6	0,6	0,6	0,6	0,6	0,6
	ψ_1												
	ψ_2												

Table 14: ULS – combination factors – leading action temperature

Accompanying variable action		Temperature				Temperature				Temperature			
		Wind				Wind				Wind			
Expression		6.10a		6.10b		6.10a		6.10b		6.10a		6.10b	
Temperature reduction		ω_N	ω_M	ω_N	ω_M	ω_N	ω_M	ω_N	ω_M	ω_N	ω_M	ω_N	ω_M
Load case	Coef.												
Self-weight of structure	γ_G	1,35	1,35	1,35	1,35	1,35	1,35	1,35	1,35	1,35	1,35	1,35	1,35
	ξ_G	1	1	0,85	0,85	1	1	0,85	0,85	1	1	0,85	0,85
Self-weight of equipment	γ_G	1,35	1,35	1,35	1,35	1,35	1,35	1,35	1,35	1,35	1,35	1,35	1,35
	ξ_G	1	1	0,85	0,85	1	1	0,85	0,85	1	1	0,85	0,85
Uneven settlements	γ_{Gset}	1,2	1,2	1,2	1,2	1,2	1,2	1,2	1,2	1,2	1,2	1,2	1,2
	ξ_G	1	1	0,85	0,85	1	1	0,85	0,85	1	1	0,85	0,85
LM1 TS	γ_Q	1,35	1,35	1,35	1,35								
	ψ_0	0,75	0,75										
	ψ_1												
	ψ_2												
LM1 UDL	γ_Q	1,35	1,35	1,35	1,35								
	ψ_0	0,4	0,4										
	ψ_1												
	ψ_2												
LM3 TS	γ_Q									1,35	1,35	1,35	1,35
	ψ_0									0	0		
	ψ_1												
	ψ_2												
LM3 UDL	γ_Q									1,35	1,35	1,35	1,35
	ψ_0									0,4	0,4		
	ψ_1												
	ψ_2												
LM4	γ_Q					1,35	1,35	1,35	1,35				
	ψ_0					0	0						
	ψ_1												
	ψ_2												
Sidewalks	γ_Q	1,35	1,35	1,35	1,35								
	ψ_0	0,4	0,4										
	ψ_1												
	ψ_2												
	coef	0,6	0,6	0,6	0,6								
Uniform temperature without reduction	γ_Q		1,5		1,5		1,5		1,5		1,5		1,5
	ψ_0		0,6		0,6		0,6		0,6		0,6		0,6
	ψ_1												
	ψ_2												
Uniform temperature with reduction	γ_Q	1,5		1,5		1,5		1,5		1,5		1,5	
	ψ_0	0,6		0,6		0,6		0,6		0,6		0,6	
	ψ_1												
	ψ_2												
Diff. temperature without reduction	γ_Q	1,5		1,5		1,5		1,5		1,5		1,5	
	ψ_0	0,6		0,6		0,6		0,6		0,6		0,6	
	ψ_1												
	ψ_2												
Diff. temperature with reduction	γ_Q		1,5		1,5		1,5		1,5		1,5		1,5
	ψ_0		0,6		0,6		0,6		0,6		0,6		0,6
	ψ_1												
	ψ_2												
Wind	γ_Q	1,5	1,5	1,5	1,5	1,5	1,5	1,5	1,5	1,5	1,5	1,5	1,5
	ψ_0	0,6	0,6	0,6	0,6	0,6	0,6	0,6	0,6	0,6	0,6	0,6	0,6
	ψ_1												
	ψ_2												

5. Prestressing

The prestressing reinforcement is designed as tendons composed of strands. Each tendon is composed of 26 strands with a diameter of 15.7 mm made of Y1860S7 steel.

5.1. Design principles

5.1.1. Cover layer

The cover layer is determined from the formula:

$c_{nom} = c_{min} + \Delta c_{dev}$, where:

- c_{min} is nominal cover layer

  $c_{min} = \max \{c_{min,b}; c_{min,dur} + \Delta c_{dur,\gamma} - \Delta c_{dur,st} - \Delta c_{dur,add}; 10 \text{ mm}\}$

  $c_{min,b} = Ø = 120 \text{ mm} > 80 \text{ mm} \Rightarrow C_{min,b} = 80 \text{ mm}$

  $c_{min,dur} = 55 \text{ mm}$

  $\Delta c_{dur,\gamma} = 0 \text{ mm}$

  $\Delta c_{dur,st} = 0 \text{ mm}$

  $\Delta c_{dur,add} = 0 \text{ mm}$

  $c_{min} = \max \{80 \text{ mm}; 55 + 0 - 0 - 0; 10 \text{ mm}\} = 80 \text{ mm}$

- $\Delta c_{dev} = 10 \text{ mm}$

$c_{nom} = c_{min} + \Delta c_{dev} = 80 + 10 = 90 \text{ mm}$

5.1.2. Clear spacing between ducts

Horizontal direction

≥ diameter of the duct (120 mm)
≥ 50 mm
≥ d_g + 5 mm,
where d_g is the maximum size of aggregate grains

Vertical direction

≥ diameter of the duct (120 mm)
≥ 40 mm
≥ d_g

5.2. Design of prestressing reinforcement

The prestressing reinforcement is designed as curved tendons made of 26 strands with a diameter of 15.7 mm. Preliminarily 6 tendons were designed in two layers of 2 and 4 tendons each. The course of the curved tendons and the effects of prestressing are shown in the drawing part of the diploma thesis.

Area of the cross section of one prestressing strand

$A_{p1} = 150 \text{ mm}^2$.

Maximum stress in prestressing reinforcement after tensioning

$б_{p,max} = \min \{0.8 f_{pk}; 0.9 \times f_{p0,1k}\} = \min \{0,8 \times 1860.0; 0,9 \times 1636.8\} =$
$= \min \{1488.00; 1473.12\} = 1473.12 \text{ MPa} \approx 1473.0 \text{ MPa}$

Maximum force in prestressing reinforcement (6 tendons)

$P_{max} = A_p \times б_{p,max} = 0.0234 \times 1473,0 = 34.468 \text{ MN}$

5.3. Prestressing layout

In each beam, there are installed six tendons. Each pair of tendons has a different geometry, either in terms of elevation or in plan. The tendon course has been inserted into the SCIA Engineer software to provide better visualization and to obtain more accurate results. More precise layout of the tendons can be seen in attachments.

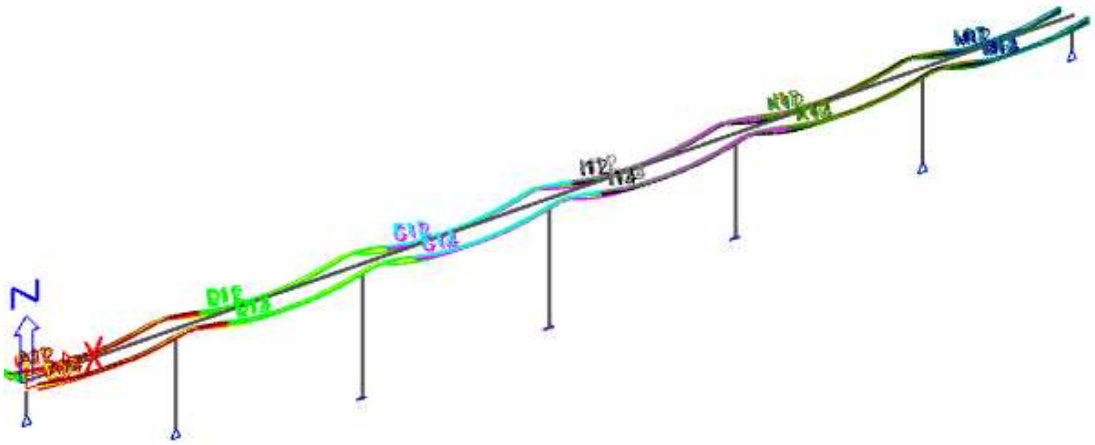

Figure 95: Display of prestressing reinforcement in the TDA model

6. Serviceability limit states

6.1. Introduction

The structure was checked in terms of serviceability limit states (SLS) as a stress limitation and a crack control.

Load combinations as characteristic, quasi-permanent and frequent were developed for the SLS check.

Normal stresses entering the SLS combinations were obtained using SCIA Engineer software.

6.2. Stress limit of concrete

For combinations representing serviceability limit states, the maximum compressive stress in the concrete is limited by the risk of cracks, excessive creep, etc. The limit values of the normal stress for different conditions and combinations are specified in the following expressions.

6.2.1. Finished structure

Maximum compressive stress

Characteristic combination of actions

$\sigma_{c,lim} = 0.6\ f_{ck} = 0.6 \times 40 = 24.0$ MPa

Quasi-permanent combination of actions

$\sigma_{c,lim} = 0.45 \times f_{ck} = 0.45 \times 40 = 18.0$ MPa

Tensile stresses

Frequent combination of actions

Under the frequent combination, decompression must be checked in critical fibers.

6.2.2. Construction stages

The estimated time of transfer of prestressing is 7 days after casting the structure.

Maximum compressive stress

Characteristic combination of actions

$\sigma_{c,lim} = 0.6\ f_{ck}(t) = 0.6 \times 31.312 = 18.787$ MPa

Quasi-permanent combination of actions

$\sigma_{c,lim} = 0.45 \times f_{ck}(t) = 0.45 \times 31.312 = 14.090$ MPa

Maximum tensile stress

The maximum tensile stress under the quasi-permanent combination shall not exceed the mean value of the tensile strength of concrete $f_{ctm}(t) = 2.867$ MPa in critical fibers.

6.3. Determination of normal stresses

The normal stresses due to permanent loads, i.e. the self-weight of the structure, the self-weight of the equipment and the prestressing effects, were obtained from the TDA model.

For short-term loads, models were developed separately for each construction stage and variable loads were applied to them. For the calculation during construction, these models were prepared twice.

Specifically, the first case is where the structure is without a scaffolding system, and the second one is where a scaffolding system is placed on the piers and the remaining part of the span is loaded by the weight of fresh concrete (27 kN/m^3).

For this purpose, girders of a scaffolding system were designed. A rough calculation indicated 15 girders with the depth of 2.8 m. These girders are supported by piers, and the cantilever from the previous span is attached to the girders using prestressing bars.

The scheme of the arrangement for these two considered situations for the first construction stage can be seen in Figure 96 and Figure 97. The scaffolding system girders are placed in other bridge spans in a similar way.

Figure 96: First construction stage – without scaffolding system girders

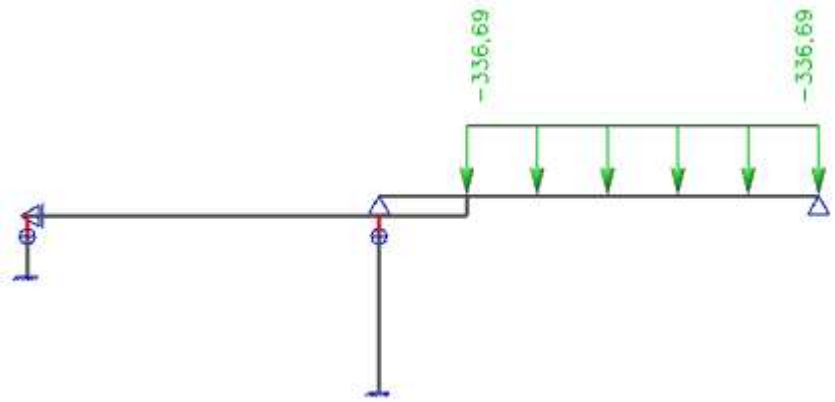

Figure 97: First construction stage – with scaffolding system

6.4. Resulting normal stresses

For the stress analysis, the stresses from the long-term loads, i.e. the self-weight, the effects of prestressing, and later the self-weight of the equipment have been determined first. To these stresses, the effects of short-term loads have been applied in each stage.

The check of the limit stresses has been carried out on these combinations and has been performed twice. Once for the construction stages without the action of the scaffolding system, and for the second time for the construction stages with the scaffolding system installed and with the weight of fresh concrete in the remaining part of the span.

The following part illustrates the stress diagrams in the upper and lower fibres due to long-term loads in all stages of construction.

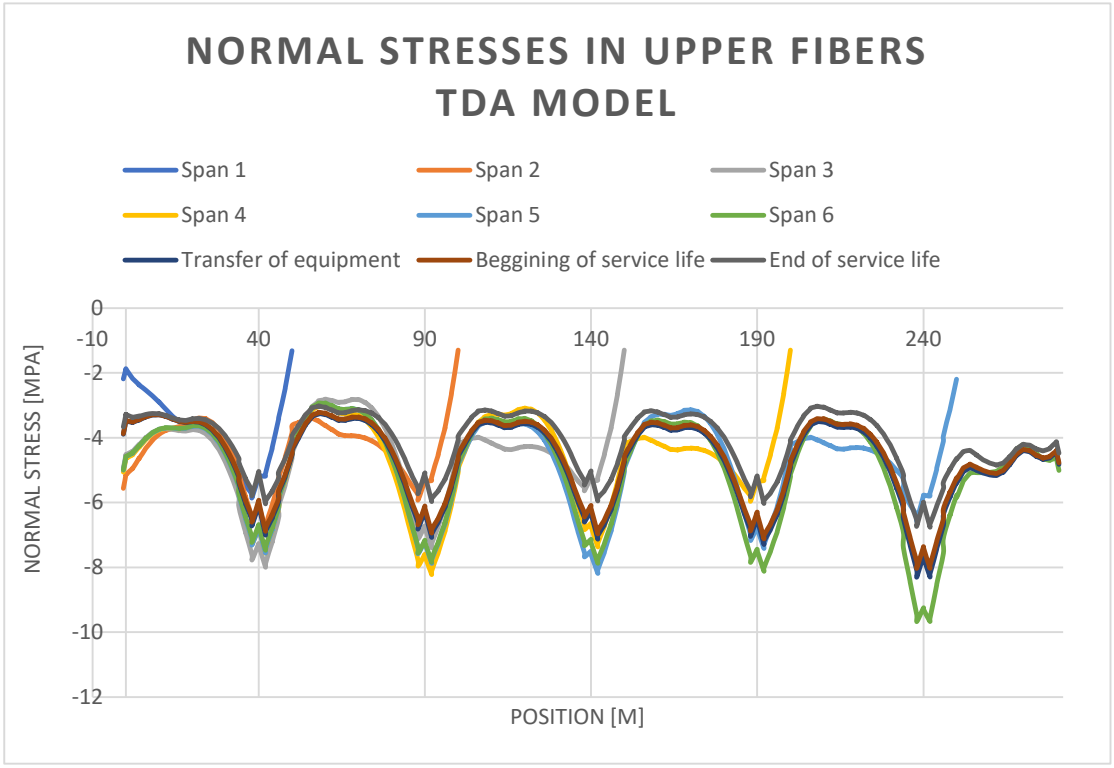

Figure 98: Normal stresses in upper fibers – long-term loads

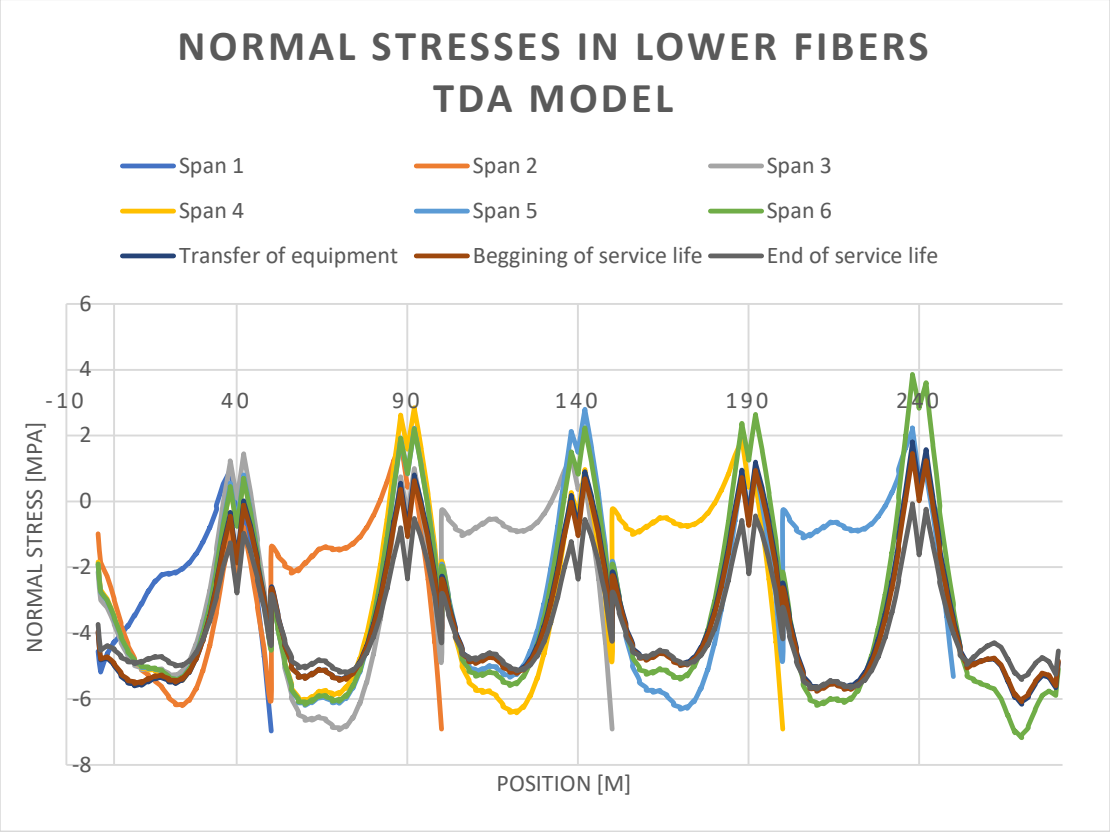

Figure 99: Normal stress in lower fibers – long-term loads

6.4.1. Construction stages - check of the case without the action of the fresh concrete

During construction, worse results came out for combinations where the leading variable action was the temperature change load. The resulting diagrams are therefore only presented for this combination.

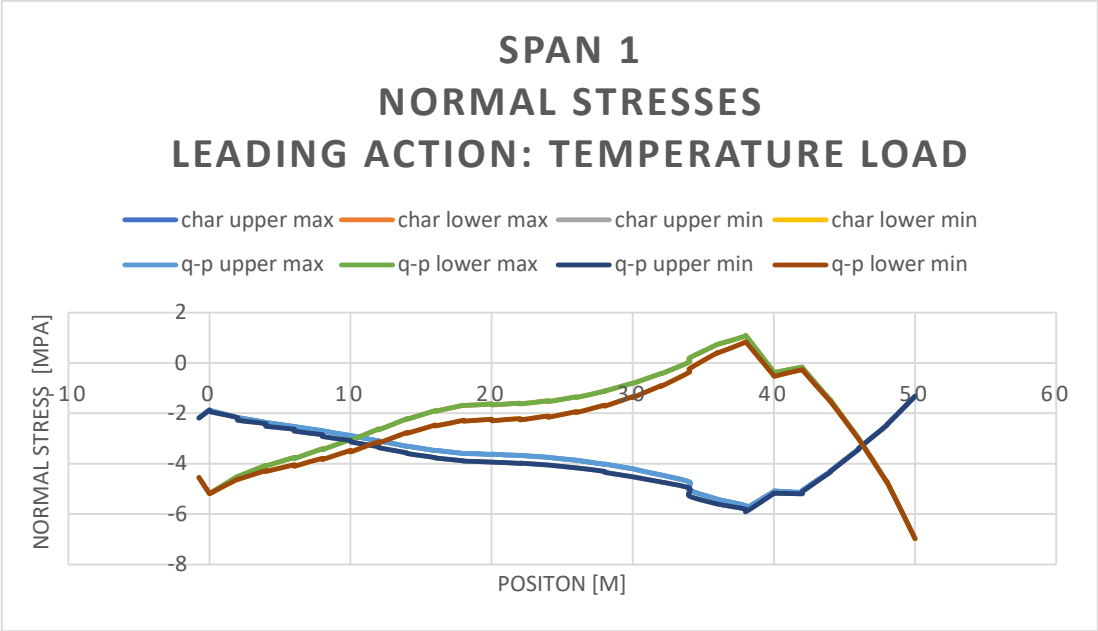

Figure 100: Construction without action of the fresh concrete: Normal stresses – span 1

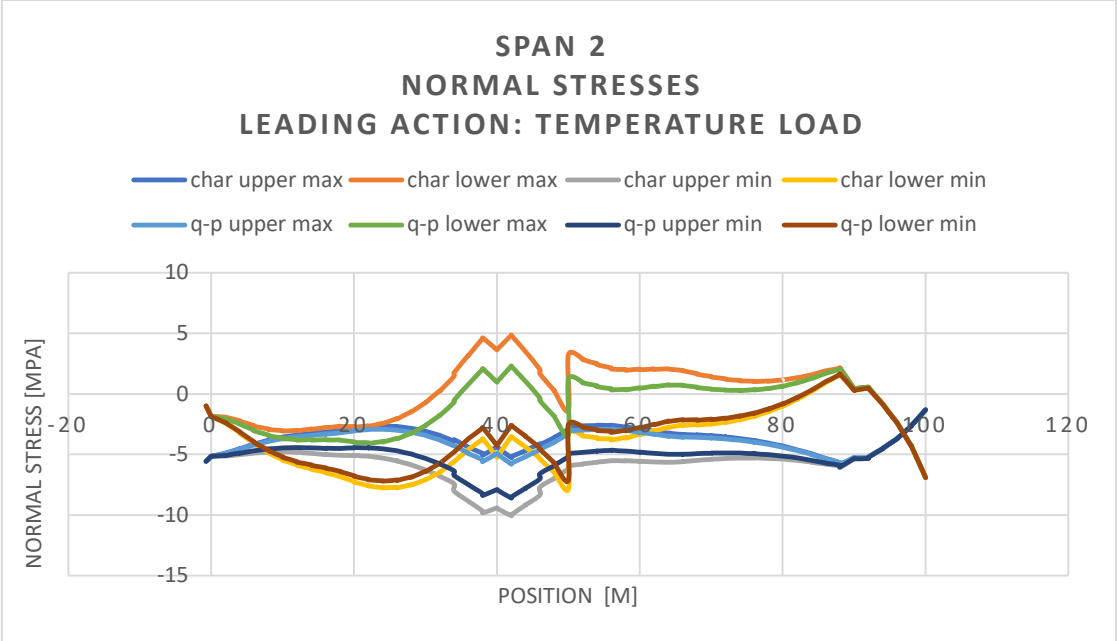

Figure 101: Construction without action of the fresh concrete: Normal stresses – span 2

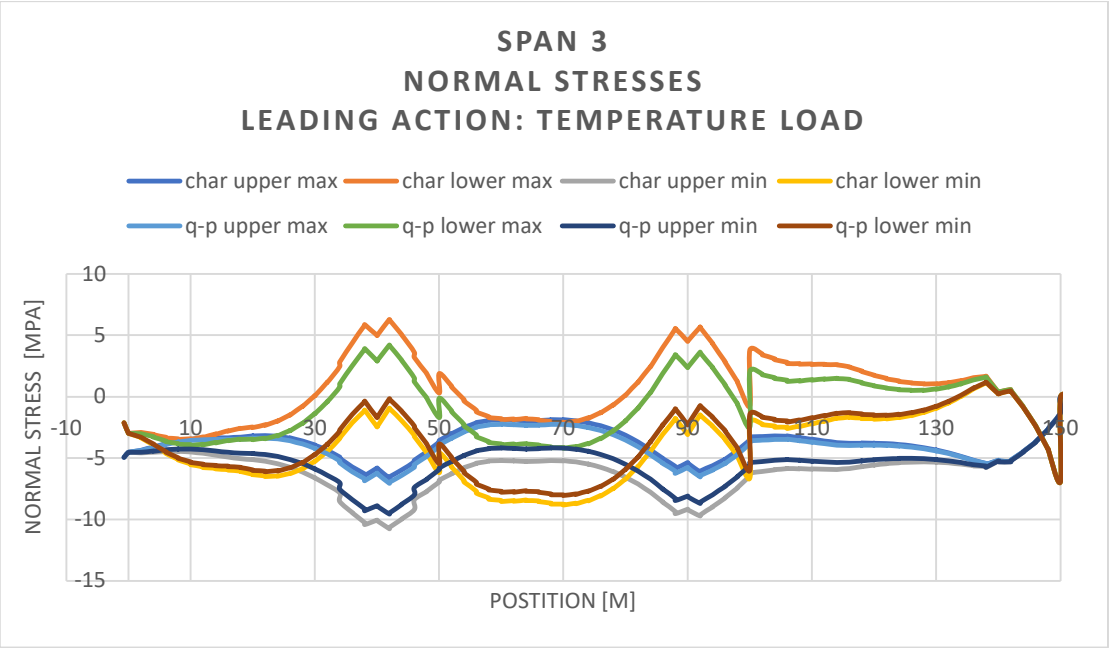

Figure 102: Construction without action of the fresh concrete: Normal stresses – span 3

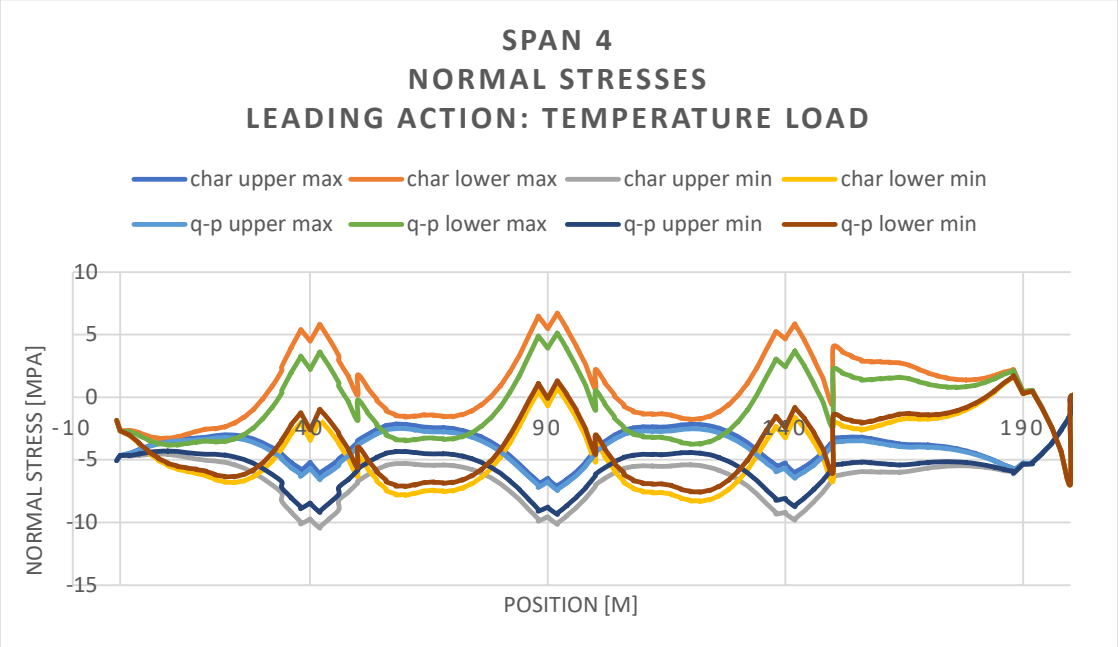

Figure 103: Construction without action of the fresh concrete: Normal stresses – span 4

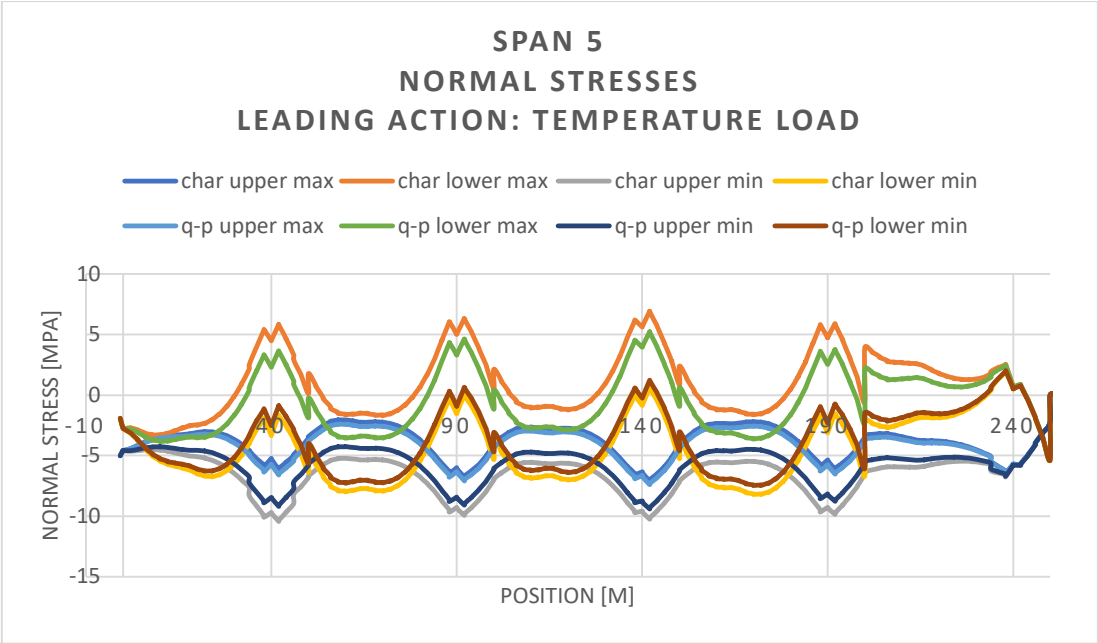

Figure 104: Construction without action of the fresh concrete: Normal stresses – span 5

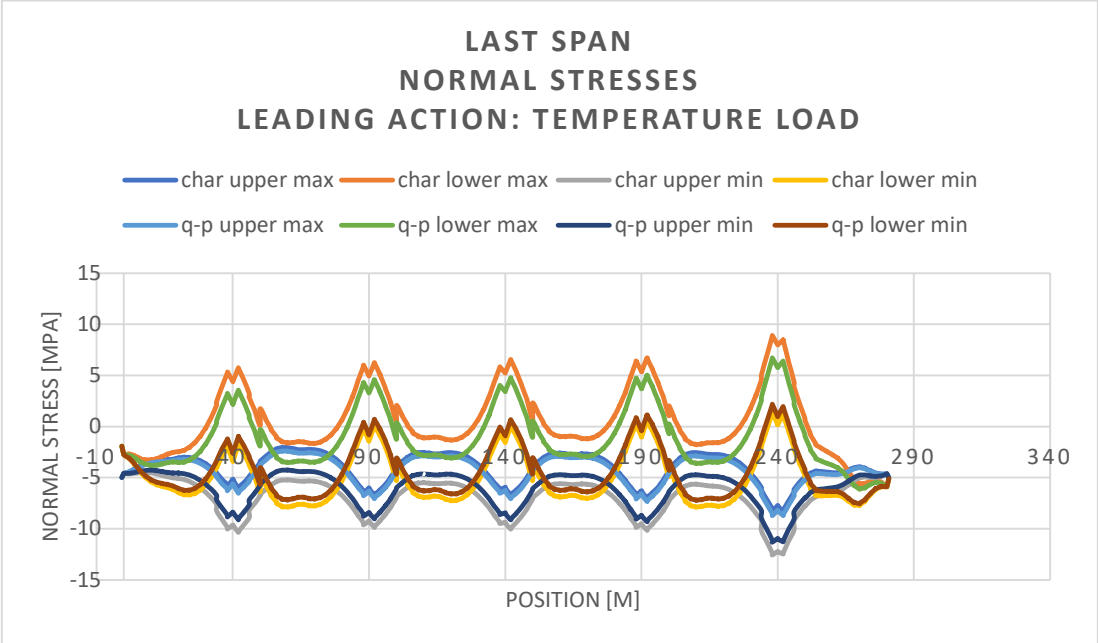

Figure 105: Construction without action of the fresh concrete: Normal stresses – span 6

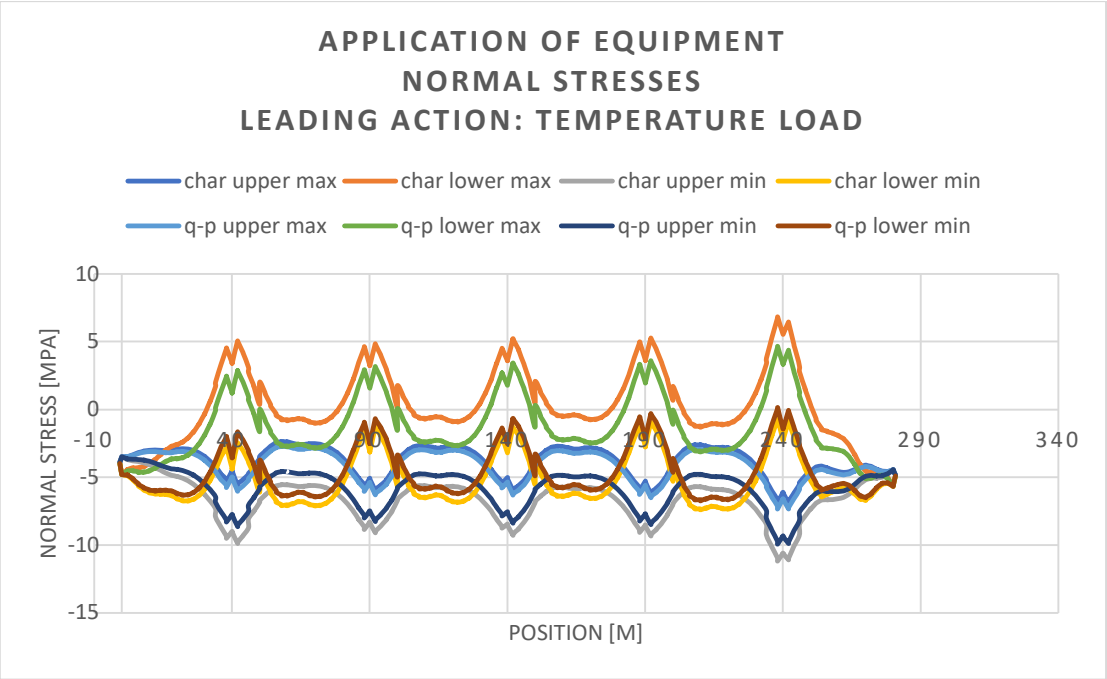

Figure 106: Construction without action of the fresh concrete: Normal stresses – application of equipment

It is apparent from the diagrams above that the design meets the limit requirements in the critical fibres.

6.4.2. Construction stages - check of the case with the action of the fresh concrete on the scaffolding system

For this case, worse results are also obtained when the main variable load is temperature variation. The final stresses are therefore also shown only for this combination.

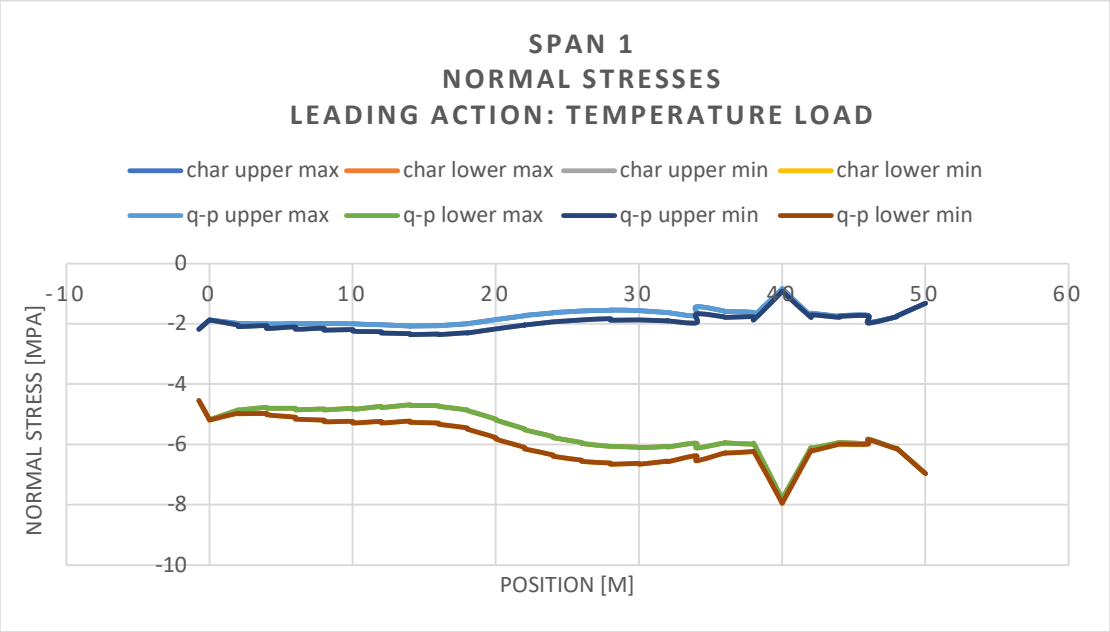

Figure 107: Construction with action of the fresh concrete: Normal stress – span 1

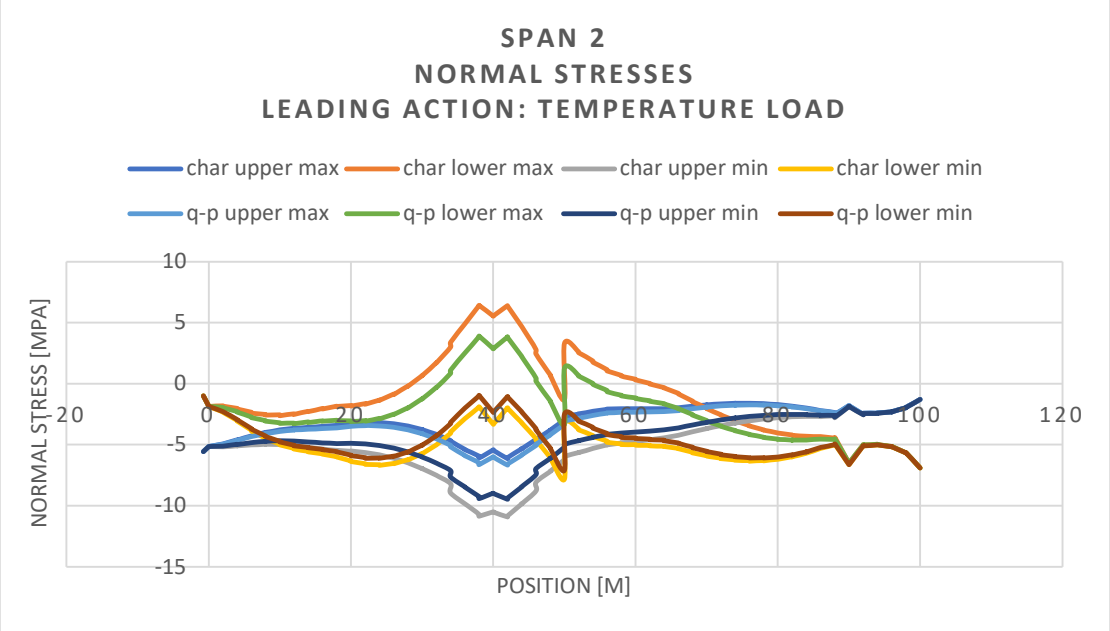

Figure 108: Construction with action of the fresh concrete: Normal stress – span 2

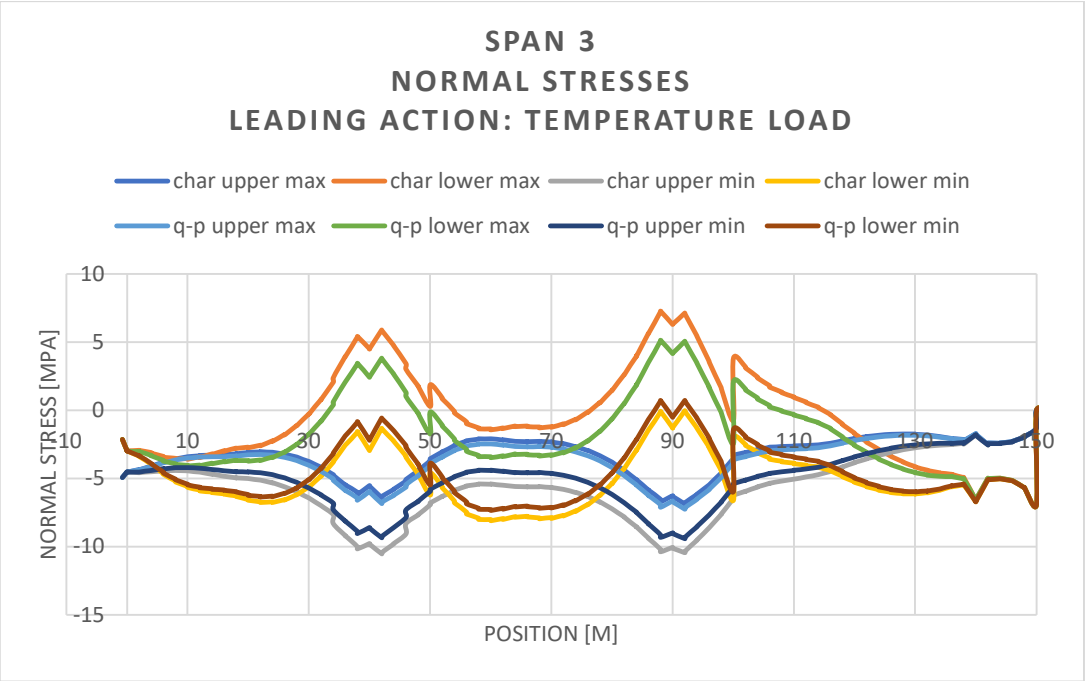

Figure 109: Construction with action of the fresh concrete: Normal stress – span 3

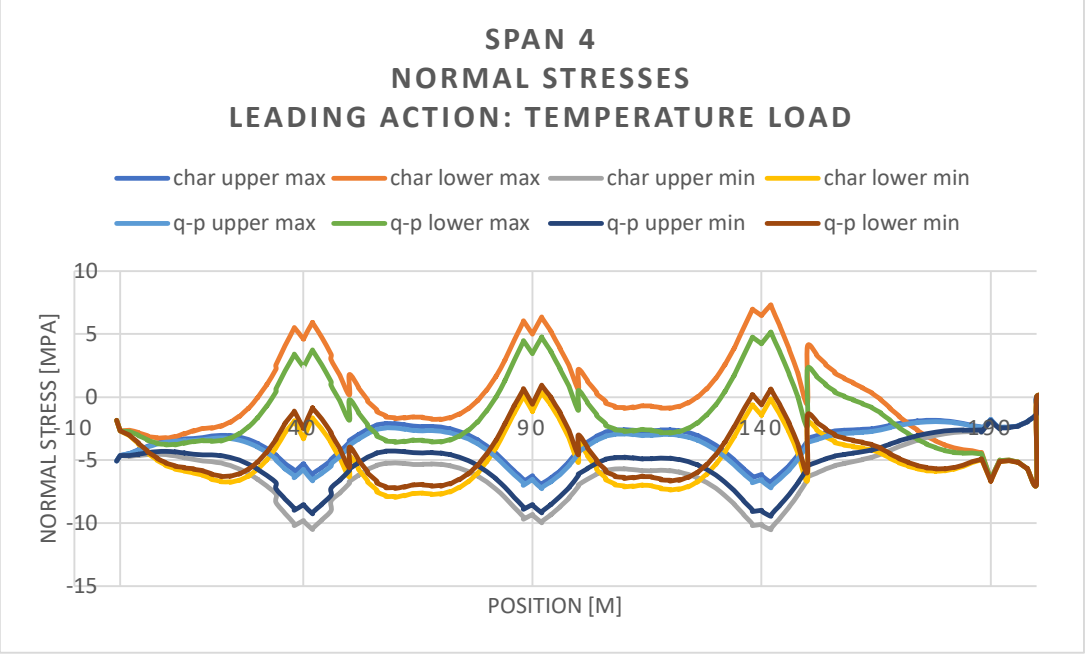

Figure 110: Construction with action of the fresh concrete: Normal stress – span 4

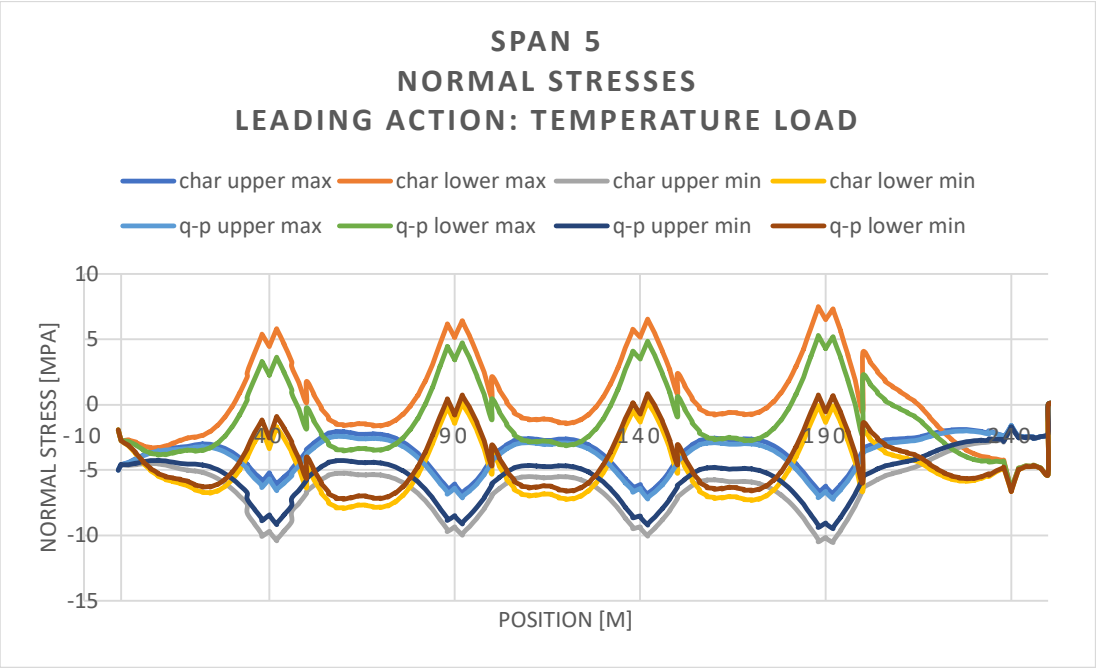

Figure 111: Construction with action of the fresh concrete: Normal stress – span 5

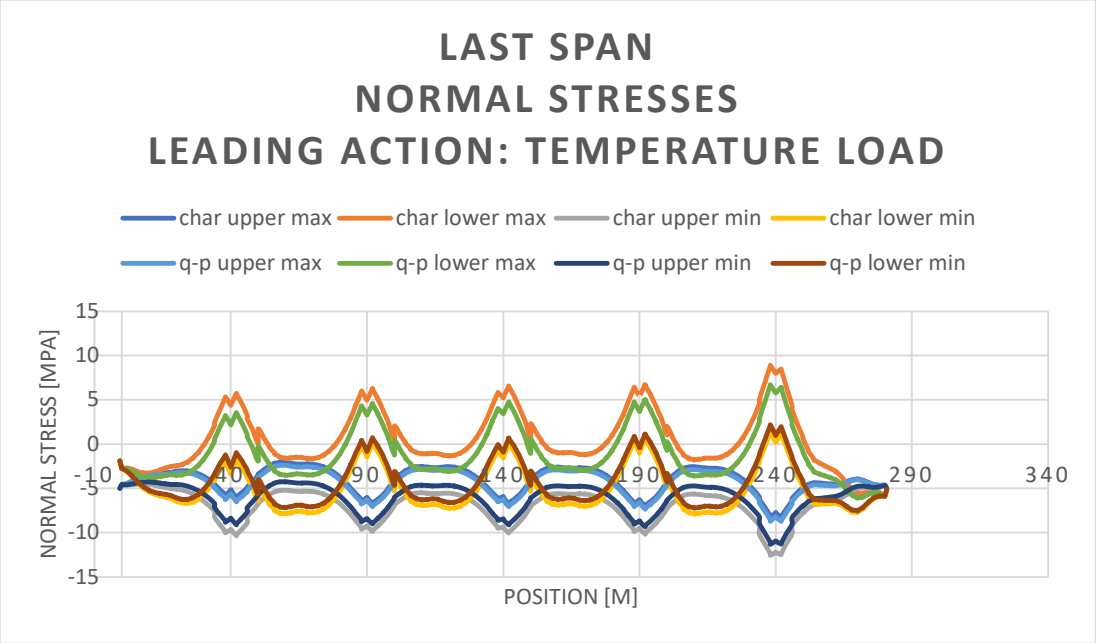

Figure 112: Construction with action of the fresh concrete: Normal stress – span 6

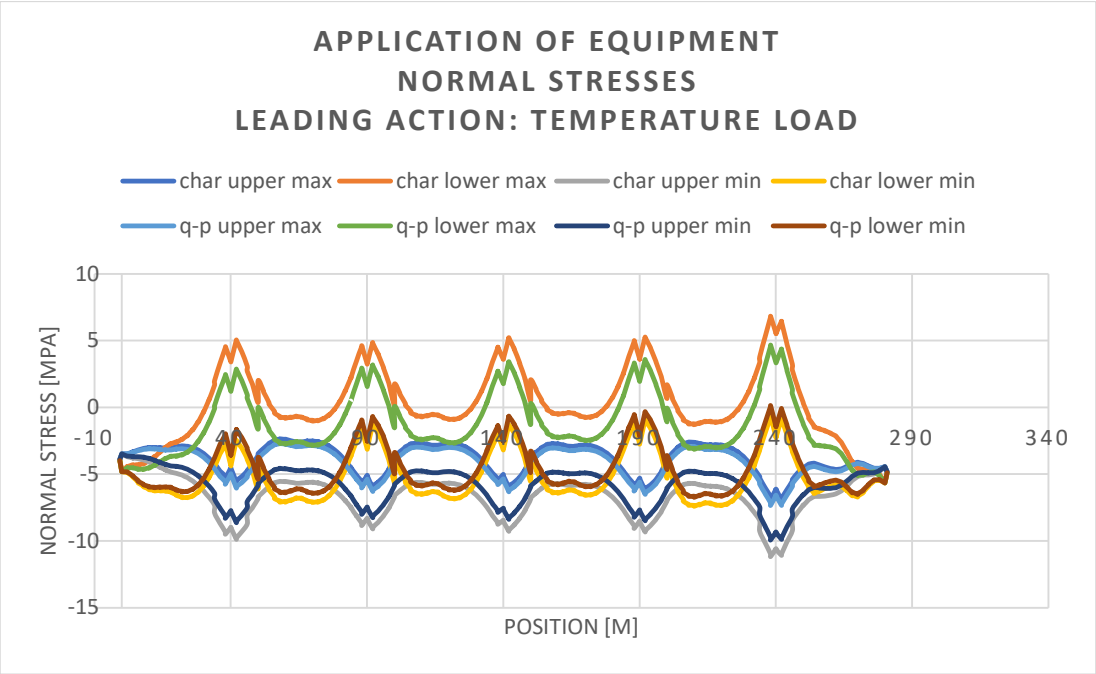

Figure 113: Construction with action of the fresh concrete: Normal stress – application of equipment

It is apparent from the diagrams above that the design meets the limit requirements in the critical fibres.

Tensile stresses in the structure would be solved by use of passive reinforcement.

6.4.3. Finished structure – check of limit stresses

In the service life, the stresses are always presented separately for the upper and lower fibers. For greater transparency, only the maximum and minimum values from each of the combinations (characteristic, quasi-permanent, frequent) are illustrated.

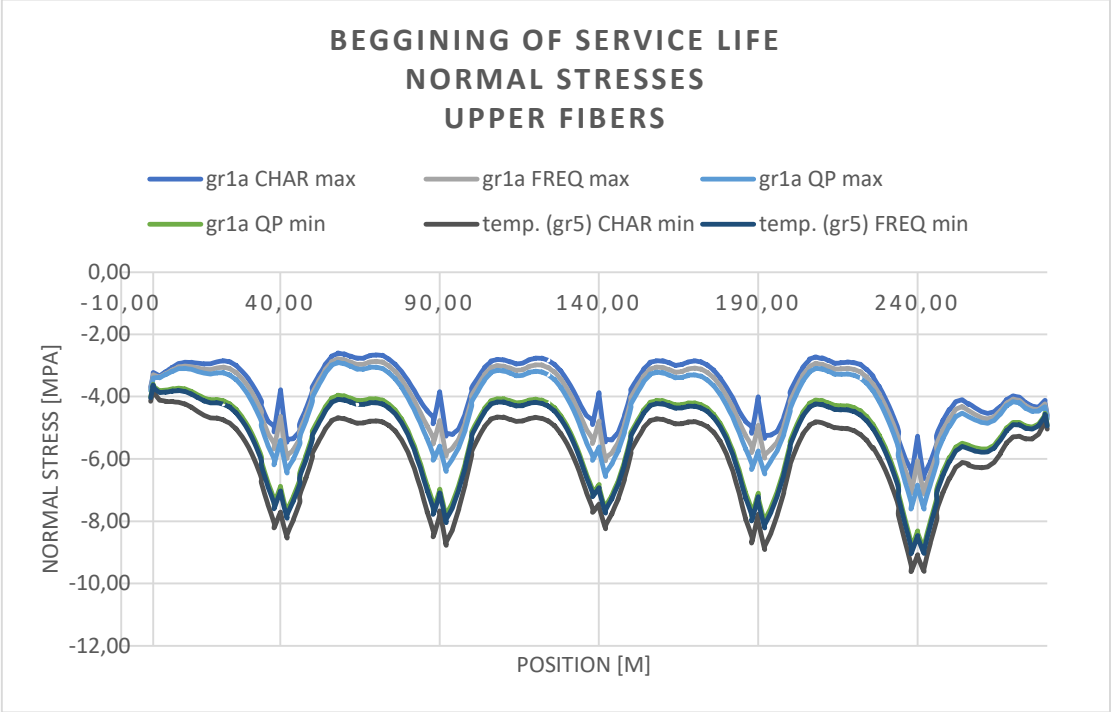

Figure 114: Normal stress in upper fibers – beggining of service life

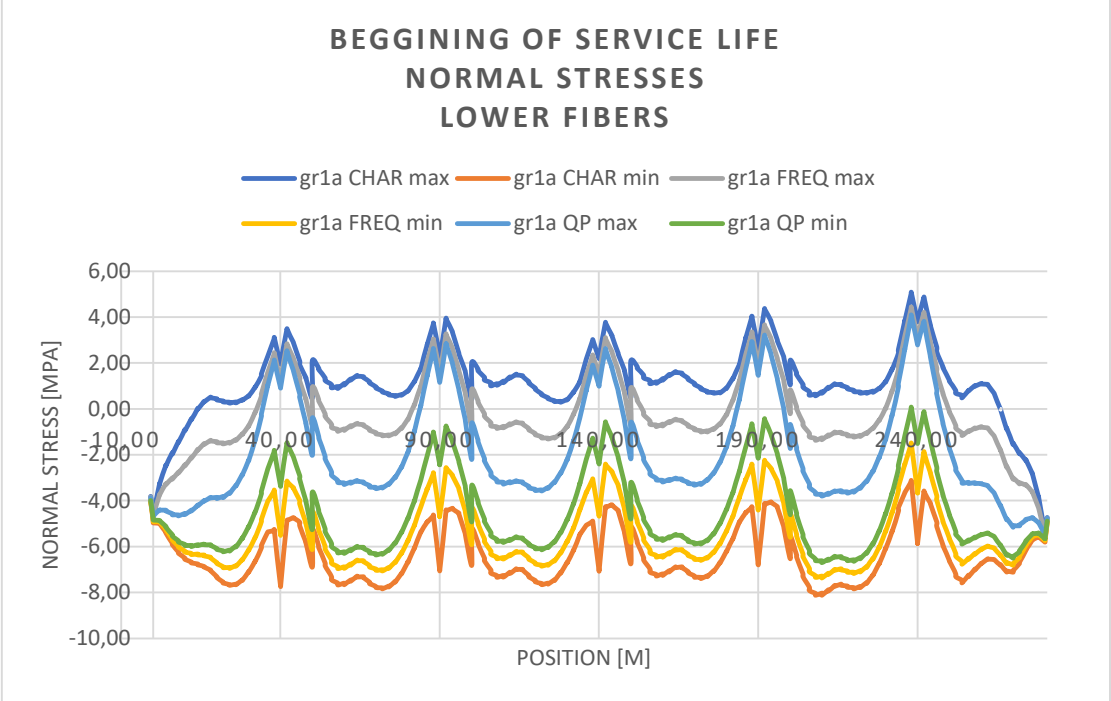

Figure 115: Normal stress in upper fibers – beggining of service life

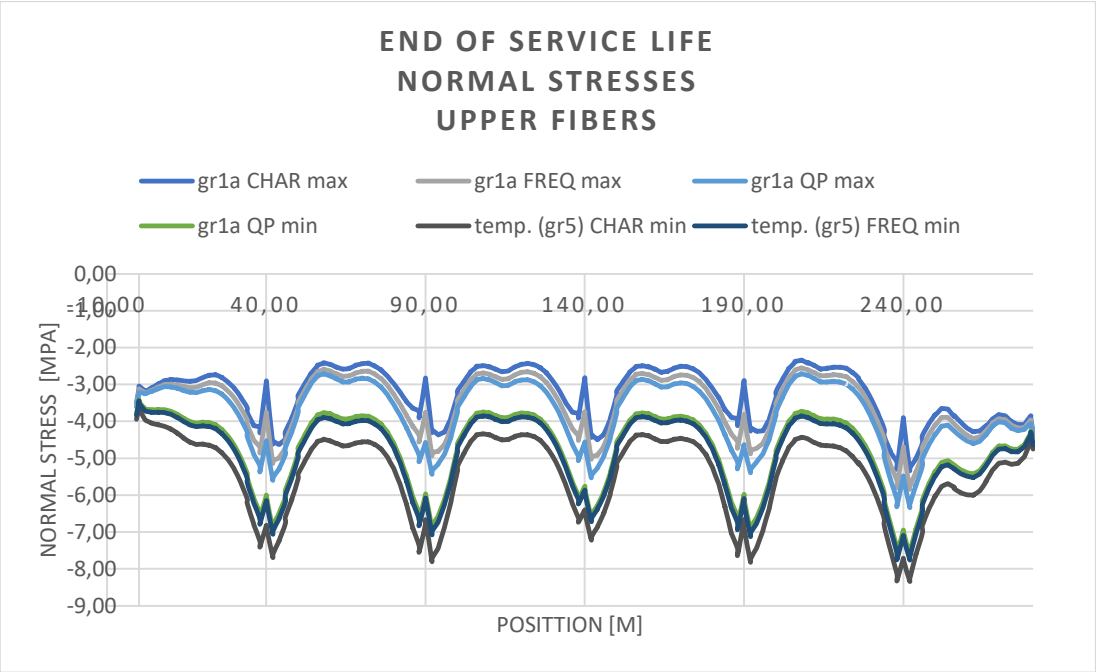

Figure 116: Normal stress in upper fibers – end of service life

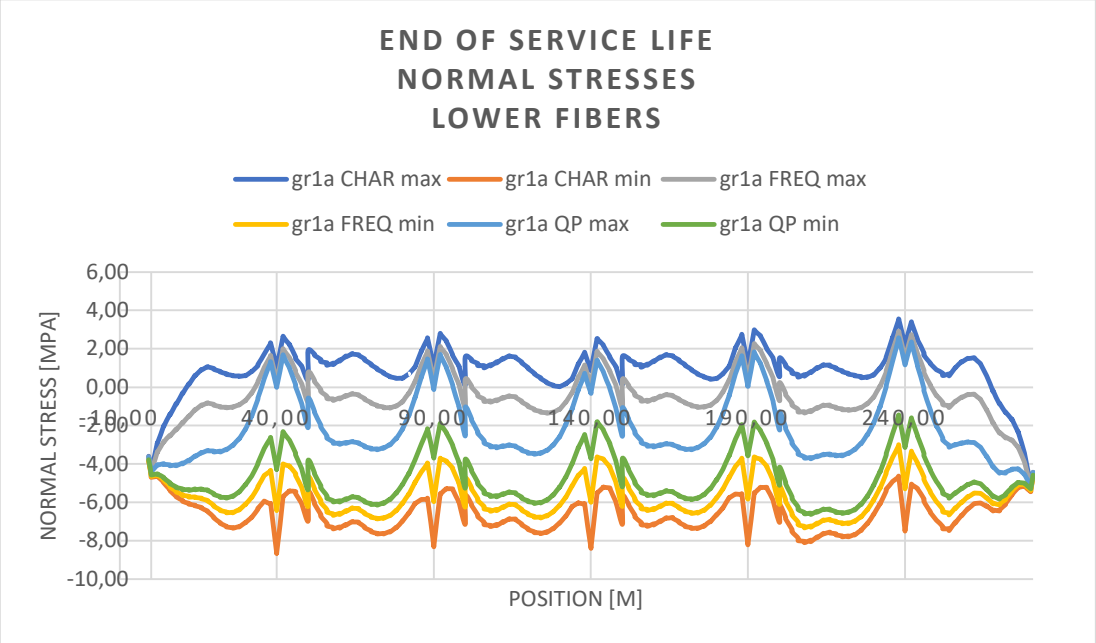

Figure 117: Normal stress in upper fibers – end of service life

7. Ultimate limit states

7.1. Introduction

To check the ultimate limit states, combinations 6.10a and 6.10b were created. From these combinations, the maximum mid-span bending moments and minimum bending moments above support were determined. The extreme effects in these two cross sections were checked.

7.2. Resulting internal forces

The extreme bending moments for all types of combinations are shown in the following diagrams. The minimum moment in the cross-section above the pier and the maximum moment in the cross-section in the middle of span were obtained from these plots and are checked in the next part.

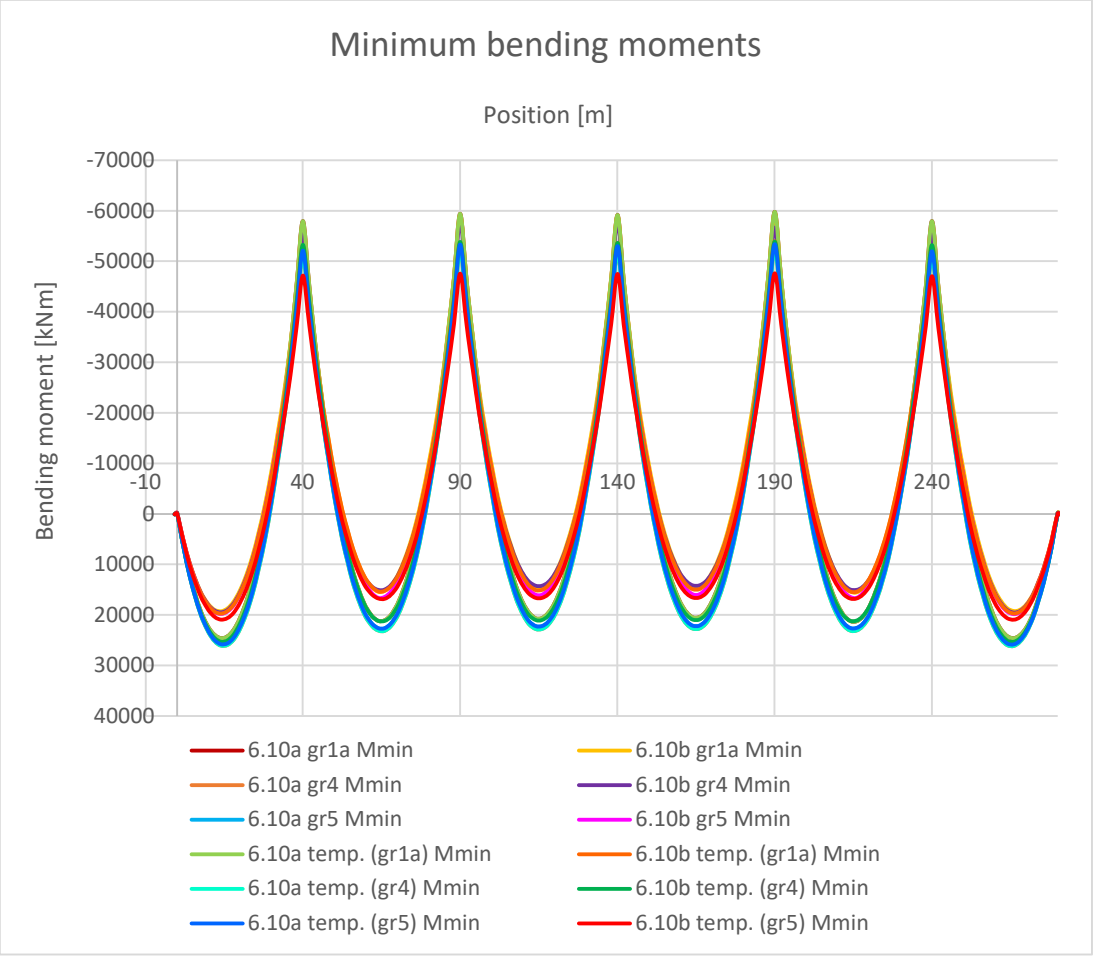

Figure 118: Minimum bending moments

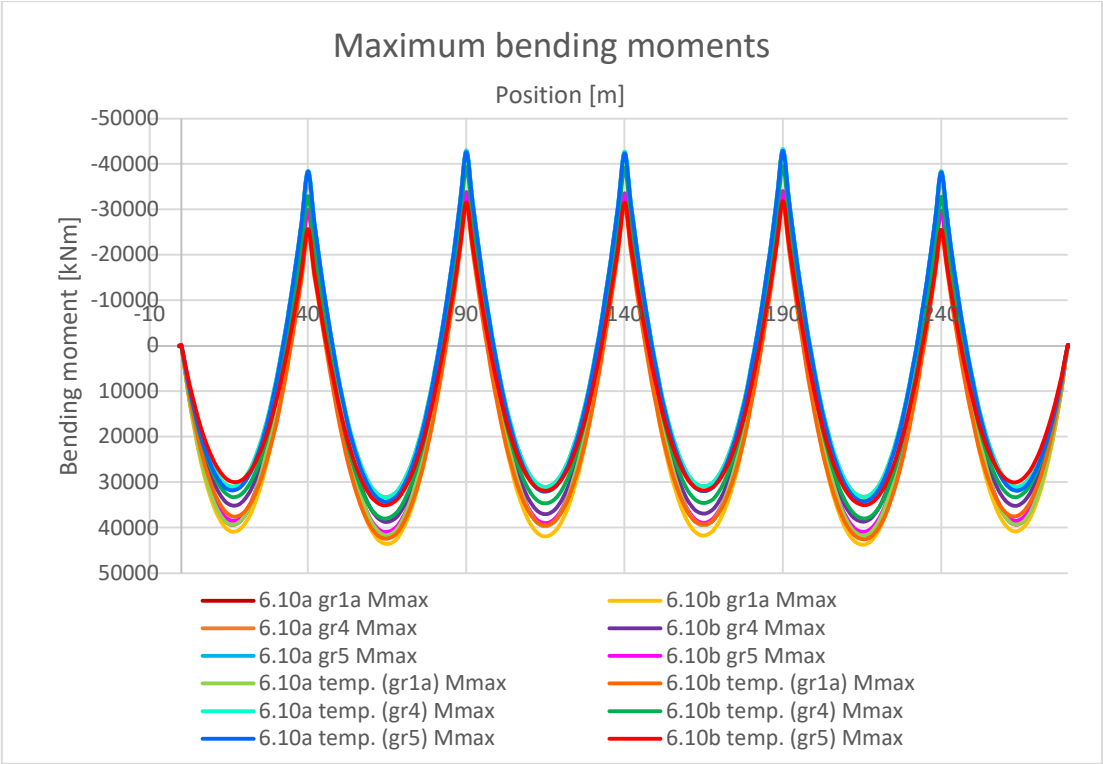

Figure 119: Maximum bending moments

7.3. Check of the cross section at span

The maximum bending moment at span was achieved specifically at span 5 and under the combination 6.10b with the leading variable load gr1a.

The cross section is checked for the time of the beginning of the service life. A detailed calculation was performed in Microsoft Excel prepared by doc. Ing. Roman Šafář, Ph.D. The original of the calculation is archived by its author.

7.3.1. Check of the cross section at span – beginning of service life

Check of ultimate limit state - resistance moment

Cross section		At span 5	
Time		Beggining of service life	
Cross section characteristics	depth	3000	mm
	centroid	2001	mm
	width	7250	mm
Design compressive strength	f_{cd}	26,67	MPa

Design moment	M_{Ed}	42,52	MNm
Design normal force	N_{Ed}	0,61	MN
Total moment from prestressing - maximum tensioning force	M_0	-30,86	MN
Percentage of maximum stress at in the beggining of service life		76,61	%
Total moment from prestressing with losses	M_0	-23,64	MN
Statically indeterminate moment	ΔM_p	23,96	MN

Prestressing reinforcement

Layer	Position from the bottom	Excentricity	Number of tendons	Number of strands	Area of 1 tendon	Total area of tendons	Stress in tendons	Force in tendons	Moment
	m	m	pcs	pcs	mm^2	m^2	MPa	MN	MNm
I	0,15	1,851	2	26	150	0,0078	1140,28	8,894	16,463
K	0,15	1,851	2	26	150	0,0078	1076,29	8,395	15,539
J	0,29	1,711	2	26	150	0,0078	1168,67	9,116	15,597
							Total	26,405	47,599

Concrete reinforcing

bottom	8 x 20 mm
top	72 x 12 mm

After detaild calculation

Force in concrete	N_{cd}	-31,174	MN
Force in prestressing tendons	N_{pd}	33,306	MN
Force in concrete reinforcint - upper layer	N_{sd1}	-2,613	MN
Force in concrete reinforcint - lower layer	N_{sd2}	1,092	MN
Normal force from external actions	N_{Ed}	-0,61	MN
Efective depth of the compression zone of concrete	x_u	0,288	m

Resistance moment	M_{Rd}	90,523	MNm	OK
Design moment increased by the static moment from prestressing	$M_{Ed} + \Delta M_p$	66,48	MNm	

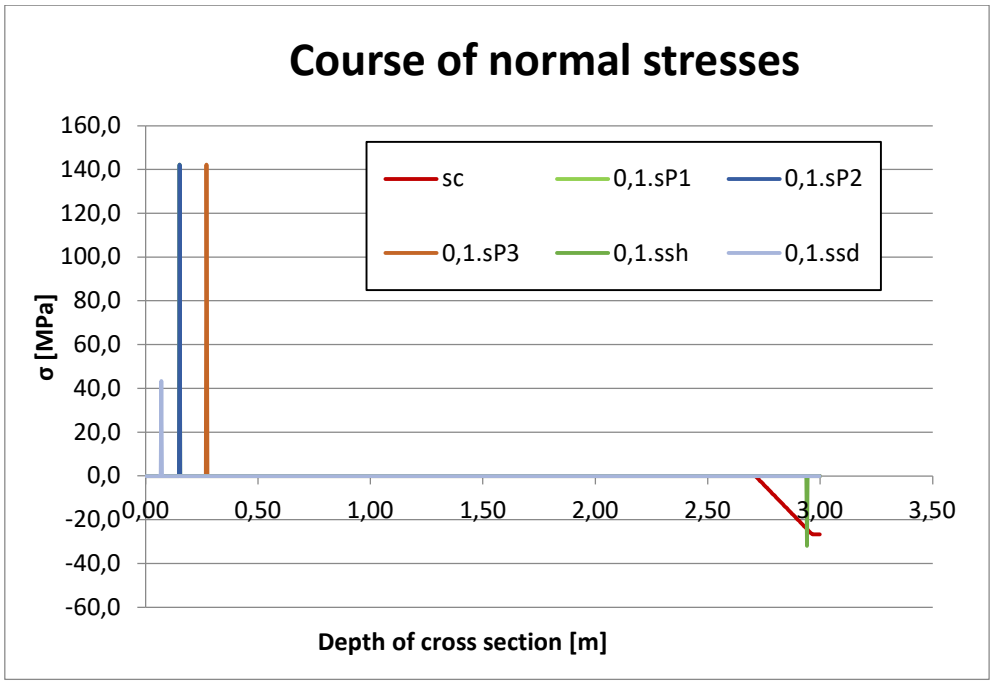

Figure 120: Course of normal stresses – cross section at span – beggining of service life

7.4. Check of the cross section at pier

The maximum bending moment at span was achieved specifically in cross section at pier 4 and under the combination 6.10a with the temperature changes load as the leading variable action and group of loads gr1a.

The cross section is checked for the time of the end of the service life. A detailed calculation was performed in Microsoft Excel prepared by doc. Ing. Roman Šafář, Ph.D. The original of the calculation is archived by its author.

7.4.1. Check of the cross section at pier– end of service life

Check of ultimate limit state - resistance moment

Cross section		At pier 4	
Time		End of service life	
Cross section characteristics	depth	3000	mm
	centroid	999	mm
	width	1280	mm
Design compressive strength	f_{cd}	26,67	MPa

Design moment	M_{Sd}	-59,794	MNm
Design normal force	N_{Sd}	-0,096	MN
Total moment from prestressing - maximum tensioning force	M_P	44,27	MN
Percentage of maximum stress at the end service life		76,16	%
Total moment from prestressing with losses	M_P	33,72	MN
Statically indeterminate moment	ΔM_P	12,47	MN

Prestressing reinforcement

Layer	Position from the top	Excentricity	Number of tendons	Number of strands	Area of 1 tendon	Total area of tendons	Stress in tendons	Force in tendons	Moment
	m	m	pcs	pcs	mm^2	m^2	MPa	MN	MNm
I	0,15	0,849	2	26	150	0,0078	1215,09	9,478	8,047
K	0,15	0,849	2	26	150	0,0078	1199,14	9,353	7,941
J	0,29	0,709	2	26	150	0,0078	951,5	7,422	5,262
							Total	26,253	21,249

Concrete reinforcing

bottom	8 x 20 mm
top	72 x 12 mm

After detail calculation

Force in concrete	N_{cd}	-32,744	MN
Force in prestressing tendons	N_{pd}	31,523	MN
Force in concrete reinforcint - upper layer	N_{sd1}	2,081	MN
Force in concrete reinforcint - lower layer	N_{sd2}	-0,955	MN
Normal force from external actions	$-N_{Sd}$	0,096	MN
Efective depth of the compression zone of concrete	x_u	1,794	m

Resistance moment	M_{Rd}	-74,961	MNm	OK
Design moment increased by the static moment from prestressing	$M_{Sd} + \Delta M_P$	-47,33	MNm	

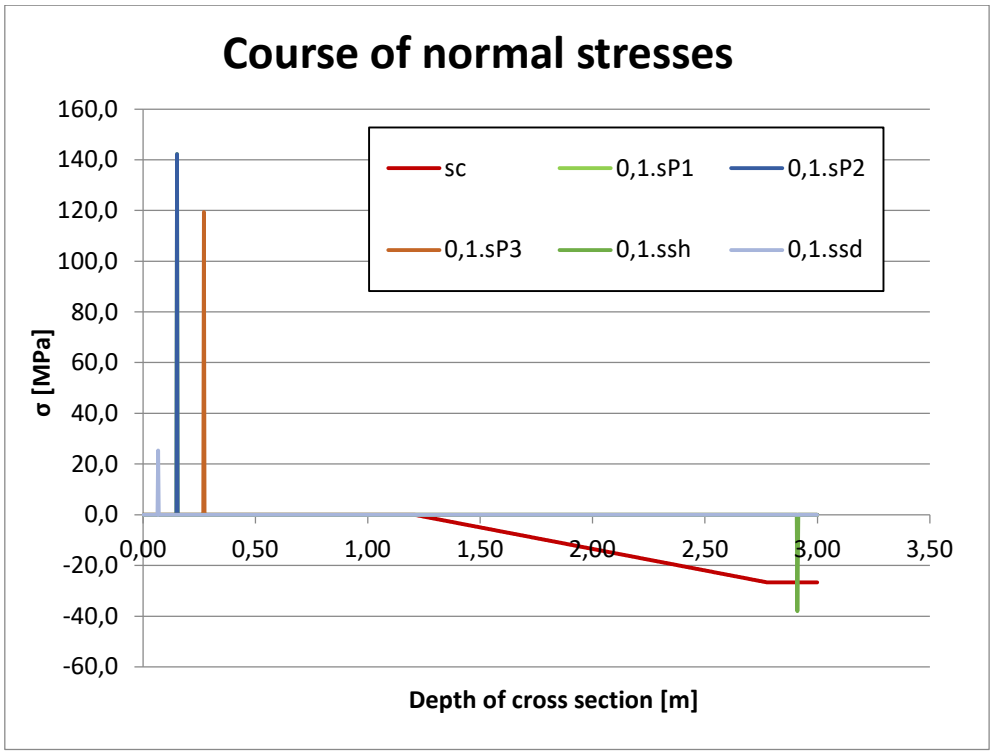

Figure 121: Course of normal stresses – cross section at pier – end of service life

Both cross sections meet the requirements of the ultimate limit state.

8. Conclusion

In this thesis, a case study of the design of the V1 road viaduct located near Lisbon, Portugal, was carried out.

The thesis is divided into three parts, namely a technical report, a structural analysis, and a set of drawings.

In the technical report, general information about the bridge and its location can be found. Furthermore, other structural solutions for this structure are proposed, which have been considered for the final design. The last part of the technical report describes the bridge elements in terms of materials, shapes, and equipment.

In the structural analysis, the calculation models that were used for the analysis are presented and the characteristics of the structure needed for further calculation are also evaluated there. Subsequently, the parameters of the materials used are defined.

The next section describes the analysis of actions and internal forces for whose effects the prestressing reinforcement was designed. The last part of the structural analysis includes main safety checks.

The superstructure was designed according to the standards and the requirements were met.

The third part of the thesis, a set of drawings, is included in the attachments.

List of figures

Figure 1: Box girder built on a movable scaffolding system – cross section 13
Figure 2: Box girder built on a movable scaffolding system – longitudinal section 13
Figure 3: Arch bridge – cross section 14
Figure 4: Arch bridge – longitudinal section 14
Figure 5: System of UHPFRC precast segments – cross section 15
Figure 6: System of UHPFRC precast segments – longitudinal section 15
Figure 7: Composite steel-concrete structure – cross section 16
Figure 8: Composite steel-concrete – longitudinal section 16
Figure 9: Scheme for empirical design 21
Figure 10: Scheme for dimensioning of the double-beam 21
Figure 11: Cross section simplified for the structural analysis 23
Figure 12: 3D model 23
Figure 13: Rendered 3D model 24
Figure 14: Casting the substructure 25
Figure 15: Casting the span 1 25
Figure 16: Casting the span 2 25
Figure 17: Casting the span 3 25
Figure 18: Casting the span 4 25
Figure 19: Casting the span 5 25
Figure 20: Casting the span 6 25
Figure 21: Completed structure 25
Figure 22: Bar 2D model 26
Figure 23: Rendered 2D model 26
Figure 24: Model for short-term loads during construction – stage 1 27
Figure 25: Effective cross section above the piers P1 and P5 28
Figure 26: Self-weight of cornices 31
Figure 27: Self-weight of handrails and barriers 32
Figure 28: Self-weight of pavement layers 32
Figure 29: Self-weight of bridge equipment: mean value 33
Figure 30: Self-weight of bridge equipment: Upper characteristic value 34
Figure 31: Self-weight of bridge equipment: lower characteristic value 35
Figure 32: Dispersion of axle forces of LM1 TS 35
Figure 33: Scheme of the Load Model 1 – tandem system 37
Figure 34: Dispersion of axle forces of LM3 38
Figure 35: Scheme of the Load Model 3 – special vehicle 1200/150 38
Figure 36: Action of footways 39
Figure 37: Elastic response spectrum 46
Figure 38: Design response spectrum 47
Figure 39: Normal force N: Self-weight of superstructure 49
Figure 40: Shear force V_z: Self-weight of superstructure 49
Figure 41: Bending moment M_y: Self-weight of superstructure 49
Figure 42: Torsion moment M_x: Self-weight of superstructure 49
Figure 43: Normal force N: Self-weight of equipment 50
Figure 44: Shear force V_z: Self-weight of equipment 50
Figure 45: Bending moment M_y: Self-weight of equipment 50
Figure 46: Torsion moment M_x: Self-weight of equipment 50

Figure 47: Normal force N: Uneven settlements 51
Figure 48: Shear force V_z: Uneven settlements 51
Figure 49: Bending moment M_y: Uneven settlements 51
Figure 50: Torsional moment M_x: Uneven settlements 51
Figure 51: Normal force N: LM1 TS 52
Figure 52: Shear force V_z: LM1 TS 52
Figure 53: Bending moment M_y: LM1 TS 52
Figure 54: Torsion moment M_x: LM1 TS 52
Figure 55: Normal force N: LM1 UDL 53
Figure 56: Shear force V_z: LM1 UDL 53
Figure 57: Bending moment M_y: LM1 UDL 53
Figure 58: Torsion moment M_x: LM1 UDL 53
Figure 59: Normal force N: Load on sidewalks 54
Figure 60: Shear force V_z: Load on sidewalks 54
Figure 61: Bending moment M_y: Load on sidewalks 54
Figure 62: Torsion moment M_x: Load on sidewalks 54
Figure 63: Normal force N: LM3 TS 55
Figure 64: Shear force V_z: LM3 TS 55
Figure 65: Bending moment M_y: LM3 TS 55
Figure 66: Torsion moment M_x: LM3 TS 55
Figure 67: Normal force N: LM3 UDL 56
Figure 68: Shear force V_z: LM3 UDL 56
Figure 69: Bending moment M_y: LM3 UDL 56
Figure 70: Torsion moment M_x: LM3 UDL 56
Figure 71: Normal force N: LM4 57
Figure 72: Shear force V_z: LM4 57
Figure 73: Bending moment M_y: LM4 57
Figure 74: Torsion moment M_x: LM4 57
Figure 75: Normal force N: Uniform temperature load 58
Figure 76: Shear force V_z: Uniform temperature load 58
Figure 77: Bending moment M_y: Uniform temperature load 58
Figure 78: Torsion moment M_x: Uniform temperature load 58
Figure 79: Normal force N: Differential temperature load 59
Figure 80: Shear force V_z: Differential temperature load 59
Figure 81: Bending moment M_y: Differential temperature load 59
Figure 82: Torsion moment M_x: Differential temperature load 59
Figure 83: Normal force N: Wind load – longitudinal direction 60
Figure 84: Shear force V_z: Wind load – longitudinal direction 60
Figure 85: Bending moment M_y: Wind load – longitudinal direction 60
Figure 86: Torsion moment M_x: Wind load – longitudinal direction 60
Figure 87: Normal force N: Wind load – transverse direction 61
Figure 88: Shear force V_z: Wind load – transverse direction 61
Figure 89: Bending moment M_y: Wind load – transverse direction 61
Figure 90: Torsion moment M_x: Wind load – transverse direction 61
Figure 91: First mode shape of the structure 62
Figure 92: Second mode shape of the structure 62
Figure 93: Bending moments in piers: Combination of seismic action – direction x 62

Figure 94: Bending moments in piers: Combination of seismic action – direction y 63
Figure 95: Display of prestressing reinforcement in the TDA model 71
Figure 96: First construction stage – without scaffolding system girders 73
Figure 97: First construction stage – with scaffolding system 73
Figure 98: Normal stresses in upper fibers – long-term loads 74
Figure 99: Normal stress in lower fibers – long-term loads 75
Figure 100: Construction without action of the fresh concrete: Normal stresses – span 1 76
Figure 101: Construction without action of the fresh concrete: Normal stresses – span 2 76
Figure 102: Construction without action of the fresh concrete: Normal stresses – span 3 77
Figure 103: Construction without action of the fresh concrete: Normal stresses – span 4 77
Figure 104: Construction without action of the fresh concrete: Normal stresses – span 5 78
Figure 105: Construction without action of the fresh concrete: Normal stresses – span 6 78
Figure 106: Construction without action of the fresh concrete: Normal stresses – application of equipment 79
Figure 107: Construction with action of the fresh concrete: Normal stress – span 1 80
Figure 108: Construction with action of the fresh concrete: Normal stress – span 2 80
Figure 109: Construction with action of the fresh concrete: Normal stress – span 3 81
Figure 110: Construction with action of the fresh concrete: Normal stress – span 4 81
Figure 111: Construction with action of the fresh concrete: Normal stress – span 5 82
Figure 112: Construction with action of the fresh concrete: Normal stress – span 6 82
Figure 113: Construction with action of the fresh concrete: Normal stress – application of equipment 83
Figure 114: Normal stress in upper fibers – beggining of service life 84
Figure 115: Normal stress in upper fibers – beggining of service life 84
Figure 116: Normal stress in upper fibers – end of service life 85
Figure 117: Normal stress in upper fibers – end of service life 85
Figure 118: Minimum bending moments 86
Figure 119: Maximum bending moments 87
Figure 120: Course of normal stresses – cross section at span – beggining of service life 89
Figure 121: Course of normal stresses – cross section at pier – end of service life 92

List of tables

Table 1: Construction stages 26
Table 2: Load Model 1 – tandem system – characteristic values of action 36
Table 3: Load Model 1 – uniformly distributed load – characteristic values of action: 37
Table 4: Horizontal forces overview 40
Table 5: Values of the factor k_{sur} 41
Table 6: Elastic response spectrum parameters 45
Table 7: Design response spectrum parameters 46
Table 8: Overview of load cases 48
Table 9: Partial factors γ and reduction factor ξ 65
Table 10: Values of combination coefficients ψ (road bridges) 65
Table 11: SLS – combination factors – leading traffic action 66
Table 12: SLS – combination factors – leading action temperature 67
Table 13: ULS – combination factors – leading action traffic 68
Table 14: ULS – combination factors – leading action temperature 69

References

[1] **ŠAFÁŘ, Roman, Milan PETŘÍK a Petr TEJ.** *Concrete bridges: worked examples*. Praha: České vysoké učení technické v Praze, 2013. ISBN 978-80-01-05179-5.

[2] **ŠAFÁŘ, Roman.** *Concrete bridges: lectures*. V Praze: České vysoké učení technické, 2015. ISBN 978-80-01-05631-8.

[3] **EN 1990 (2002) (English):** Eurocode: Basis of structural design [Authority: The European Union Per Regulation 305/2011, Directive 98/34/EC, Directive 2004/18/EC]

[4] **EN 1991-1-4 (2005) (English):** Eurocode 1: Actions on structures – Part 1-4: General actions – Wind actions [Authority: The European Union Per Regulation 305/2011, Directive 98/34/EC, Directive 2004/18/EC]

[5] **NP EN 1991-1-4 (2010):** Eurocode 1: Actions on structures – Part 1-4: General actions Wind actions (Versão portuguesa da EN 1991-1-4:2005 + AC:2010)

[6] **EN 1991-1-5 (2003) (English):** *Eurocode 1: Actions on structures – Part 1-5: General actions – Thermal actions* [Authority: The European Union Per Regulation 305/2011, Directive 98/34/EC, Directive 2004/18/EC]

[7] **NP EN 1991-1-5 (2009):** *Eurocode 1: Actions on structures – Part 1-5: General actions – Thermal actions* (Versão portuguesa da EN 1991-1-5:2003 + AC:2009)

[8] **EN 1991-2 (2003) (English):** *Eurocode 1: Actions on structures – Part 2: Traffic loads on bridges* [Authority: The European Union Per Regulation 305/2011, Directive 98/34/EC, Directive 2004/18/EC]

[9] **NP EN 1991-2 (2017):** *Eurocode 1: Actions on structures – Part 2: Traffic loads on bridges* (Versão portuguesa da EN 1991-2:2003 + AC:2010)

[10] **EN 1992-1-1 (2004) (English):** *Eurocode 2: Design of concrete structures – Part 1-1: General rules and rules for buildings* [Authority: The European Union Per Regulation 305/2011, Directive 98/34/EC, Directive 2004/18/EC]

[11] **NP EN 1992-1-1 (2010):** *Eurocode 2: Design of concrete structures: Part 1-1: General rules and rules for buildings* (Versão portuguesa da EN 1992-1-1:2004 + AC:2008)

[12] **EN 1992-2 (2005) (English)**: *Eurocode 2: Design of concrete structures – Part 2: Concrete bridges – Design and detailing rules* [Authority: The European Union Per Regulation 305/2011, Directive 98/34/EC, Directive 2004/18/EC]

[13] **NP EN 1992-2 (2018)**: *Eurocode 2: Design of concrete structures – Concrete bridges – Design and detailing rules* (Versão portuguesa da EN 1992-2:2005 + AC:2008)

[14] **EN 1998-2 (2005) (English):** Eurocode 8: Design of structures for earthquake resistance – Part 2: Bridges [Authority: The European Union Per Regulation 305/2011, Directive 98/34/EC, Directive 2004/18/EC]

[15] **NP EN 1998-1 2010:** Eurocode 8: Design of structures for earthquake resistence – Part 1: General rules, seismic actions and rules for buildings (Versão portuguesa da EN 1998-1:2004 + AC:2009)

CZECH TECHNICAL UNIVERSITY IN PRAGUE

Faculty of Civil Engineering

Department of Concrete and Masonry Structures

Design of a prestressed concrete road viaduct close to Lisbon

Part C
Drawings

List of attachments		
Attachment number	Content	Scale
1	Plan	1:200
2	Longitudinal section	1:200
3	Cross section at span	1:50
4	Cross section at pier	1:50
5	Cross section at abutment	1:50
6	Prestressing reinforcement - longitudinal section	1:200
7	Prestressing reinforcement - plan	1:200